AD-A153 264 THE CONSTRUCTION AND STUDY OF IMPROVED AL(X)GA(1-X)AS-GAAS HETEROSTRUCTUR..(U) ILLINOIS UNIV AT URBANA DEPT OF ELECTRICAL ENGINEERING 1/1

UNCLASSIFIED N HOLONYAK ET AL. MAR 85 ARO-18509.51-EL F/G 9/1 NL

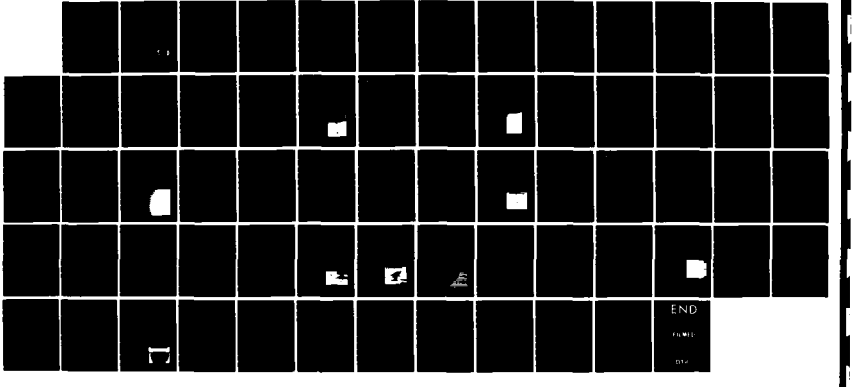

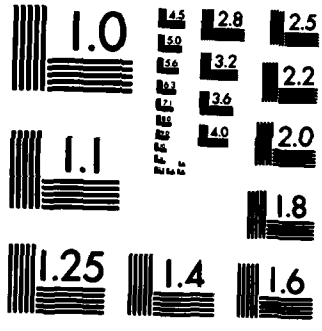

MICROCOPY RESOLUTION TEST CHART
NATIONAL BUREAU OF STANDARDS-1963-A

THE CONSTRUCTION AND STUDY OF IMPROVED $Al_xGa_{1-x}As$-GaAs HETEROSTRUCTURE DEVICES

FINAL report

N. Holonyak, Jr./G. E. Stillman/K. Hess/J. J. Coleman

March 1985

U.S. ARMY RESEARCH OFFICE

DAAG 29-82-K-0059

DEPARTMENT OF ELECTRICAL ENGINEERING
UNIVERSITY OF ILLINOIS AT URBANA-CHAMPAIGN
URBANA, IL 61801

APPROVED FOR PUBLIC RELEASE;
DISTRIBUTION UNLIMITED

UNCLASSIFIED
SECURITY CLASSIFICATION OF THIS PAGE (When Data Entered)

MASTER COPY - FOR REPRODUCTION PURPOSES

REPORT DOCUMENTATION PAGE		READ INSTRUCTIONS BEFORE COMPLETING FORM
1. REPORT NUMBER ARO 18509.51-EL	2. GOVT ACCESSION NO. AD-A153 264 N/A	3. RECIPIENT'S CATALOG NUMBER N/A
4. TITLE (and Subtitle) The construction and study of improved $Al_xGa_{1-x}As$-GaAs heterostructure devices.		5. TYPE OF REPORT & PERIOD COVERED 2/15/82 - 3/31/85 6. PERFORMING ORG. REPORT NUMBER
7. AUTHOR(s) N. Holonyak, Jr., G. E. Stillman, K. Hess, J. J. Coleman		8. CONTRACT OR GRANT NUMBER(s) DAA G29-82-K-0059
9. PERFORMING ORGANIZATION NAME AND ADDRESS Department of Electrical Engineering University of Illinois Urbana, IL 61801		10. PROGRAM ELEMENT, PROJECT, TASK AREA & WORK UNIT NUMBERS
11. CONTROLLING OFFICE NAME AND ADDRESS U. S. Army Research Office Post Office Box 12211 Research Triangle Park, NC 27709		12. REPORT DATE March 1985 13. NUMBER OF PAGES
14. MONITORING AGENCY NAME & ADDRESS (if different from Controlling Office)		15. SECURITY CLASS. (of this report) Unclassified 15a. DECLASSIFICATION/DOWNGRADING SCHEDULE NA

16. DISTRIBUTION STATEMENT (of this Report)

Approved for public release; distribution unlimited.

17. DISTRIBUTION STATEMENT (of the abstract entered in Block 20, if different from Report)

NA

18. SUPPLEMENTARY NOTES

The view, opinions, and/or findings contained in this report are those of the author(s) and should not be construed as an official Department of the Army position, policy, or decision, unless so designated by other documentation.

19. KEY WORDS (Continue on reverse side if necessary and identify by block number)

Heterostructure, Submicron Structures, Semiconductor Laser, Heterojunction Transport

Sub x subl - x

20. ABSTRACT (Continue on reverse side if necessary and identify by block number)

The III-V materials GaAs, $Al_xGa_{1-x}As$, AlAs offer important advantages that make possible the fabrication of a large range of sophisticated heterostructure devices. The devices that have concerned us most are: quantum-well heterostructure lasers, heterostructure phototransistors, real-space transfer devices and high electron mobility transistors. In this report we describe extensive studies of the optical and electrical properties of these devices as well as the physical properties of semiconductor heterolayer structures. → See p 4

DD FORM 1 JAN 73 1473 EDITION OF 1 NOV 65 IS OBSOLETE

UNCLASSIFIED
SECURITY CLASSIFICATION OF THIS PAGE (When Data Entered)

During the period of this contract, 53 manuscripts (abstracts, reprints and preprints attached) were published or accepted for publication. 9 manuscripts have been published or submitted for publication in the last period of this contract (July 1, 1984 - February 15, 1985). Since the manuscripts are attached, only a short description of the major scientific progress is given here.

1. Progress in Quantum Well Laser Operation:

(a) Low-Threshold High-Power Lasers

One of the major accomplishments of our quantum well laser research was achieved by experimental and theoretical investigations that led to the development of low threshold, high power quantum well lasers. We have demonstrated (with Burnham of Xerox) threshold currents below 100A/cm^2 and cw operation in the visible at appreciable power levels (>10mW). This represents major improvement over conventional structures. Details can be found in manuscripts 10, 11, 19, and 22.

(b) Pattern Generation by Impurity Diffusion and Ion-Implantation into Superlattices

We have shown that superlattices can be selectively converted via impurity-induced disordering (accepted or donor) into bulk-crystal alloys with significantly different dielectric properties.

It is thought by many groups in the U.S. and Japan that these processes may form an important basis for future optoelectronic integrated circuits (manuscripts 34-36 and 50).

(c) Wavelength Modification of Quantum Well Lasers

Methods of wavelength modification and broadband tuning have been established (manuscripts 23, 37, and 38).

2. Strained Layer Superlattices

We have shown that high quality strained heterolayer structures can be produced which support a quasi-two-dimensional electron gas, display resonant tunneling effects, and even show stimulated emission. Although this demonstrates clearly that the interface defect density of the as-grown crystal is low enough for many device applications, drastic degradation effects have been observed in cw laser operation and also in FET operation of strained layer structures. Details can be found in manuscripts 6-9 and 18.

3. Electronic properties and Device Applications

We have continued to pursue the concept of real space transfer and have demonstrated its high potential for device applications.

We have also developed the first two-dimensional model of the high electron mobility transistor. This model is capable of simulating size quantization and velocity overshoot effects and the ultimate switching speed of these devices (manuscripts 27-29, 41, 42, 51 and 52).

4. Physics of Optoelectronics in Quantum Well Structures

A wide variety of important physical effects in heterolayers has been explored. We have performed detailed investigations of the dynamics of electron-hole collection in quantum wells (manuscript 1), the influence of high pressure on the optical properties of superlattices (manuscripts 3, 5, 7,

and 48) and magneto-transport (manuscript 25) in low threshold quantum well lasers. This research has resulted in a better understanding of material constants such as deformation potential constants and the electron-phonon interaction in these structures.

5. Construction of an MOCVD Reactor

A reactor for metalorganic chemical vapor deposition of GaAs-AlGaAs epilaxial layers has been designed and completed. The system is computer controlled and is capable of growing high uniformity superstructures with excellent control of interface abruptness on the scale of monatomic layers (manuscript 43, 44, and 53).

6. Activities in the Present Reporting Period (#6)

In the present reporting period 9 papers (manuscripts 45-53) have been published or accepted for publication. Emphasis ~~has been~~ was placed on superlattice disordering and pattern generation by silicon diffusion; stripe- geometry and buried-heterostructure lasers have been realized by this method (i.e., impurity-induced disordering). Tunable laser operation in external gratings as well as under hydrostatic pressure has been accomplished with quantum-well heterostructures. This has resulted, for the first time, in tunable semiconductor laser operation over a 100meV range (and not the previous limit of $\Delta\hbar\omega \lesssim 40$meV). The theory of the dielectric constant of superlattices has also been considerably refined. Two manuscripts have been devoted to the two-dimensional modeling of the high mobility transistor and one manuscript discusses the interface quality of our MOCVD-grown superlattices.

Additional keywords: Submicron Structures; heterojunction transport.

7. Scientific Personnel:

N. Holonyak, Jr., Co-Principal Investigator

G. E. Stillman, Co-Principal Investigator

K. Hess, Co-Principal Investigator

J. J. Coleman, Co-Principal Investigator

P. Garvilovic, Ph.D. Degree Student

B. J. Skromme, Ph.D. Degree Student, Ph.D. completed 1984

K. Meehan, Ph.D. Degree Student

D. S. Ruby, Ph.D. Degree Student (no change)

N. Tabatabaie, Ph.D. Degree Student (no change), Ph.D. completed 1984

M. Artaki, Ph.D. Degree Student

G. Costrini, Ph.D. Degree Student

M. Camras, Ph.D. Degree Student, Ph.D. completed 1984

L. Mawst, Masters Degree Student

D. Widiger, Ph.D. Degree Student, IBM Fellow, Ph.D. completed 1984

8. List of Publications:

1. J. Y. Tang, K. Hess, N. Holonyak, Jr., J. J. Coleman, and P. D. Dapkus. 'The dynamics of electron-hole collection in quantum well heterostructures. J. Appl. Phys. 53, 6043-6046 (Sept. 1982).

2. M. D. Camras, N. Holonyak, Jr., K. Hess, J. J. Coleman, R. D. Burnham, and D. R. Scifres. High energy $Al_xGa_{1-x}As(0\leq x\leq 0.1)$ quantum-well heterostructure laser operation. Appl. Phys. Lett. 41, 317-319 (Aug. 15, 1982).

3. S. W. Kirchoefer, K. Meehan, N. Holonyak, Kr., D. A. Gulino, H. G. Drickamer, R. D. Burnham, and D. R. Scifres. High pressure measurements on visible spectrum $Al_xGa_{1-x}As$ heterostructure lasers: 7100-6750-Å 300-K operation. Appl. Phys. Lett. 41, 406-407 (Sept. 1, 1982).

4. N. Holonyak, Jr. Quantum-well and superlattice lasers: fundamental effects. from: The Physics of Submicron Structures, Edited by H. L. Grubin, K. Hess, G. J. Iafrate, and D. K. Ferry (Plenum Publishing Corp., 1984).

5. S. E. Kirchoefer, N. Holonyak, Jr., K. Hess, K. Meehan, D. A. Gulino, H. G. Drickamer, J. J. Coleman, and P. D. Dapkus. High pressure measurements on $Al_xGa_{1-x}As$-GaAs(x=0.5 and 1) superlattices and quantum-well heterostructure lasers. J. Appl. Phys. 53, 6037-6042 (Sept. 1982).

6 M. J. Ludowise, W. T. Dietze, C. R. Lewis, N. Holonyak, Jr., K. Hess, M. D. Camras, and M. A. Nixon. Stimulated emission in strained $GaAs_{1-x}P_x$-$GaAs_{1-y}P_y$ superlattices. Appl. Phys. Lett. 42, 257-259 (Feb. 1, 1983).

7. P. Gavrilovic, K. Meehan, N. Holonyak, Jr., K. Hess, W. P. Zurawsky, H. G. Drickamer, M. J. Ludowise, W. T. Dietze, and C. R. Lewis. Absorption measurements at high pressure (0-10 kbar) on strained superlattices. Solid State Communications, 45:9, 803-806 (1983).

8. M. D. Camras, N. Holonyak, Jr., K. Hess, M. J. Ludowise, W. T. Dietze, and C. R. Lewis. Impurity induced disordering of strained GaP-$GaAs_{1-x}P_x$(x~0.6) superlattices. Appl. Phys. Lett. 42, 185-187 (Jan. 15, 1983).

9. M. J. Ludowise, W. T. Dietze, C. R. Lewis, M. D. Camras, N. Holonyak, Jr., B. K. Fuller, and M. A. Nixon. Continuous 300-K laser operation of strained superlattices. Appl. Phys. Lett. 42, 487-489 (Mar. 15, 1983).

10. R. D. Burnham, W. Streifer, D. R. Scifres, N. Holonyak, Jr., K. Hess, and M. D. Camras. Low threshold photopumped $Al_xGa_{1-x}As$ quantum-well heterostructure lasers. J. Appl. Phys. 54, 2618-2622 (May 1983).

11. R. D. Burnham, W. Streifer, D. R. Scifres, C. Lindstrom, T. L. Paoli, and N. Holonyak. Low-threshold single quantum well (60 Å) GaAlAs lasers grown by MO-CVD with Mg as p-type dopant. Electronics Lett. 18:25/26, 1095-1097 (Dec. 9, 1982).

12. M. D. Camras, J. J. Coleman, N. Holonyak, Jr., K. Hess, P. D. Dapkus, and C. G. Kirkpatrick. Disorder of AlAs/GaAs superlattices by the implantation and diffusion of impurities. Inst. Phys. Conf. Ser. 65 233-239 (1982).

13. J. P. Leburton and K. Hess. A simple model for the index of refraction of GaAs-AlAs superlattices and heterostructure layers: contributions of the states around Γ. J. Vac. Sci. Technol. B. 1, 415 (1983).

14. K. Hess. Electronic transport in GaAs-GaAlAs heterolayers and high mobility transistors. Philadelphia Meeting of the American Physical Society. (Nov. 3-5, 1982) to be published.

15. T. C. Hsieh, K. Hess, J. J. Coleman, and P. D. Dapkus. Carrier Density distribution in modulation doped GaAs-$Al_xGa_{1-x}As$ quantum well heterostructures. Solid-State Electronics 26, 1173-1176 (1983).

16. N. Holonyak, Jr. and K. Hess. Quantum-well heterostructure lasers. Synthetic Modulated Materials, edited by L. L. Chang and B. C. Giessen (New York: Academic Press, 1983).

17. J. M. Brown, N. Holonyak, Jr., M. J. Ludowise, W. T. Dietze, and C. R. Lewis. Direct observation of lattice distortion in a strained-layer superlattice. Appl. Phys. Lett. 43, 863-865 (Nov. 1, 1983).

18. J. M. Brown, M. E. Mochel, N. Holonyak, Jr., M. D. Camras, M. J. Ludowise, W. T. Dietze, and C. R. Lewis. Defect studies in strained-layer quantum well heterostructures. Proc. of the 41st Annual Meeting of the Electron Microscopy Society of America, 120-121 (1983).

19. M. D. Camras, N. Holonyak, Jr., M. A. Nixon, R. D. Burnham, W. Streifer, D. R. Scifres, T. L. Paoli, and C. Lindstrom. Photopumped low threshold $Al_{x'}Ga_{1-x'}As$-$Al_xGa_{1-x}As$-$Al_{x'}Ga_{1-x'}As$-$Al_xGa_{1-x}As$ ($x' \sim 0.85$, $x' \sim 0.3$, $x=0$) single quantum well lasers. Appl. Phys. Lett. 42, 761-763 (May 1, 1983).

20. R. D. Burnham, C. Lindstrom, T. L. Paoli, D. R. Scifres, W. Streifer, and N. Holonyak, Jr. 100 mW CW room temperature, 6μm shallow proton stripe GaAlAs single quantum well visible diode lasers. ECS Meeting (May 1983, San Francisco) to be published.

21. R. D. Burnham, C. Lindstrom, T. L. Paoli, D. R. Scifres, W. Streifer, and N. Holonyak, Jr. cw room-temperature operation of GaAlAs single quantum well visible (7300 Å) diode lasers at 100 mW. Appl. Phys. Lett. 42, 937-939 (June 1, 1983).

22. M. D. Camras, N. Holonyak, Jr., J. J. Coleman, H. G. Drickamer, R. D. Burnham, W. Streifer, K. R. Scifres, C. Lindstrom, and T. P. Paoli. High pressure measurements on photopumped low threshold $Al_xGa_{1-x}As$ quantum well lasers. J. Appl. Phys. 54, 4386-4389 (Aug. 1983).

23. M. D. Camras, N. Holonyak, Jr., R. D. Burnham, W. Streifer, D. R. Scifres, T. L. Paoli, and C. Lindstrom. Wavelength modification of $Al_xGa_{1-x}As$ quantum well heterostructure lasers by layer interdiffusion. J. Appl. Phys. 54, 5637-5641 (Oct. 1983).

24. J. P. Leburton, K. Hess, N. Holonyak, Jr., J. J. Coleman, and M. Camras. Index of refraction of AlAs-GaAs superlattices. J. Appl. Phys. 54, 4230-4231 (July 1983).

25. P. Gavrilovic, K. Hess, N. Holonyak, Jr., R. D. Burnham, T. L. Paoli, and W. Streifer. Quantum well laser operation at low temperature in strong magnetic fields. Solid State Communications, 48:8, 671-673 (1983).

26. P. A. Martin, K. Meehan, P. Gavrilovic, K. Hess, N. Holonyak, Jr., and J. J. Coleman. Transient cpacitance spectroscopy on large quantum well heterostructures. J. Appl. Phys. 54, 4689-4691 (Aug. 1983).

27. K. Hess. Superlattices. Proc. NATO Summer School (St. Miniato, Italy, 1983) to be published.

28. K. Hess. Principles of hot electron thermionic emission (real space transfer) in semiconductor heterolayers and device applications. MITI Workshop on Future Electron Devices (Tokyo, Feb. 1984) to be published.

29. K. Hess, G. J. Iafrate. Hot electrons in semiconductor heterostructures and superlattices. Book chapter, Springer (1985), L. Reggiani, editor, to be published.

30. M. D. Camras, J. M. Brown, N. Holonyak, Jr., M. A. Nixon, R. W. Kaliski, M. J. Ludowise, W. T. Dietze, and C. R. Lewis. Stimulated emission in strained-layer quantum-well heterostructures. J. Appl. Phys. 54, 6183-6189 (Nov. 1983).

31. J. E. Epler, N. Holonyak, Jr., R. D. Burnham, C. Lindstrom, W. Streifer, and T. L. Paoli. broadband tuning (ΔE~100 meV) of $Al_xGa_{1-x}As$ quantum well heterostructure lasers with an external grating. Appl. Phys. Lett. 43, 740-742 (Oct. 15, 1983).

32. K. Meehan, N. Holonyak, Jr., R. D. Burnham, T. L. Paoli, and W. Streifer. Wavelength modification ($\Delta h\omega$ = 10-40 meV) of room temperature continuous quantum-well heterostructure laser diodes by thermal annealing. J. Appl. Phys. 54, 7190-7191 (Dec. 1983).

33. K. Meehan, J. M. Brown, P. Gavrilovic, N. Holonyak, Jr., R. D. Burnham, T. L. Paoli, and W. Streifer. Thermal-anneal wavelength modification of multiple-well p-n $Al_xGa_{1-x}As$-GaAs quantum-well lasers. J. Appl. Phys. 55, 2672-2675 (Apr. 1984).

34. K. Meehan, J. M. Brown, M. D. Camras, N. Holonyak, Jr., R. D. Burnham, T. L. Paoli, and W. Streifer. Impurity-induced disordering of single well $Al_xGa_{1-x}As$-GaAs quantum well heterostructures. Appl. Phys. Lett. 44, 428-430 (Feb. 15, 1984).

35. K. Meehan, J. M. Brown, N. Holonyak, Jr., R. D. Burnham, T. L. Paoli, and W. Streifer. Stripe-geometry AlGaAs-GaAs quantum-well heterostructure lasers defined by impurity-induced layer disordering. Appl. Phys. Lett. 44, 700-702 (Apr. 1, 1984).

36. K. Meehan, N. Holonyak, Jr., J. M. Brown, M. A. Nixon, P. Gavrilovic, and R. D. Burnham. Disorder of an $Al_xGa_{1-x}As$-GaAs superlattice by donor diffusion. Appl. Phys. Lett. 45, 549-551 (Sept. 1, 1984).

37. J. E. Epler, N. Holonyak, Jr., J. M. Brown, R. D. Burnham, W. Streifer, and T. L Paoli. High-energy (λ7300Å) 300 K operation of single- and multiple-stripe quantum-well heterostructure laser diodes in an external grating cavity. J. Appl. Phys. 56, 670-675 (Aug. 1, 1984).

38. J. E. Epler, N. Holonyak, Jr., R. D. Burnham, T. L. Paoli, and W. Streifer. Far-field supermode patterns of a multiple-stripe quantum well heterostructure laser operated (~7300 Å, 300 K) in an external grating cavity. Appl. Phys. Lett. 45, 406-408 (Aug. 15, 1984).

39. J. M. Brown, N. Holonyak, Jr., R. W. Kaliski, M. J. Ludowise, W. T. Dietze, and C. R. Lewis. Effect of layer size on lattice distortion in strained-layer superlattices. Appl. Phys. Lett. 44, 1158-1160 (June 15, 1984).

40. R. D. Burnham, W. Streifer, T. L. Paoli, and N. Holonyak, Jr. Growth and characterization of AlGaAs/GaAs quantum wll lasers. J. of Crystal Growth 68, 370-382 (North-Holland, Amsterdam, 1984).

41. D. Widiger, K. Hess, and J. J. Coleman. Two-dimensional numerical analysis of the high electron mobility transistor. IEEE-EDL-5, 266 (1984).

42. D. Widiger, I. C. Kizilyalli, K. Hess, and J. J. Coleman. Two-dimensional transient simulation of the high electron mobility transistor. Proc. of the IEDM, (San Francisco, 1984) to appear.

43. S. J. Jeng, C. M. Wayman, G. Costrini, and J. J. Coleman. Interface structure of GaAs/AlAs semiconductor superlattices prepared by MOCVD. Materials Lett. 2:5A, 359-361 (June 1984).

44. G. Costrini and J. J. Coleman. Conditions for Uniform Growth of GaAs by Metalorganic Chemical Vapor Deposition in a Vertical Reactor. J. Appl. Phys. submitted.

45. K. Meehan, P. Gavrilovic, N. Holonyak, Jr., R. D. Burnham, and R. L. Thornton. Stripe-geometry $Al_xGa_{1-x}As$-GaAs quantum well heterostructure lasers defined by Si diffusion and disordering. Appl. Phys. Lett. 46,

75-77 (Jan. 1, 1985).

46. K. Meehan, P. Gavrilovic, J. E. Epler, K. C. Hsieh, and N. Holonyak, Jr. Donor-induced disorder-defined buried-heterostructure $Al_xGa_{1-x}As$-GaAs quantum well lasers. J. Appl. Phys. 57, to appear.

47. J. E. Epler, N. Holonyak, Jr., R. D. Burnham, T. L. Paoli, and W. Streifer. Supermodes of multiple-stripe quantum well heterostructure laser diodes oOperated (cw, 300 K) in an external grating cavity. J. Appl. Phys. 57, (Jan. 1, 1985).

48. R. W. Kaliski, J. E. Epler, N. Holonyak, Jr., M. J. Peanasky, G. A. Herrmannsfeldt, H. G. Drickamer, M. J. Tsai, M. S. Camras, F. G. Kellert, C. H. Wu, and M. B. Craford. Pressure dependence of $Al_xGa_{1-x}As$ light emitting diodes near the direct-inderect transition. J. Appl. Phys. 57, to appear.

49. J. E. Epler, R. W. Kaliski, N. Holonyak, Jr., M. J. Peanasky, G. A. Herrmannsfeldt, H. G. Drickamer, R. D. Burnham, and R. L. Thornton. Hydorstatic pressure measurements (12 kbar) on single- and multiple-stripe quantum-well heterostructure laser diodes. J. Appl. Phys. 57, to appear.

50. K. B. Kahen, J. P. Leburton, and K. Hess. General model of the transverse dielectric constant of GaAs-AlAs superlattices. J. of Superlattices and Microstructures, Academic Press, to appear.

51. D. Widiger, I. C. Kizilyalli, K. Hess, and J. J. Coleman. Two-dimensional numerical analysis of the high electron mobility transistor. J. of Superlattices and Microstructures, Academic Press, to appear.

52. D. Widiger, I. C. Kizilyalli, K. Hess, and J. J. Coleman. Two-dimensional transient simulation of an idealized high electron mobility transistor. IEEE Trans. on ED, submitted.

53. S. J. Jeng, C. M. Wayman, J. J. Coleman, and G. Costrini. Interface characteristics of GaAs/$Al_xGa_{1-x}As$ superlattices grown by MOCVD. Materials Lett., submitted.

The dynamics of electron-hole collection in quantum well heterostructures

J. Y. Tang and K. Hess
Department of Electrical Engineering and Coordinated Science Laboratory, University of Illinois, Urbana, Illinois 61801

N. Holonyak, Jr. and J. J. Coleman
Electrical Engineering Research Laboratory and Materials Research Laboratory, University of Illinois, Urbana, Illinois 61801

P. D. Dapkus
Microelectronics Research and Development Center, Rockwell International, Thousand Oaks, California 91360

(Received 26 March 1982; accepted for publication 13 May 1982)

The dynamics of carrier collection in quantum-well heterostructures are studied by photoemission experiments and Monte Carlo simulations. It is shown that carrier scattering decreases rapidly for well sizes $L_z \lesssim 100$ Å. The collection mechanism depends sensitively on details of the band structure. The energy distribution function of the carriers after collection exhibits significant structure with respect to multiples of the phonon energy. This feature is also reflected by the experimental results.

PACS numbers: 42.55.Px, 71.38. + i, 78.55.Ds, 63.20.Kr

I. INTRODUCTION

If excess carriers are photogenerated or injected in the confining layers of a single quantum-well heterostructure within a diffusion length of the narrower gap active region, the carriers will diffuse to the quantum well, be collected and recombine in the well (GaAs) if it is large enough.[1] The process of excess carrier collection by single and multiple quantum-well heterostructures (QWH) has been studied experimentally and theoretically[2] by means of Fermi's age theory. The main goal of this theory has been to explain the experimentally observed cutoff of confined-particle recombination for single-well sizes $L_z \lesssim 80$ Å.

It is the purpose of this paper to present a more refined theory of the dynamics of carrier collection in quantum wells, which includes details of the band structure and the electron-phonon interaction, and to compare this theory with experimental results. We use a Monte Carlo simulation of the electrons percolating down in energy in a QWH by phonon emission. This simulation gives a detailed account of the history of the electrons in the Γ, X, and L valleys and shows that the cutoff features for confined-particle recombination depend sensitively on the valley type in which the electron resides when approaching and traversing the quantum well. The transient energy distribution reflects also characteristic structure with respect to the phonon energy which can be related to similar structure in the QWH laser spectrum. The theory is not complete, however, since effects of size quantization are not included in the simulation. The effects of a subband structure become increasingly important at low energy, i.e., when the electron has cascaded down a substantial fraction of the QW. At higher energies, however, size quantization plays a minor role, because of the small deBroglie wavelength, and we have to account only for the quantum mechanical transmission probability from the wider-gap confining layers to the GaAs well. Therefore, our numerical model is three dimensional with respect to the scattering and transport of electrons in the GaAs. We assume that the electrons transmitted into the GaAs stay in the valley type in which they started and simply gain kinetic energy in the amount of the band edge discontinuity ΔE_c. This assumption is supported by investigations of the quantum mechanical transmission coefficient by Osbourn and Smith.[3]

II. NUMERICAL RESULTS

The Monte Carlo program used for the computations is a revised version of that described in previous papers.[4] Without going into details of the Monte Carlo model, we would like to emphasize the importance of the inclusion of the realistic band structure in this problem because the electrons are injected into the GaAs with a significant amount of kinetic energy (ΔE_c). They are scattered initially high up in the GaAs conduction band where a simple effective mass approximation no longer holds. Therefore, the inclusion of the band structure is absolutely necessary. We use ~7000 mesh points and interpolations between these points. The E(k) relation is calculated by the empirical pseudopotential method. The band structure is not simulated too well by this model at very low energies (few points only), and the results at low energies are therefore estimated to be in error by ± 20%. Within the model assumptions, our formalism (which is equivalent to the semiclassical Boltzmann formalism) is valid in the considered range of energies and scattering rates even if very strict criteria are applied.

The percentage of electrons scattered according to this model at a certain distance in the GaAs is shown in Fig. 1. This percentage does not directly reflect the percentage of electrons captured in the quantum well because of possible multiple electron reflection at the well boundaries and the possibility of phonon absorption and electron re-emission. Phonon absorption contributes only a few percent to the results at room temperature and is entirely negligible at low temperatures.

The influence of multiple reflection is displayed by the

 0021-8979/82/096043-04$02.40

(2)

High energy $Al_xGa_{1-x}As$ ($0<x<0.1$) quantum-well heterostructure laser operation

M. D. Camras, N. Holonyak, Jr., K. Hess, and J. J. Coleman
Electrical Engineering Research Laboratory and Materials Research Laboratory, University of Illinois at Urbana–Champaign, Urbana, Illinois 61801

R. D. Burnham and D. R. Scifres
Xerox Palo Alto Research Center, Palo Alto, California 94304

(Received 17 May 1982; accepted for publication 28 May 1982)

Besides high pressure or bulk crystal composition change, a size-determined direct-indirect transition can be obtained in an $Al_xGa_{1-x}As$ ($0<x<0.1$) quantum-well heterostructure (QWH), in fact, at higher energy ($E\sim2.05$ eV) than in bulk $Al_xGa_{1-x}As$ (~1.98 eV). Laser operation is demonstrated at 6700–6500 Å on a QWH grown by metalorganic chemical vapor deposition (MOCVD).

PACS numbers: 42.55.Px, 71.50. + t, 78.65.Jd, 78.55.Ds

Previous work[1] indicates that if the GaAs active layers of a quantum-well heterostructure (QWH) in the AlAs-$Al_xGa_{1-x}As$-GaAs system are made small enough ($L_z \lesssim 30$ Å), then it should be possible to shift the recombination radiation and stimulated emission well into the visible. In fact, the possibility exists of using small GaAs well size (L_z), or small wells of $Al_xGa_{1-x}As$ of low composition ($x<0.1$), to shift the various confined-particle states of the Γ, L, and X valleys of the conduction band and Γ of the valence band to high enough energy to create a size-determined direct-indirect transition *exceeding* in energy the bulk crystal direct-indirect transition of $Al_xGa_{1-x}As$ ($x=x_c\simeq0.44$, $E_g\sim1.98$ eV). The physical reason for this behavior is that the "disorder bowing" of the band edge, i.e., nonlinear contributions of x in $E_g(x)$, can be avoided in a QWH or superlattice (SL). In this letter we examine this possibility and indicate to what extent the bulk crystal direct-indirect transition can be exceeded, in a QWH, by a size-determined direct-indirect transition ($\Delta E\sim2.05-1.98\sim0.07$ eV). Data (300 K) are presented on a 20-period $Al_xGa_{1-x}As$-GaAs QWH (a small superlattice, SL) grown by metalorganic chemical vapor deposition (MOCVD)[2–5] that are consistent with the conclusion that an $Al_xGa_{1-x}As$-GaAs (or $Al_{x'}Ga_{1-x'}As$-$Al_xGa_{1-x}As$, $x'>x$) QWH can exceed an

 0003-6951/82/040317-03$01.00

High pressure measurements on visible spectrum $Al_xGa_{1-x}As$ heterostructure lasers: 7100–6750-Å 300-K operation

S. W. Kirchoefer, K. Meehan, and N. Holonyak, Jr.
Electrical Engineering Research Laboratory and Materials Research Laboratory, University of Illinois at Urbana–Champaign, Urbana, Illinois 61801

D. A. Gulino and H. G. Drickamer
School of Chemical Sciences and Materials Research Laboratory, University of Illinois at Urbana–Champaign, Urbana, Illinois 61801

R. D. Burnham and D. R. Scifres
Xerox Palo Alto Research Center, Palo Alto, California 94304

(Received 29 April 1982; accepted for publication 2 June 1982)

Pressure applied to high performance cw 300-K bulk-limit ($L_z \sim 600$ Å) single quantum well heterostructure $Al_xGa_{1-x}As$ ($x \sim 0.28$, $\lambda \sim 7100$ Å) laser diodes is used to simulate composition change and determine the threshold increase at shorter wavelength. Unless small quantum well sizes are employed in more sophisticated designs it is unlikely that λ (for cw 300-K operation) can be made much less than 6900 Å.

PACS numbers: 71.25.Tn, 73.40.Lq, 62.50. + p, 78.60.Fi

In spite of the fact that the semiconductor laser was first demonstrated in the alloy $GaAs_{1-x}P_x$[1] as soon as in GaAs[2] and now is almost 20 years old, it still is not a commonly available visible spectrum device. It simply has been too difficult, even in the most advanced form of a lattice-matched heterostructure, to shift the operation from longer wavelength toward ~7000 Å and simultaneously maintain a low threshold current. Recently Burnham and coworkers[3,4] have shown that large ($L_z \sim 600$ Å) single quantum well heterostructure (QWH) $Al_xGa_{1-x}As$ lasers[5,6] grown by metalorganic chemical vapor deposition (MOCVD)[7–9] can be operated continuously at room temperature at significantly shorter wavelengths and lower thresholds than the double heterojunctions (DH) of previous work. Figure 2 of Ref. 3 shows recent MOCVD $Al_xGa_{1-x}As$ QWH laser thresholds, at various crystal compostions x, compared with the earlier results of others on DH's. The data of Refs. 3 (and 4) stop at $x \sim 0.28$ and $\lambda \sim 7100$ Å, and give little idea of how rapidly the threshold current density in the $Al_xGa_{1-x}As$ system would increase at still higher crystal composition (shorter wavelength), which can in fact be simulated with pressure. In other words, hydrostatic pressure applied to the high performance visible spectrum QWH lasers of Refs. 3 and 4 affords a unique means to probe the range (and limits) over which stimulated emission (300 K) can be achieved in the $Al_xGa_{1-x}As$ system.

Hydrostatic pressure measurements have been performed on these visible spectrum QWH laser diodes. The techniques used in these high pressure experiments are the same as those used previously for studies on other QWH laser diodes.[10,11] The diodes are placed in a high pressure cell[12] outfitted with a sapphire window and standard Bridgman electric seals. The cell is filled with a dielectric fluid consisting of 10% isooctane in methylcyclohexane. An intensifier (previously calibrated against a manganin gauge) is connected to the cell and used to apply pressure. This apparatus is operable to ~12 kbar.

The single quantum well heterostructure laser diodes tested here are grown by MOCVD as described in Refs. 3 and 4. Their structure consists of (1) GaAs:Se buffer layer ~0.3 μm thick, $N_d \sim 10^{18}$ cm^{-3}; (2) $Al_xGa_{1-x}As$:Se ~0.5 μm thick, $x \sim 0.25$, $N_d \sim 3\times10^{17}$ cm^{-3}; (3) $Al_xGa_{1-x}As$:Se ~3 μm thick, $x > 0.6$, $N_d \sim 3\times10^{17}$ cm^{-3}; (4) $Al_xGa_{1-x}As$ (undoped) active layer ~600 Å thick, $0 < x < 0.28$, $N_d \sim 3\times10^{16}$ cm^{-3}; (5) $Al_xGa_{1-x}As$:Zn ~2.75 μm thick, $x > 0.6$, $N_a \sim 3\times10^{17}$ cm^{-3}; (6) $Al_xGa_{1-x}As$:Zn ~0.25 μm thick, $x \sim 0.25$, $N_a \sim 10^{18}$ cm^{-3}; and (7) GaAs:Zn contact layer ~0.5 μm thick, $N_a \sim 5\times10^{19}$ cm^{-3}. These diodes are fabricated in a stripe geometry configuration and are metallized with Au/Ge on the n side and Cr/Au on the p side. Although cw 300-K laser operation is possible with these devices,[4] pulsed operation is used to avoid confusion of the data by heating effects. The diodes are pulsed as near to threshold as possible to avoid band filling.

The change in the photon energy of the peak lasing intensity with pressure is shown in Fig. 1. The data points are fitted by the least-squares method, and a pressure coefficient of ~8.2 meV/bar is measured. This result for the pressure

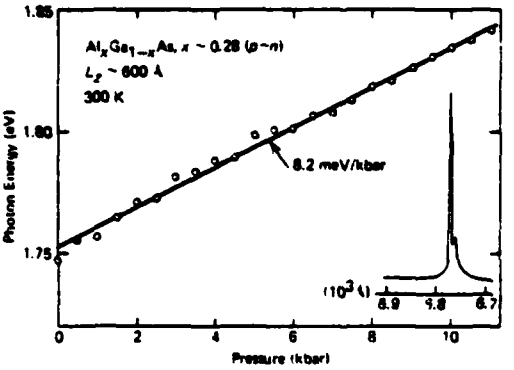

FIG. 1. Peak laser energy vs pressure for a bulk-limit ($L_z \sim 600$ Å) single quantum well laser diode operated under hydrostatic pressure. The inset is the room-temperature pulsed spectrum of the diode at a pressure of 10 kbar. The diode exhibits a linear energy vs pressure dependence of ~8.2 meV/kbar over the entire range 0–11 kbar (7100–6750 Å).

 0003-6951/82/050406-02$01.00

(4)

From: THE PHYSICS OF SUBMICRON STRUCTURES
Edited by H.L. Grubin, K. Hess, G.J. Iafrate,
D.K. Ferry
(Plenum Publishing Corporation, 1984)

QUANTUM-WELL AND SUPERLATTICE LASERS: FUNDAMENTAL EFFECTS

N. Holonyak, Jr.

Electrical Engineering Research Laboratory and
Materials Research Laboratory
University of Illinois at Urbana-Champaign
Urbana, Illinois 61801

ABSTRACT

Besides the improvements that can be effected in laser design and operation by the use of a quantum-well (QW) or superlattice (SL) configuration, various fundamental effects also can be observed. Some of these are: 1) electron-hole asymmetry (mass and velocity and its use to measure band-edge discontinuities, 2) identification of phonon-sideband laser operation, 3) alloy clustering and reduction of "band-to-band" (e+h) recombination energies, 4) impurity-induced layer disordering, 5) high pressure measurements that permit observation of the behavior (pressure coefficients) of the "inside" of an energy band, and 6) a quantum-well or size-induced "direct-indirect" transition (in the AlAs-AlGaAs-GaAs system) higher in energy than the bulk value of the disordered alloy.

INTRODUCTION

In the usual double heterojunction (DH) laser the narrow gap active region is greater in thickness than $\sim$ 500 Å and, as a consequence, bulk-crystal properties are observed. If the active layer thickness, L_z, is in the range $L_z \lesssim$ 500 Å, i.e., $\lambda \sim h/p \sim L_z$, confined-particle or quantum size effects are manifest. Apart from the fact that improvements can be effected in laser design and operation[1-3] by resorting to a quantum-well (QW) or superlattice (SL) configuration, various fundamental effects also can be observed. Some of these, including the electron-hole asymmetry and the peculiarities of carrier collection, phonon generation, alloy clustering, layer disorder, high pressure effects, and size-induced direct-indirect transition, are described below.

High pressure measurements on $Al_xGa_{1-x}As$-GaAs ($x = 0.5$ and 1) superlattices and quantum-well heterostructure lasers

S. W. Kirchoefer, N. Holonyak, Jr., K. Hess, and K. Meehan
Electrical Engineering Research Laboratory and Materials Research Laboratory, University of Illinois at Urbana-Champaign, Urbana, Illinois 61801

D. A. Gulino and H. G. Drickamer
School of Chemical Sciences and Materials Research Laboratory, University of Illinois at Urbana-Champaign, Urbana, Illinois 61801

J. J. Coleman[a] and P. D. Dapkus
Rockwell International, Electronics Research Center, Anaheim, California 92803

(Received 18 March 1982; accepted for publication 13 May 1982)

Absorption data on AlAs-GaAs and $Al_xGa_{1-x}As$-GaAs superlattices (SL's) and emission data on $Al_xGa_{1-x}As$-GaAs quantum-well heterostructure (QWH) laser diodes subjected to hydrostatic pressure (0–10 kbar) at 300 K are presented. Superlattice absorption data show that the confined-particle transitions, which partition and "label" the Γ energy band high above the band edge, *all move* with the same pressure coefficient of 11.5 meV/kbar. (For bulk GaAs, the pressure coefficient is 12.5 meV/kbar.) The effect of the L indirect minima on the highest observed confined-particle transitions is small; the effect of the X minima is large. At lower pressures, QWH diodes exhibit a pressure dependence similar to that of the free (unconstrained) SL's. The data on QWH diodes demonstrate, however, a size-dependent [L_z(GaAs) < 500 Å] shift in slope to a lower (8.5 meV/kbar) energy gap versus pressure coefficient at higher pressures. This change in slope can be explained by considering the effect on the light- and heavy-hole subbands of shear stresses generated within the p-n diode heterostructure.

PACS numbers: 42.55.Px, 62.50. + p, 71.25.Tn, 73.60.Fw

I. INTRODUCTION

The effects of hydrostatic pressure on the band structure of semiconductors have long formed the basis for the measurement of important physical parameters in these materials. In particular, the pressure dependence of the conduction band minima in GaAs, and to a lesser extent in $Al_xGa_{1-x}As$, has been characterized and is known to be linear for "low" pressures (i.e., $p < 100$ kbar). Recent experiments on quantum-well heterostructures (QWH's) grown by metalorganic chemical vapor deposition (MO-CVD), however, have shown departures from GaAs-like pressure dependence for $p < 10$ kbar in both doped samples operated as p-n junction laser diodes[1] and in undoped superlattices used as absorption samples.[2] These results suggest that effects associated with the presence of heterointerfaces and thin layers, and bulk p-layer n-layer mismatch (diodes), in these materials are responsible for their anomalous hydrostatic pressure behavior.

It is important to recognize that most heterostructure materials do not experience true hydrostatic pressure effects. Since the layers of such structures are composed of dissimilar materials with differing bulk compressibilities, externally applied hydrostatic pressure might be expected to induce shear stresses at the interfaces, thus producing a nonhydrostatic condition. In order to conform actually to a hydrostatic environment, a sample must be homogeneous, a bulk sample, and be free of any stress-inducing mechanical connections. Any type of a heterostructure or p-n junction violates these assumptions to some degree, and so one might expect to see effects associated with directional stresses in such materials subjected to hydrostatic pressure.

It has been observed recently that QWH's are excellent detectors of the presence of such directional stresses. This is in fact due to the breaking of the Γ degeneracy of light- and heavy-hole subbands (at zero pressure) in QWH's. Relative movement between light- and heavy-hole subbands in a QWH can be more easily detected because of their built-in separation. Since movement of the light holes relative to the heavy holes is known to be associated with uniaxial stress in the [100] direction in GaAs,[3,4] observations of such an effect indicate the presence of some form of directional stress in the crystal. This property of heterostructures under pressure is used here to examine a number of $Al_xGa_{1-x}As$-GaAs p-n junction laser diodes. For reference and comparison, several AlAs-GaAs and $Al_xGa_{1-x}As$-GaAs superlattice platelets, unconstrained samples that are free of p and n bulk "contact" layers, are examined in absorption.

II. SAMPLE PREPARATION

Superlattice (SL) crystals composed of alternating layers of AlAs-GaAs and $Al_xGa_{1-x}As$-GaAs ($x \sim 0.5$), and with various layer sizes L_z and L_B, have been grown by MO-CVD.[5] Experimental samples cleaved from these SL crystals are of excellent quality, operating as 300 K cw lasers in platelet form.[6] The samples are prepared for absorption measurements (and photopumped laser experiments) by first removing the GaAs substrate by mechanical polishing and selective etching. The resulting thin platelets are attached to a sapphire sample holder with silicone grease. The holder is

[a] Now at the University of Illinois.

 0021-8979/82/096037-06$02.40

Stimulated emission in strained $GaAs_{1-x}P_x$-$GaAs_{1-y}P_y$ superlattices

M. J. Ludowise, W. T. Dietze, and C. R. Lewis
Corporate Solid State Laboratory, Varian Associates, Incorporated, Palo Alto, California 94303

N. Holonyak, Jr., K. Hess, M. D. Camras, and M. A. Nixon
Electrical Engineering Research Laboratory and Materials Research Laboratory University of Illinois at Urbana-Champaign, Urbana, Illinois 61801

(Received 3 September 1982; accepted for publication 3 November 1982)

Photoluminescence data are presented on a direct-well $GaAs_{1-x}P_x$-GaAs ($x \sim 0.25$) strained superlattice (SL) (barrier $L_B \sim 75$ Å, quantum well $L_z \sim 75$ Å) and on indirect-well GaP-$GaAs_{1-x}P_x$ ($x \sim 0.6$) strained SL's ($L_B, L_z \sim 120$ Å and $L_B, L_z \sim 60$ Å) grown by organometallic vapor phase epitaxy. Stimulated emission (at 300 and at 77 K) is observed in the former but only weak luminescence in the latter, thus establishing that a large density of defects at the heterointerfaces is not necessarily an issue in strained SL's and that so far zone-folding effects, and SL "indirect-direct" conversion, have not been observed in indirect systems.

PACS numbers: 42.55.Px, 68.48. + f, 78.20. − e, 68.55. + b

Although a good deal of flexibility exists in the III-V family of semiconductors which permits formation of a wide range of lattice-matched heterostructures, there is, nevertheless, the practical constraint of limited availability of high quality binary substrates at desired lattice sizes. Thus, lattice matching is not always practical, and it would be of considerable value if strained-layer heterostructures, with limited interface defects and a high degree of stability, could be grown. A specific case is that of $GaAs_{1-x}P_x$ grown on GaAs or on GaP, which, in the usual thick-layer heterostructure, results in a large defect density at the heterointerfaces.[1-3] If the layers are thin enough, however, as in a strained-layer superlattice (SL), the layers deform elastically, and presumably the interface defect density can be kept low. This cannot easily be concluded, however, from the GaP-$GaAs_{1-x}P_x$ strained SL's recently described[4,5] in which the quantum wells are indirect-gap $GaAs_{1-x}P_x$ [$x > x_c(77) \approx 0.46$].[6] That is, unless a high level of luminescence is measured, it is not obvious whether a "quantum-well" indirect-gap crystal has failed to act direct (a zone-folding effect) or whether the heterointerface defect density is large. (We return to this point later.) Accordingly, a better demonstration of the freedom of a strained-SL heterointerface from defects would be to consider such a structure with direct-gap quantum wells, and observe on it unambiguously a high level of luminescence. In this letter we demonstrate stimulated emission, and thus a low heterointerface defect density, on photopumped $GaAs_{1-x}P_x$-GaAs ($x \sim 0.25$) strained SL's with 66 periods or 132 heterointerfaces.

The strained $GaAs_{1-x}P_x$-GaAs SL's of interest here have been grown by the organometallic vapor phase epitaxial (OMVPE) process reported on elsewhere.[7] The SL's themselves resemble the $Al_xGa_{1-x}As$-GaAs or AlAs-GaAs SL's described earlier grown by metalorganic chemical vapor deposition (MOCVD).[8,9] A typical shallow angle cross section of the $GaAs_{1-x}P_x$-GaAs strained SL's of interest here is shown in Fig. 1. Note that the vertical striations are polishing scratches. Out of view at the bottom is a GaAs substrate and then a $GaAs_{1-y}P_y$ layer graded from $y = 0$ to $y \approx 0.125$, the averge composition of the SL. The strained SL begins at the upward arrow and extends 1 μm to the top arrow with 66 $GaAs_{1-x}P_x$ ($x \sim 0.25$) layers of thickness $L_B \sim 75$ Å alternating with 66 GaAs quantum wells also of thickness $L_z \sim 75$ Å. Above the top arrow is the crystal surface and some noticeable, as well as typical, cross-hatch characteristic of $GaAs_{1-x}P_x$ grown on GaAs.

For the photopumping experiments of interest here, the GaAs substrate is polished and etched off as much as is possible. Small wafers polished to thin dimensions (~ 25 μm) and then etched (no stop layer) to a thickness of 2 μm or less tend to have feathered edges that are free of substrate. It is from this region that samples are cleaved and are heat sunk under diamond in annealed copper. The samples are photopumped with a cavity dumped Ar^+ laser (5145 Å).

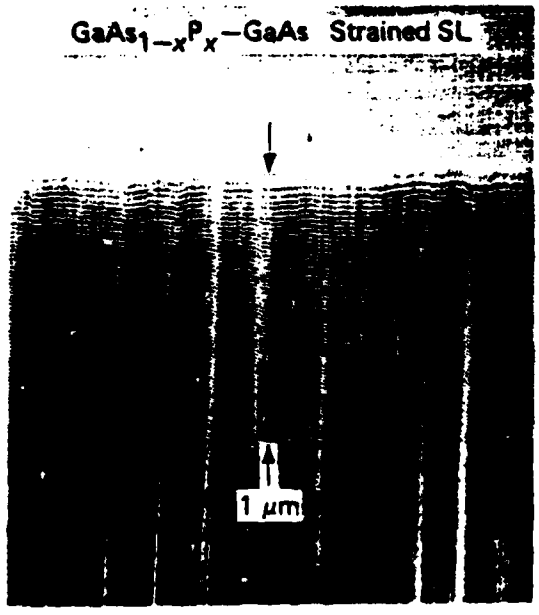

FIG. 1. Shallow-angle ($< 0.5°$) cross section of a 66-period strained SL consisting of $L_z \sim 75$-Å GaAs quantum wells coupled by $L_B \sim 75$-Å $GaAs_{1-x}P_x$ ($x \sim 0.25$) barriers. The upper arrow indicates the "corner" with the lightly cross-hatched wafer surface. The ~ 1-μm SL is shown between the arrows. Beneath the lower arrow is a graded region of $GaAs_{1-y}P_y$ ($0.125 > y > 0$) grown on a GaAs substrate. The vertical striations are polishing scratches.

 0003-6951/83/030257-03$01.00

Solid State Communications, Vol.45,No.9, pp.803-806, 1983.
Printed in Great Britain.

0038-1098/83/090803-04$03.00/0
Pergamon Press Ltd.

ABSORPTION MEASUREMENTS AT HIGH PRESSURE (0-10 kbar) ON STRAINED SUPERLATTICES

P. Gavrilovic, K. Meehan, N. Holonyak, Jr., and K. Hess
Electrical Engineering Research Laboratory and Materials Research Laboratory
University of Illinois at Urbana-Champaign, Urbana, Illinois 61801

W.P. Zurawsky and M.G. Drickamer
School of Chemical Sciences and Materials Research Laboratory
University of Illinois at Urbana-Champaign, Urbana, Illinois 61801

M.J. Ludowise, W.T. Dietze, and C.R. Lewis
Corporate Solid State Laboratory, Varian Associates, Inc.
611 Hansen Way, Palo Alto, California 94303

(Received 5 November 1982 by A.A. Maradudin)

Absorption data on strained $GaAs_{1-x}P_x$-GaAs superlattices (SL, 128-period, barrier size L_B~ 75 Å, quantum-well size L_z~ 75 Å, alloy composition x ~ 0.25) are presented in the range 0-10 kbars. The absorption curves obtained show no exciton peaks such as seen in lattice-matched $Al_xGa_{1-x}As$-GaAs SL's, and the pressure coefficient decreases from 11.5 meV/kbar to ~ 10.5 meV/kbar in the wells and ~ 6.5 meV/kbar at energies approaching and above the barrier energies. This behavior is attributed to the fluctuations in strain caused by the alloy disorder, and clustering, of the barriers.

Although most heterostructures have been constructed in lattice-matched III-V systems, for fundamental and various practical reasons mismatched strained-layer heterostructures and superlattices are beginning to gain attention, particularly since newer crystal growth methods now permit successful growth of these structures. For example, recently attempts to observe zone-folding effects on GaP-$GaAs_{1-x}P_x$ strained superlattices (SL) have been reported.[1] Also, impurity-induced layer disordering experiments have been reported on the same type of SL's.[2] Most recently successful laser operation, both pulsed and continuous (cw), has been obtained (300 K) on GaAs-$In_xGa_{1-x}As$ and $GaAs_{1-x}P_x$-GaAs strained SL's.[3,4] The results of Refs. 3 and 4 are important in showing that these as-grown strained SL's, with many interfaces and thus many possibilities for defect formation, are nevertheless relatively free of defects. Otherwise the laser operation of Refs. 3 and 4 would not be possible. Immediately then an interesting and important question concerning a strained SL, particularly one relatively free of defects (i.e., good enough to operate as a cw 300 K photopumped laser),[4] is that of how it compares to a lattice-matched SL. For example, how does a $GaAs_{1-x}P_x$-GaAs strained SL compare in fundamental behavior to an $Al_xGa_{1-x}As$-GaAs SL?[5] Concerning this question, in this paper we report high pressure absorption measurements (300 K) showing that the confined-particle exciton transitions, normally visible in a lattice-matched SL,[5] vanish in the case of a strained SL. In addition, a lesser pressure coefficient is measured because of the built-in strain and the alloy randomness coupled (via strain) from the alloy barriers ($GaAs_{1-x}P_x$) into the binary wells (GaAs).

Two fundamentally different strained SL's, a 66-period GaAs-$In_xGa_{1-x}As$ (x ~ 0.20) SL and a 128-period $GaAs_{1-x}P_x$-GaAs (x ~ 0.25) SL with L_B~ 75-Å barriers and L_z~ 75-Å quantum wells, have been grown for these experiments. These SL's have been grown by organometallic vapor phase epitaxy (OMVPE),[6] or metalorganic chemical vapor deposition (MOCVD), and, as for highly uniform $Al_xGa_{1-x}As$-GaAs SL's grown earlier by VPE,[7] the crystal growth apparatus is electronically operated and computer controlled so as to ensure the growth of equally uniform as well as reproducible layers (shown in Figs. 1 of Refs. 3 and 4). The crystal growth is accomplished at 625°C for GaAs-$In_xGa_{1-x}As$ SL's and at 750°C for $GaAs_{1-x}P_x$-GaAs SL's. The growth rates used are 400 Å/min as determined from separate thick-layer calibration experiments.

In order to compare the behavior of strained SL's with lattice-matched SL's,[5] both with the same kind of binary quantum wells (GaAs), we present data below on only the $GaAs_{1-x}P_x$-GaAs (x ~ 0.25) strained SL. Unlike previous SL's, however, this SL has been provided (and improved) with higher gap confining layers, specifically $Al_yGa_{1-y}As_{1-x}P_x$ (x ~ 0.25, y ~ 0.6) confining layers that are ~ 800 Å thick. One of these confining layers is grown on the top side of the SL and one on the bottom side immediately following a $GaAs_{1-x}P_x$ graded layer that is grown first on a GaAs substrate and is changed in composition over 0.1 μm thickness from x=0 to x = 0.125 (i.e., to the average composition of the SL). The bottom Al-containing confining layer acts as a convenient "stop layer" that permits polishing and etch removal of <u>all</u> of the substrate and graded region so that absorption (or emission) measurements can

Impurity induced disordering of strained GaP-GaAs$_{1-x}$P$_x$ ($x \sim 0.6$) superlattices

M. D. Camras, N. Holonyak, Jr., and K. Hess
Electrical Engineering Research Laboratory and Materials Research Laboratory, University of Illinois at Urbana–Champaign, Urbana, Illinois 61801

M. J. Ludowise, W. T. Dietze, and C. R. Lewis
Solid State Laboratory, Varian Associates, Incorporated, 611 Hansen Way, Palo Alto, California 94303

(Received 16 August 1982; accepted for publication 18 October 1982)

Data are presented showing that Zn diffusion into a strained GaP-GaAs$_{1-x}$P$_x$ ($x \sim 0.6$) superlattice (40 periods, $L_z \sim 120$ Å GaAsP quantum wells, $L_B \sim 120$ Å GaP barriers) enhances the interdiffusion of As and P (anion interchange) at the heteriointerfaces, thus resulting in disordered indirect gap bulk crystal GaAs$_{1-x}$P$_x$ ($x \sim 0.8$).

PACS numbers: 66.30.Jt, 64.70.Kb, 64.75. + g, 68.48. + f

Recent work on AlAs-GaAs and Al$_x$Ga$_{1-x}$As-GaAs supperlattices (SL's), as well as on similar quantum well heterostructures (QWH's), has shown that the heterointerfaces, and thus the crystal, are unstable against either Zn diffusion (500–600 °C)[1–4] or Si ion implantation.[5] To explain this behavior it has been proposed[1] that in the usual interstitial-substitutional Zn diffusion process in a material such as GaAs a closely associated interstitial Zn, vacancy pair or "molecule" (Zn_i, V) plays an important role in permitting Al and Ga atoms to interchange. The (Zn_i, V) pair or "molecule" acts as a high concentration pseudovacancy that is available for the Al-Ga interchange, particularly at a heter-

 0003-6951/83/020185-03$01.00

Continuous 300-K laser operation of strained superlattices

M. J. Ludowise, W. T. Dietze, and C. R. Lewis
Corporate Solid State Laboratory, Varian Associates, Incorporated, 611 Hansen Way, Palo Alto, California 94303

M. D. Camras, N. Holonyak, Jr., B. K. Fuller, and M. A. Nixon
Electrical Engineering Research Laboratory and Materials Research Laboratory, University of Illinois at Urbana-Champaign, Urbana, Illinois 61801

(Received 26 October 1982; accepted for publication 3 January 1983)

Continuous (cw) 300-K laser operation of a 66-period lower energy GaAs-$In_xGa_{1-x}As$ ($x\sim0.2$) strained superlattice (SL) and a higher energy 128-period $GaAs_{1-x}P_x$-GaAs ($x\sim0.25$) strained SL is demonstrated. The strained SL's are grown by organometallic vapor phase epitaxy (OMVPE) or metalorganic chemical vapor deposition (MOCVD) with higher gap quaternary confining layers and $L_b\sim75$ Å barriers and $L_z\sim75$ Å quantum wells. These SL's are unstable during high level excitation, failing in 2–20 min when operated cw at 300 K as photopumped lasers.

PACS numbers: 42.55.Px, 78.45. + h, 78.20. − e, 78.55.Ds

Essentially all heterostructure devices of any practical merit have been constructed in lattice-matched III-V systems. For various reasons it is interesting to consider heterostructures constructed in mismatched systems. Not the least of these is the fact that high quality binary substrates are not available at all the interesting or desired lattice sizes, and hence mismatched III-V layer growth in some circumstances is inevitable. Also, in many cases it is of some interest, for physical and band structure reasons (e.g., zone-folding experiments),[1] to grow (in thin layer form) one mismatched material on another. In addition, it is of some importance for general understanding to establish what limitations and consequences arise from growing heterostructures with mismatched, and thus strained thin layers. For example, recently we[2] have shown that a $GaAs_{1-x}P_x$-GaAs ($x\sim0.25$) strained superlattice (SL) is capable of pulsed-excitation photopumped laser operation at 300 K, which would not be possible if a high density of defects existed at the large number (132) of heterointerfaces. Since a strained SL will operate as a laser,[2] an immediate unanswered question is that of whether a strained SL is capable of continuous (cw) 300-K laser operation, and whether the operation and thus the SL are stable. In this letter, we demonstrate the former, but at the high excitation level characteristic of cw 300-K laser operation ($\sim10^3$ A/cm^2) the luminescence decays as the strained SL degrades.

Two fundamentally different strained SL's, a 66-period GaAs-$In_xGa_{1-x}As$ ($x\sim0.20$) SL and a 128-period $GaAs_{1-x}P_x$-GaAs ($x\sim0.25$) SL, have been grown for these experiments by organometallic vapor phase epitaxy (OMVPE) or metalorganic chemical vapor deposition (MOCVD).[3] As for the case of highly uniform $Al_xGa_{1-x}As$-GaAs SL's grown earlier by VPE,[4] in the present case the crystal growth apparatus is electronically operated and computer controlled. The crystal growth is first calibrated with respect to composition (x) and growth rate (layer thickness) on easily examined thicker layers. Growth rates are typically 400 Å/min for these structures. A special feature of the crystal growth apparatus is its capability for handling the four components Ga, In, Al, and As in the case of GaAs-In_x-$Ga_{1-x}As$ SL's and Ga, Al, As, and P in the case of $GaAs_{1-x}P_x$-GaAs SL's. This has made it possible to provide higher gap $In_xAl_yGa_{1-x-y}As$ ($x\sim0.1$, $y\sim0.6$) confining layers on the 66-period SL with $In_xGa_{1-x}As$ quantum wells and higher gap $Al_yGa_{1-y}As_{1-x}P_x$ ($x\sim0.25$, $y\sim0.6$) confining layers on the 128-period SL with GaAs quantum wells.

A shallow-angle ($<0.5°$) or slant cross section of the alloy well SL is shown in Fig. 1. At the bottom of the figure is a GaAs substrate, which is followed by a thin $In_xGa_{1-x}As$ layer (g) linearly graded from $x=0$ (GaAs) to $x=0.1$, i.e., to

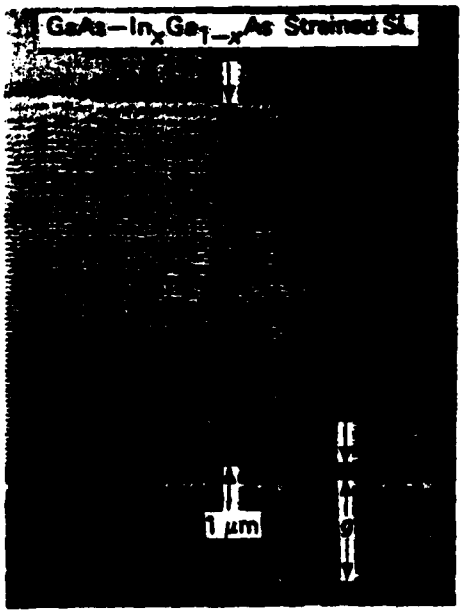

FIG. 1. Shallow-angle ($<0.5°$) cross section of a 66-period strained SL consisting of $L_z\sim75$ Å $In_xGa_{1-x}As$ ($x\sim0.2$) quantum wells coupled by $L_b\sim75$ Å GaAs barriers. A graded region (g) of $In_xGa_{1-x}As$ ($0<x<0.1$) is first grown on a GaAs substrate (by OMVPE). This is followed by an ~800-Å $In_xAl_yGa_{1-x-y}As$ confining layer (arrows at lower right). The ~1-μm strained SL is next (center arrows), with an ~800-Å $In_xAl_yGa_{1-x-y}As$ ($x\sim0.1$, $y\sim0.6$) confining layer on top. (The upper layers appear thicker because of rounding of the "corner" formed by the slant cross section and the wafer surface.)

 0003-6951/83/060487-03$01.00

(10)

Low threshold photopumped $Al_xGa_{1-x}As$ quantum-well heterostructure lasers

R. D. Burnham, W. Streifer, and D. R. Scifres
Xerox Palo Alto Research Center, Palo Alto, California 94304

N. Holonyak, Jr., K. Hess, and M. D. Camras
Electrical Engineering Research Laboratory and Materials Research Laboratory, University of Illinois at Urbana-Champaign, Urbana, Illinois 61801

(Received 19 November 1982; accepted for publication 20 January 1983)

Data are presented on very low threshold photopumped separate-confinement quantum-well heterostructure (SC QWH) lasers grown by metalorganic chemical vapor deposition (MOCVD). An unusually thin *single* quantum well (size $L_z \lesssim 60$ Å) is employed in the QWH with the carriers confined ("trapped") in the interior "cladding" region, which serves also as the optical waveguide. Excess carriers, which are photogenerated (or injected), are confined in the thin interior cladding region (size $L_{z'} \sim 1000$ Å) and, in this charge reservoir and waveguide region, are thermionically "emitted" back and forth across the well until scattered to lower energy in the well ($\Delta E \sim \hbar\omega_{LO}$) and collected. Continuous (cw) 300 K photopumed laser operation of these QWH's is demonstrated for very short cavities. For one QWH wafer laser operation occurs at $\lambda \sim 7730$ Å with a photopumping threshold of 380 W/cm^2 ($J_{eq} \sim 160$ A/cm^2) and for another wafer at $\lambda \sim 7000$ Å with threshold 10^3 W/cm^2 ($J_{eq} \sim 410$ A/cm^2). The photopumped samples are as small as 20×40 μm, thus making these laser thresholds (for such short cavity lengths) a factor of 3–10 better than the lowest previously reported.

PACS numbers: 78.45. + h, 42.55.Px, 78.55. − m, 78.20. − e

I. INTRODUCTION

Recently a single quantum-well heterostructure (QWH) laser has been introduced that consists of an ultra thin quantum well ($L_z < 80$ Å) inserted into the center of the narrower gap thin interior "cladding" region (see inset of Fig. 1).[1] This is an interesting and useful design because the laser waveguide properties are determined by the interior cladding portion of the structure ($L_{z'}$) and the carrier recombination by the quantum well (L_z), which, in fact, can be much smaller in size than $L_z \simeq 80$ Å (the collecting limit of a GaAs quantum well confined between *thick* $Al_xGa_{1-x}As$ layers).[2] In the central region of dimension $L_{z'} \simeq 0.1$ μm (inset of Fig. 1) the excess injected or photogenerated electrons recombine or are collected in the well and then recombine. The injected carriers are confined ("*trapped*") near the quantum well within distance $L_{z'}$, and if an electron is not scattered to lower energy ($\Delta E \sim \hbar\omega_{LO}$) and collected on its first excursion over the well, it will repeat the traversals until captured in the well or until after a long enough time it recombines outside of the well (in the confinement region $L_{z'}$ of Fig. 1). Before this occurs, however, the confined carriers experience an increased probability of capture in the quantum well because of being in a constant state of transport (thermionic "emission") across the well. In essence, because of the carrier's multiple opportunities to scatter into the well, the extremely small well appears magnified in respect to carrier capture (and recombination) but is not itself the source of much absorption. In other words, the internal cladding region of width $L_{z'}$ acts as a reservoir for excess carriers. In addition, the very thin QW absorbs very little light in its unpumped state and only very little current then renders it transparent. Thus an extremely small *single* quantum well can be used to advantage in a QWH laser. In this paper we show that a single quantum-well heterostructure as described is capable of extremely low threshold continuous

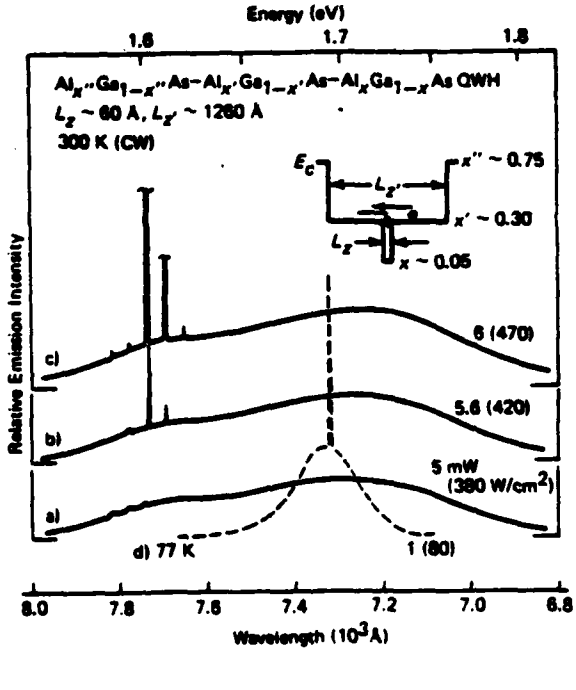

FIG. 1. Low threshold cw 300 K $Al_xGa_{1-x}As$ quantum-well heterostructure laser ($\lambda \sim 7730$ Å) as shown (conduction band) in the inset. The photopumped sample (20×40 μm area) reaches threshold at 5 mW of measured photopumping (Ar$^+$ laser, 5145 Å). Half of this power is transmitted to and is focused on the the sample, or 380 W/cm^2 ($J_{eq} \sim 160$ A/cm^2). The dashed curve (d) corresponds to 77 K.

 0021-8979/83/052618-05$02.40

LOW-THRESHOLD SINGLE QUANTUM WELL (60 Å) GaAlAs LASERS GROWN BY MO-CVD WITH Mg AS *p*-TYPE DOPANT

Indexing terms: Semiconductor devices and materials, Semiconductor lasers

The letter reports low-threshold MO-CVD GaAlAs DH (~7730 Å) lasers containing Mg as the *p*-type dopant. The structure consists of symmetric stepped index cladding layers on both sides of a thin single quantum well (~60 Å) active region. Broad-area threshold current densities of 460 A cm^{-2} and 270 A cm^{-2} are achieved for cavity lengths of 250 and 500 μm, respectively. Broad-area room-temperature lasers without facet coatings emit in excess of 400 mW/facet CW output power.

We report low-threshold operation of a quantum well diode laser, whose *p*-side cladding regions and active region are magnesium-doped. Mg is expected to be more attractive than Zn as a *p*-type dopant in GaAs and related III-V compounds because the diffusion coefficient of Mg is about 10^4 times lower than that of Zn in GaAs.[1] Zn has been shown[2] to migrate in $Ga_{1-x}Al_xAs$ at low temperature and produce compositional disorder at a $Ga_{1-x}Al_xAs$-GaAs interface. Mukai *et al.*[3] showed that Mg can be incorporated as an acceptor in liquid phase epitaxy (LPE) grown $Ga_{1-x}Al_xAs$ and that the resistivity of $Ga_{1-x}Al_xAs$ doped with Mg exhibits a low temperature dependence. Wolf *et al.*[4] reported very low degradation (about 10^{-5} h^{-1} at 100–120°C) GaAlAs DH (8800 Å) oxide stripe lasers grown by liquid phase epitaxy using Mg as the *p*-type dopant in the cladding layer. Recently, a metalorganic compound bis(cyclopentadienyl) magnesium $(C_5H_5)_2Mg$ was reported to yield excellent results as a source of Mg in MO-CVD growth.[5] However, diode lasers grown by MO-CVD with Mg as a *p*-type dopant have not been reported.

Tsang[6,7] and Hersee *et al.*[8] have used a graded aluminium fraction (x) in the $Ga_{1-x}Al_xAs$ optical cavity cladding a quantum well active region[9,10] to substantially reduce the broad-area lasing threshold compared with a conventional double heterostructure laser. The lasers were grown by MBE[6,7] with undoped active and graded cladding regions and by low-pressure MO-CVD with Zn as a *p*-type dopant. Using atmospheric pressure MO-CVD in a vertical reactor,[11–13] we too have grown and characterised broad-area lasers with a similar structure.† These devices contain a symmetric step index in the cladding regions (in contrast to graded index layers[6,8]) bounding a single quantum well that is not intentionally doped. Threshold current densities below 300 A cm^{-2} were measured for various well thicknesses between 60 and 200 Å. All these devices utilised Zn as the *p*-type dopant.

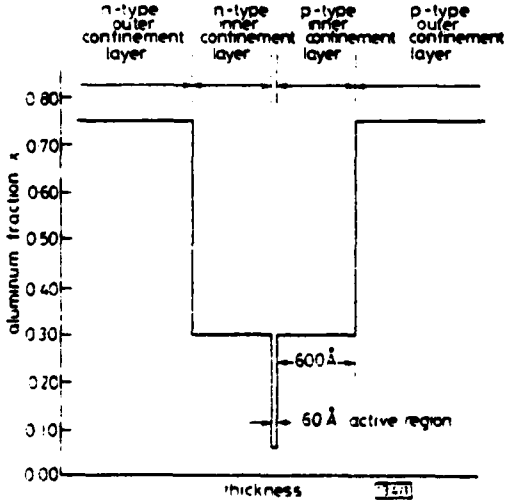

Fig. 1 *Illustrating the variation of aluminium fraction x with layer thickness for the laser*

† BURNHAM, R. D., SCIFRES, D. R., and STREIFER, W.: Unpublished results

Our purpose in this letter is to describe a similar laser with the same reduction in broad-area threshold current density, but employing Mg as the *p*-type dopant in both the cladding and active layers. The structure, layer compositions and thicknesses are shown in Fig. 1. The active region contains ~ 5% Al and is 60 Å thick; the inner claddings are composed of ~ 30% Al and are 600 Å thick; the outer regions contain ~ 75% Al.

Fig. 2 shows typical broad-area light-output/pulsed-current (L/I) characteristics at 300 K for two different cavity lengths. For a laser 250 μm long and 216 μm wide, $J_{th} \simeq 460$ A cm^{-2}, whereas 500 μm-long lasers of the same width have thresholds of $J_{th} \simeq 270$ A cm^{-2}. Although the Al constituted only 5% of the active layer, the 500 μm- and 250 μm-long devices lased simultaneously in several longitudinal modes centred at 7718 Å and 7755 Å, respectively; the difference in photon energy

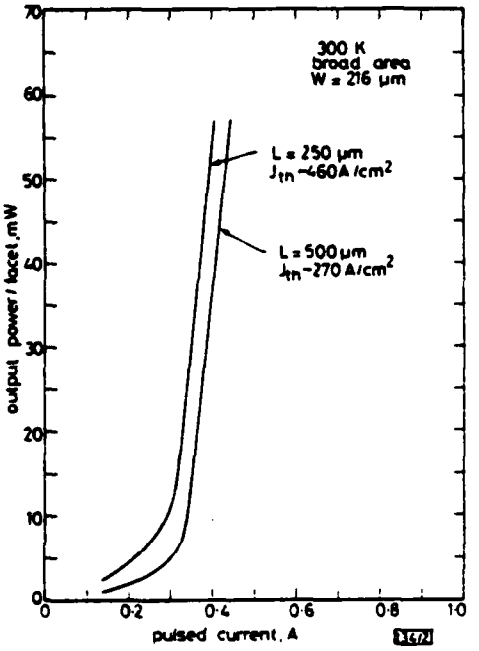

Fig. 2 *Pulsed room-temperature L.I characteristics for a symmetric step index $Ga_{1-x}Al_xAs$ single quantum well heterostructure laser diode with 250 μm- and 500 μm-long cavity lengths*

between the lasers and the bandgap of $Ga_{0.95}Al_{0.05}As$ is ≃ 120 meV, which results from the quantum size effect.[9,10,14] In particular, this energy is in good agreement with the lowest confined carrier transition. The theoretical lasing wavelength for a transition from an $n = 1$ electron and a light hole, in a 55–60 Å quantum well with a barrier height of 310 meV, is 7775–7845 Å. This indicates efficient carrier scattering into the well, enhanced by the particular symmetric stepped index cladding layers. Moreover, the wavelength difference with laser length arises because the peak gain of the quantum well laser may shift slightly with active region charge density. We also note that the differential efficiencies of the 250 μm and 500 μm length lasers are approximately equal. This result, which is similar to that reported by Tsang,[7] indicates that either the internal losses are negligible compared with the facet transmission losses and/or the internal efficiency η_i decreases with increasing active region charge density (corresponding to reduced laser length). Indeed the internal losses may well be small, but we believe it more likely that carrier leakage effects[15] are responsible for a decrease in the apparent internal efficiency. It is also possible that circulating modes[16] are present and act to reduce η_i.

Fig. 3 compares the light-output current (L/I) characteristic for the laser with a 250 μm-long cavity and a 216 μm-width under pulsed and CW operation. Under pulsed conditions, $I_{th} \simeq 300$ mA and the differential quantum efficiency is ≃ 67%. For CW operation $I_{th} \simeq 350$ mA and the differential quantum efficiency is ≃ 57%. The reduced differential quantum efficiency under CW conditions is probably a consequence of laser heating. Laser threshold increases with

Inst. Phys. Conf. Ser. No. 65: Chapter 4
Paper presented at Int. Symp. GaAs and Related Compounds, Albuquerque, 1982

Disorder of AlAs/GaAs superlattices by the implantation and diffusion of impurities

M D Camras, J J Coleman, N Holonyak, Jr., and K Hess

Electrical Engineering Research Laboratory and
Materials Research Laboratory
University of Illinois at Urbana-Champaign, Urbana, IL 61801
USA

P D Dapkus* and C G Kirkpatrick
Rockwell International Microelectronics Research and
Development Center
Thousand Oaks, California 91360, USA

Abstract

Three methods are examined for disordering AlAs-GaAs superlattices (SL's) grown by metalorganic chemical vapor deposition (MOCVD): Zn diffusion, Si ion implantation and Zn ion implantation. Disordering occurs in a binary SL when the ordered structure of alternating AlAs layers and GaAs layers is scrambled to form a compositionally homogeneous alloy of $Al_xGa_{1-x}As$. Each of the methods permits disordering of selected regions and each has its own characteristic attributes. The concentration of Zn necessary to produce disordering is estimated and models for the enhancement of Al-Ga interdiffusion by the formation of impurity-vacancy molecules are discussed.

1. Introduction

In recent work we have shown (Coleman et al 1982, Holonyak et al 1981, Laidig et al 1981) that the structure of quantum-well heterostructures (QWH) and superlattices (SL) containing alternating, thin layers of the binary compounds AlAs and GaAs can be fundamentally altered at relatively low temperatures by impurity incorporation. In selected regions delineated by photolithographic techniques, the presence and movement of impurities such as Zn and Si cause the sharply defined alternating layers of pure AlAs and GaAs to intermix, resulting in disordered $Al_xGa_{1-x}As$. The composition parameter x, of the resulting alloy depends on the relative thicknesses of the original AlAs and GaAs layers. In earlier work, we described the observation of this disordering phenomenon occurring in AlAs-GaAs superlattices grown by metalorganic chemical vapor deposition (MOCVD) (Coleman et al 1981) that have been diffused with Zn or implanted with Si ions. For both of these species the temperature (diffusion temperature or implant anneal temperature) at which disordering occurs is much lower than either the original growth temperature of the layers (~ 750 °C) or the temperature at which thermal disordering is known

* Present Address: Department of Electrical Engineering, University of Southern California, Los Angeles, California, USA

0305-2346/83/0065-0233 $02.25

JVSTB,830600P12074B-S
Running Title: A simple model for the index

A simple model for the index of refraction of GaAs–AlAs superlattices and heterostructure layers: Contributions of the states around Γ

J. P. Leburton and K. Hess

Department of Electrical Engineering and Coordinated Science Laboratory, University of Illinois at Urbana-Champaign, Urbana, Illinois 61801

(Received 18 January 1983; accepted 3 March 1983)

We present a simple theory of the dielectric function in superlattices. The calculation is performed separately for different symmetry points of the band structure. We assume that among the contributing states only the Γ states are influenced substantially by size quantization and the electronic states at Γ are calculated by using a simplified k·p method. New features of the dielectric constant of superlattices are a fine structure due to zone folding (subbands) and a small anisotropy due to the lower symmetry. Except for these finer details, the index of refraction of a superlattice is well approximated by the corresponding constant for an alloy $Al_{\bar{x}}Ga_{1-\bar{x}}As$ where $\bar{x}$ is the averaged Al mole fraction of the superlattice.

PACS numbers: 77.20. + y, 78.65. − s, 77.55. + f, 78.20.Dj

I. INTRODUCTION

Although some experimental results have been reported,[1,2] the dielectric constant (index of refraction) of superlattices and heterostructures has not yet been investigated theoretically. This paper addresses two major issues. First, we examine the modifications of the dielectric constant by size quantization and by the anisotropy introduced by the lower symmetry of the superlattice compared to the host material. Secondly, we determine theoretically the absolute value of the index of refraction, which is essential for device applications. Recently Holonyak and co-workers[3,4] have shown that superlattices can be *selectively* interdiffused generating patterns of AlGaAs alloy and GaAs–AlAs superlattice regions. The experimental findings show that the intermixed and the superlattice regions exhibit differences in the dielectric constant band gap and electronic properties. The obvious potential of these structures for applications in integrated optics makes the detailed knowledge of parameters determining the dielectric constant and especially the index of refraction desirable. Unfortunately, the simplest approach, the Penn model,[5] cannot be directly applied to a superlattice structure for the following reasons.

(i) The Penn model considers only two bands having a peak in the density of states at the band edges. The dielectric constant of a real semiconductor contains major contributions from several symmetry points within the bands. These points are shifted (quantized) differently by the additional periodicity of the superlattice.

(ii) The Penn model has spherical symmetry while the superlattice has cylindrical symmetry.

Therefore, we introduce a model for the dielectric constant which considers differently contributions from Γ and other transitions such as X and L. The Γ valley is treated by the k·p method. The influence of the superstructure (using a Kronig–Penney model) is only included for the states at Γ. Although the states around X and L also are shifted, the shift is weaker because of the larger effective mass and because of the parallel curvature of valence and conduction band. We did not include these contributions in this preliminary study since there are only few experimental results of the X and L shifts available.

We are currently developing a more rigorous treatment which includes the energy changes at L and X in the same way as described below for Γ. The changes in the contributions of the third valence band (spin-orbit splitting) to the dielectric constant have been estimated to be small and, for the time being, neglected. In spite of the oversimplification, our model still describes the experiments on the index of refraction quite well and shows the physical significance of the various contributions.

II. TRANSVERSE DIELECTRIC FUNCTION

In discussing the optical properties of superlattices, the transverse dielectric function $\epsilon(\mathbf{q},\omega)$ is adequate to describe the response of electrons to a transverse perturbation such as an electromagnetic field. In optical experiments the wave vector $\mathbf{q}$ of the photons is very small and therefore, will be approximated to be zero (long wave limit). Then, in the reduced zone scheme, the real part and the imaginary part of the dielectric constant are given by[6]

$$\mathrm{Re}\epsilon(\omega) = 1 + \frac{8\pi e^2\hbar^2}{m_0^2}\sum_{\mathbf{k}_f,\mathbf{k}_i,c,v}|\langle \mathbf{k}_f,c|\hat{e}\cdot\mathbf{p}|\mathbf{k}_i,v\rangle|^2\frac{N_{\mathbf{k}_i,v}(1-N_{\mathbf{k}_f,c})}{(E_{\mathbf{k}_f,c}-E_{\mathbf{k}_i,v})\left[(E_{\mathbf{k}_f,c}-E_{\mathbf{k}_i,v})^2-\hbar^2\omega^2\right]} \tag{1}$$

and

$$\mathrm{Im}\epsilon(\omega) = \frac{4\pi^2e^2}{m_0^2\omega^2}\sum_{\mathbf{k}_f,\mathbf{k}_i,c,v}|\langle \mathbf{k}_f,c|\hat{e}\cdot\mathbf{p}|\mathbf{k}_i,v\rangle|^2\delta(E_{\mathbf{k}_f,c}-E_{\mathbf{k}_i,v}-\hbar\omega)N_{\mathbf{k}_i,v}(1-N_{\mathbf{k}_f,c}), \tag{2}$$

(19)

Abstract for an Invited Paper

for the Philadelphia Meeting of the

American Physical Society

November 3-5, 1982

Electronic Transport in GaAs-GaAlAs Heterolayers and High Mobility Transistors.*

K. HESS, University of Illinois, Urbana. (30 min.)

Lattice matched semiconductor heterojunctions have been widely used in semiconductor lasers, photodetectors, solar cells and bipolar devices. Two new epitaxial technologies have emerged in recent years (metal-organic-chemical vapor deposition (MOCVD) and molecular beam epitaxy (MBE)) and have added a variety of new possibilities[1] including the fabrication of MESFET-high mobility transistors (HMET)[2] and double semiconductor metal insulator transistors (MISS-transistors).[3] A general survey of new transport effects at low and high electric fields in heterostructure layers will be given with special emphasis on the possibility of achieving extremely high mobilities and on high field real space transfer.[4] The opportunities and disadvantages of these effects for constructing novel devices are discussed using the HMET, the MISS-transistor as well as real space transfer and optoelectronic devices (e.g., the superlattice avalanche-photodiode) as an example. It is concluded that the variability of boundary conditions offers fascinating and physically highly interesting possibilities for novel device concepts.

*Supported by the Office of Naval Research, the Army Research Office and the Joint Services Electronics Program.

[1]K. Hess and N. Holonyak, Jr., Physics Today, October 1980.

[2]T. Mimura, S. Hiyamizu, T. Fujii and K. Nanbu, Jap. J. of Appl. Phys., 19, L225 (1980).

[3]T. Hotta, H. Sakaki and H. Ohno, Res. Rep. of the IIS Electrical Eng. and Electronics, 32 2, 1 (1982).

[4]K. Hess, Journal de Physique, C7, pp. C7-3 (1981).

Solid-State Electronics Vol. 26, No. 12, pp. 1173–1176, 1983
Printed in Great Britain.

0038-1101/83 $3.00 + .00
Pergamon Press Ltd.

CARRIER DENSITY DISTRIBUTION IN MODULATION DOPED GaAs–$Al_xGa_{1-x}As$ QUANTUM WELL HETEROSTRUCTURES

T. C. HSIEH, K. HESS, and J. J. COLEMAN
Electrical Engineering Research Laboratory and Materials Research Laboratory, University of Illinois at Urbana-Champaign, Urbana, IL 61801, U.S.A.

and

P. D. DAPKUS
Department of Electrical Engineering, University of Southern California, Los Angeles, CA 90069, U.S.A.

(*Received* 4 *December* 1982; *in revised form* 20 *May* 1983)

Abstract—A theoretical model for the distribution of charged carriers at the interface of a doped $Al_xGa_{1-x}As$-undoped GaAs heterostructure is evaluated. Assuming a triangular potential well at the interface, we obtain numerically, curves describing the Fermi energy, depletion width in the alloy, and average separation of impurities and carriers, and the electron density at the interface as functions of alloy layer composition and doping level. The results obtained can be applied to multiple heterointerface quantum well heterostructures and superlattices as well. Carrie concentration profile data on a 51-layer modulation doped QWH grown by MOCVD are presented and are discussed using the results of the model.

Modulation doped GaAs–$Al_xGa_{1-x}As$ quantum well heterostructures (QWH) have found a variety of applications including lasers[1] and high mobility transistors[2]. Theoretical models for the charge distribution, depletion width, size quantization effects, etc. are available[3, 4] but have not been evaluated in much detail for modulation doped GaAs–$Al_xGa_{1-x}As$ structures. In this note we present a model for the electronic equilibrium properties of a modulation doped QWH (including size quantization effects) which is simple enough to be applied to actual device structures and we compute the Fermi energy, depletion layer width (in the $Al_xGa_{1-x}As$), impurity-electron distance and other important parameters, as a function of doping concentration and alloy composition for a single heterointerface. Many of the results thus obtained are also valid for multiple heterointerfaces and superlattices. We show that these results can be used to approximately predict the average distance of the electrons from the interface and, therefore, the basic characteristics of carrier concentration profiles in multiple quantum well heterostructures.

Shown in Fig. 1 is a typical energy band structure which is used to develop the model for a single interface of a modulation doped QWH. The simplest approximation for the self-consistent potential at the interface is a triangular well[4, 5]. The solution for the envelope function $\zeta_i(z)$ of the electron wavefunction, and the quantized energy levels have been given by Stern[5]:

$$\zeta_i(z) = A_i\left(\frac{2m_z eF_s}{\hbar^2}\right)^{1/3}\left(z - \frac{E_i}{eF_s}\right) \tag{1}$$

$$E_i = \left(\frac{\hbar^2}{2m_z}\right)^{1/3}\left(\frac{3}{2}\pi eF_s\left(i + \frac{3}{4}\right)\right)^{2/3} \tag{2}$$

Using the notation shown in Fig. 1 and assuming donor doping in the $Al_xGa_{1-x}As$ barrier layers and unintentional background doping levels in the GaAs wells, we obtain the Poisson's equation:

$$\frac{d^2\phi}{dz^2} = -\frac{e}{\epsilon_{s1}}N_{D1}^+ \qquad -l_n < z < 0$$

$$\frac{d^2\phi}{dz^2} = \frac{e}{\epsilon_{s2}}\left(N_{A2}^- + N_0\zeta_0^2(z)/\int_0^\infty \zeta_0^2(z)\,dz\right) \qquad 0 < z < l_p \tag{3}$$

From charge neutrality and the band structure of Fig. 1, we get

$$l_nN_{D1}^+ = l_p(N_{A2}^-) + N_0 \tag{4a}$$

$$E(l_p) - (E_\Delta - E(l_n)) = E_g - E_1 - E_2 \tag{4b}$$

$$E_F = (E_\Delta - E(l_n)) - E_1 \tag{4c}$$

where

$$N_0 = \frac{m_z kT}{\pi\hbar^2}\ln\left(1 + \exp\frac{E_F - E_0}{kT}\right) \tag{5a}$$

$$E(l_p) = \frac{e^2}{2\epsilon_{s2}}N_{A2}^- l_p^2 + \frac{2}{3}e^2\left(\frac{N_0}{\epsilon_{s2}}\right)\left(\frac{E_0}{eF_s}\right) \tag{5b}$$

$$E(l_n) = \frac{e^2}{2\epsilon_{s1}}N_{D1}^+ l_n^2 \tag{5c}$$

and

$$eF_s = \frac{e^2}{\epsilon_{s2}}(N_0 + n_{A2}^- l_p). \tag{6}$$

(16)

QUANTUM-WELL HETEROSTRUCTURE LASERS

N. Holonyak, Jr. and K. Hess

Electrical Engineering Research Laboratory

and Materials Research Laboratory

University of Illinois at Urbana-Champaign, Urbana, Illinois 61801

In SYNTHETIC MODULATED MATERIALS,
edited by L. L. Chang and B. C. Giessen
(New York: Academic Press, 1983).

Direct observation of lattice distortion in a strained-layer superlattice

J. M. Brown and N. Holonyak, Jr.
Electrical Engineering Research Laboratory and Materials Research Laboratory, University of Illinois at Urbana–Champaign, Urbana, Illinois 61801

M. J. Ludowise, W. T. Dietze, and C. R. Lewis
Corporate Solid State Laboratory, Varian Associates, Incorporated, 611 Hansen Way, Palo Alto, California 94303

(Received 9 June 1983; accepted for publication 17 August 1983)

The structure of strained-layer quantum well heterostructures grown by metalorganic chemical vapor deposition has been examined using both conventional and high resolution electron microscopy. It has been possible to show that the lattice mismatch in superlattice systems containing strain of up to 7.1×10^{-3} is accommodated by the introduction of a tetragonal expansion and compression of the lattice of successive layers. This can be seen in the splitting of the (001) spots in the electron diffraction pattern and by the bending of (111) lattice fringes at the heterojunction interfaces.

PACS numbers: 68.48. + f, 61.70.Jc, 61.50.Jr, 61.55. − x

It has recently been shown that a strained-layer superlattice (SL) can be grown free enough of defects (dislocations) to make possible stimulated emission.[1] The results presented in this letter were obtained on crystals grown by metalorganic chemical vapor deposition (MOCVD) that have been shown to operate as continuous (cw) 300-K lasers when photopumped with a 100-mW Ar^+ laser (5145 Å).[2] The photoluminescence from a photopumped sample made up of 150-Å $In_{0.2}Ga_{0.8}As$ quantum wells and 150-Å GaAs barriers (66 periods) grown on a (100) GaAs substrate is shown in Fig. 2 of Ref. 1. This material has a strain of 7.1×10^{-3} and has been shown to operate as a cw laser for 5 min (high excitation level, $J_{eq}\sim10^3$ A/cm^2) before failure occurs, a network of dislocations being visible in the excited regions.[2,3] The results of an electron microscope study of a variety of these strained-layer superlattices are presented here. These results show the defect-free nature of the heterointerfaces and the uniformity of the layers. Of particular interest, high resolution electron microscopy in conjunction with electron diffraction has been used to examine the manner in which the lattice mismatch is accommodated. The strain-produced distortion of the lattice is shown directly by lattice imaging and by diffraction measurements.

The SL crystals were sectioned normal to the plane of growth [(100) plane] so that the layers are visible in cross section, the electron microscope specimen normal being a

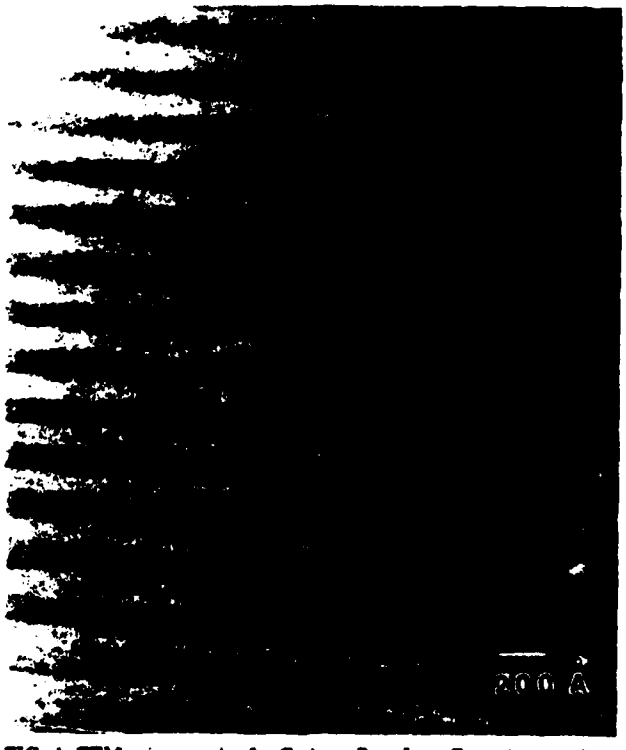

FIG. 1. TEM micrograph of a $GaAs_{0.96}P_{0.04}$-$In_{0.01}Ga_{0.99}As$ superlattice taken on a [110] pole indicating the uniformity of the (100) layers.

 0003-6951/83/210863-03$01.00

G. W. Bailey, Ed., *Proceedings of the 41st Annual Meeting of the Electron Microscopy Society of America*

(18)

DEFECT STUDIES IN STRAINED-LAYER QUANTUM WELL HETEROSTRUCTURES

J.M. Brown*, M.E. Mochel**, N. Holonyak, Jr.***, M.D. Camras***, M.J. Ludowise+, W.T. Dietze+, and C.R. Lewis+

*Dept. of Metallurgy and Materials Research Lab., Univ. of Illinois, Urbana **Materials Research Lab., Univ. of Illinois, Urbana, ***Electrical Eng. Research Lab. and Materials Research Lab., Univ. of Illinois, Urbana 61801 +Corporate Solid State Lab., Varian Associates, Inc., 611 Hansen Way, Palo Alto, CA 94303

The epitaxial growth of mismatched or strained III-V layers was shown to be viable as early as 1960.[1] Osbourn et al[2] suggested that strained layer GaP-$GaAs_{1-x}P_x$ superlattices grown by organo-metallic vapor phase epitaxy (OMVPE) could be used to fold the Brillouin zone and make indirect-crystal direct. More recently, it has been shown that a strained-layer superlattice can be grown free enough of defects at heterointerfaces to make possible stimulated emission.[3] This has been demonstrated on OMVPE $GaAs_{1-x}P_x$-GaAs (x=0.25) and GaAs-$In_xGa_{1-x}As$ (x=0.2) strained layer superlattices which have been operated as photopumped continuous (cw) 300K lasers but which at high excitation levels ($> 10^{3}Acm^{-2}$) prove to be unstable. This paper presents the results of an electron microscope study of the defects produced in a GaAs-$In_xGa_{1-x}As$ strained superlattice as a result of high excitation levels of operation.

The strained superlattice was grown by OMVPE, the crystal growth apparatus being electronically operated and computer controlled resulting in a highly uniform superlattice (SL) as is shown in fig. 1. A GaAs substrate was used, then a thin layer of $In_xGa_{1-x}As$ linearly graded from x=0 (i.e. GaAs) to x=0.1 i.e. to the average composition of the superlattice. An 850Å confining layer of $In_xAl_yGa_{1-x-y}As$ is grown prior to a 66-period GaAs-$In_xGa_{1-x}As$ (x=0.2) strained superlattice. This represents a strain of $7x10^{-3}$.

The specimens were photopumped with the 100mW or less output of an Ar^+ laser (5145Å). Regions therefore existed within the material which had failed due to damage. Specimens were sectioned perpendicular to the growth direction and then ion beam thinned for examination in the TEM. Another specimen in the plane of growth was later prepared in a similar way. Regions containing dislocations in the graded layer were found in the undamaged areas but they did not propagate into the superlattice which was virtually defect-free (fig. 2.) This type of dislocation was also found in the as-grown material and implies that it is possible to grow defect-free layered structures on a substrate that contains dislocations. In the areas of the specimen which had failed, dislocations could be seen running from one superlattice layer to another as well as along the interfaces between the layers. This is shown in fig. 3. The dislocations had <110> Burgers vectors which is the primary direction in diamond cubic structures. A specimen taken in the plane of growth clearly showed the dislocations produced by the photopumping. High densities of dislocations were centered around the path of the photopumping laser separated by regions of perfect crystal (fig. 4). These damaged regions were ~15μm wide and separated by ~ 500μm. This corresponds well with the diameter of the focused laser beam and the separation of the laser damaging passes.

The failure of these strained superlattices can therefore be seen to result from the introduction of a large number of dislocations due to laser operation. It should be noted however, that defect free, highly strained superlattices can be grown by OMVPE. These fail when used at high levels of excitation but they may be useful if used in devices requiring low energy drive levels below that at which damage occurs.[4]

(19)

Photopumped low threshold $Al_{x''}Ga_{1-x''}As$-$Al_{x'}Ga_{1-x'}As$-$Al_xGa_{1-x}As$ ($x''\sim0.85$, $x'\sim0.3$, $x=0$) single quantum well lasers

M. D. Camras, N. Holonyak, Jr., and M. A. Nixon
Electrical Engineering Research Laboratory and Materials Research Laboratory, University of Illinois at Urbana–Champaign, Urbana, Illinois 61801

R. D. Burnham, W. Streifer, D. R. Scifres, T. L. Paoli, and C. Lindström
Xerox Palo Alto Research Center, Palo Alto, California 94304

(Received 20 January 1983; accepted for publication 16 February 1983)

Data are presented showing that it is possible to photopump and operate a quantum well heterostructure laser at equivalent current densities (J_{eq}) as low as 70 A/cm^2. Continuous 300-K laser operation of a single 60-Å GaAs ($x=0$) quantum well in the center of a ~0.12-μm-thick $x'\sim0.30$ $Al_{x'}Ga_{1-x'}As$ waveguide (and carrier reservoir), which is confined by $x''\sim0.85$ $Al_{x''}Ga_{1-x''}As$ layers, is demonstrated at $I_{eq}\sim0.4$ mA (168 W/cm^2, $J_{eq}\sim70$ A/cm^2). These quantum well heterostructures are grown by organometallic vapor phase epitaxy.

PACS numbers: 42.55.Px, 78.20.Jq, 78.45.+h, 78.55.Ds

Since the first construction of semiconductor lasers[1–4] and then the demonstration of continuous (cw) 300-K operation,[5,6] a continuing goal has been that of reducing the threshold current density J_{th} for continuous (cw) 300-K operation into the range of normal power devices, say, $J_{th}\lesssim100$ A/cm^2. Low operating currents, as such, have been achieved by resorting to a variety of narrow stripe configurations,[7] and this, and not particularly low current densities ($\sim10^3$ A/cm^2), has been mainly the basis for cw 300-K semiconductor laser operation. A more fundamental approach to improving semiconductor lasers is to employ a quantum well active region (see Ref. 8 for a review). Recent

 0003-6951/83/090761-03$01.00

ECS Meeting May 1983
San Francisco

(20)

100 mW CW ROOM TEMPERATURE, 6 μm SHALLOW PROTON STRIPE GaAlAs SINGLE QUANTUM WELL VISIBLE DIODE LASERS

R. D. Burnham, C. Lindström, T. L. Paoli, D. R. Scifres and W. Streifer
Xerox Palo Alto Research Centers
Palo Alto, CA 94304

N. Holonyak, Jr.
Electrical Engineering Research Laboratory and
Materials Research Laboratory
University of Illinois at Urbana-Champaign
Urbana, IL 61801

Abstract

CW room-temperature laser operation at 7300 Å has been achieved at power levels up to 100 mW with a $Ga_{1-x}Al_xAs$ (x ~0.22), ~300 Å thick, single quantum well double heterostructure (SQW-DH) diode grown by organometallic vapor phase epitaxy. The proton-defined contact is 6 μm wide, and the front and rear laser facets are coated for anti-reflection and high-reflection, respectively. The CW threshold current is 86 mA for a 250 μm long device, and linear output power vs. current characteristics are obtained up to 100 mW with an external differential quantum efficiency of 1 W/A. CW output power exceeds 13 mW at 100°C. Between 25-55°C, the pulsed threshold current varies with temperature T as $\exp(T/T_0)$ where T_0 ~187 K.

Visible light-emitting semiconductor lasers with desirable properties such as high CW output powers and linear L-I characteristics are useful as sources in printing and optical memory systems. Gain-guided room temperature CW laser operation of (GaAl)As diodes emitting at wavelengths shorter than 7500 Å has been reported from devices grown by both liquid phase epitaxy (LPE) [1] and organometallic vapor phase epitaxy (OM-VPE) [2-4]. CW lasers grown by LPE [5-7] with built-in refractive index changes along the junction plane have also been reported to emit at wavelengths shorter than 7500 Å.

Clearly, there exist compromises between high power output and short wavelength. Among the highest CW output powers reported for "visible" diode lasers are those of Refs. 2 and 5 for gain- and real-refractive index

cw room-temperature operation of GaAlAs single quantum well visible (7300 Å) diode lasers at 100 mW

R. D. Burnham, C. Lindström, T. L. Paoli, D. R. Scifres, and W. Streifer
Xerox Palo Alto Research Centers, Palo Alto, California 94304

N. Holonyak, Jr.
Electrical Engineering Research Laboratory and Materials Research Laboratory, University of Illinois at Urbana–Champaign, Urbana, Illinois 61801

(Received 3 March 1983; accepted for publication 16 March 1983)

100-mW room-temperature cw laser operation at 7300 Å has been achieved in a $Ga_{1-x}Al_xAs$ ($x \sim 0.22$), ~300 Å thick, single quantum well double heterostructure diode grown by organometallic vapor phase epitaxy. The proton-delineated stripe contact is 6 μm wide, and the front and rear laser facets are coated for antireflection and high reflection respectively. The cw threshold current is 86 mA for a 250-μm-long device, and linear output power versus current characteristics are observed up to 100 mW with an external differential quantum efficiency of 1 W/A (59%). cw output power exceeds 13 mW at 100 °C. Between 25–55 °C, the pulsed threshold current varies exponentially with temperature T as $\exp(T/T_0)$, where $T_0 \sim 187$ K.

PACS numbers: 42.55.Px

Visible light-emitting semiconductor lasers with desirable properties such as high cw output powers and linear L-I characteristics are useful as sources in printing and optical memory systems. Gain-guided room-temperature cw laser operation of (GaAl)As diodes emitting at wavelengths shorter than 7500 Å has been reported for devices grown by both liquid phase epitaxy (LPE)[1] and organometallic vapor phase epitaxy (OMVPE).[2–4] cw lasers grown by LPE[5–7] with built-in refractive index changes along the junction plane have also been reported to emit at wavelengths shorter than 7500 Å.

Clearly, there exist compromises between high power output and short wavelength. Among the highest cw output powers reported for "visible" diode lasers are those of Refs. 2 and 5 for gain, and real-refractive index waveguide devices, respectively. As reported, $\simeq 18$ mW were obtained at 7410 Å in Ref. 2 and 7250 Å in Ref. 5, and both lasers were close to the limit imposed by catastrophic facet degradation. In this letter we report cw room-temperature operation of visible GaAlAs (~7300 Å) OMVPE-grown single quantum well double heterostructure (SQW-DH) lasers at 100 mW. The diode structure consists of nine epitaxial layers grown successively at 775 °C by atmospheric pressure OMVPE in a vertical reactor similar to that used by Manasevit[8] and Dupuis *et al.*[9] The layers are (a) n-GaAs buffer, 0.4 μm thick, Se doped $\sim 1\times10^{18}$ cm^{-3}, (b) n-$Ga_{0.85}Al_{0.15}As$, ~0.4 μm thick, Se doped $\sim 1\times10^{18}$ cm^{-3}, (c) n-$Ga_{0.6}Al_{0.4}As$, ~1.4 μm thick, Se doped $\sim 5\times10^{17}$ cm^{-3}, (d) n-$Ga_{1-y}Al_yAs$ where $y \sim 0.85$, ~1.3 μm thick, Se doped $\sim 3\times10^{17}$ cm^{-3}, (e) undoped $Ga_{1-x}Al_xAs$ where $x \sim 0.22$, $L_z \sim 300$ Å, (f) p-$Ga_{1-y}Al_yAs$ where $y \sim 0.85$, ~1.25 μm thick, Mg doped 2×10^{18} cm^{-3}, (g) p-$Ga_{0.6}Al_{0.4}As$, ~1 μm thick, Mg doped 1×10^{18} cm^{-3}, (h) p-$Ga_{0.85}Al_{0.15}As$, ~0.4 μm thick, Mg doped $\sim 1\times10^{18}$ cm^{-3}, (i) p-GaAs, ~0.2 μm thick, Mg doped greater than 4×10^{19} cm^{-3}. The use of Mg as a p-type dopant in OMVPE growth was first reported by Lewis *et al.*,[10] and more recently by Burnham *et al.*[11] and Lindström *et al.*[12] After growth, the wafer is masked with ~4 μm-thick photoresist, and 6-μm lines on 500-μm centers are exposed with the use of a projection mask aligner. Following development, the wafer is proton bombarded at 100 keV to produce damage to a depth of ~1 μm in the region outside the masked stripes. After polishing the wafer, Cr/Au and AuGe contacts are applied to the p and n sides, respectively. The wafer is cleaved into 250-μm-long bars and diced into chips

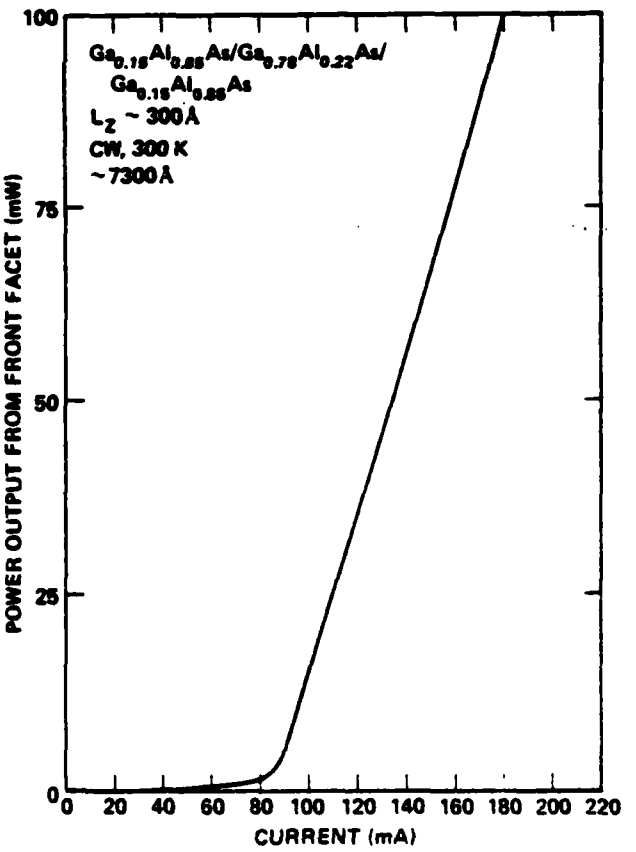

FIG. 1. cw room-temperature L-I characteristics for a $Ga_{1-x}Al_xAs$ SQW-DH laser diode with $L_z \sim 300$ Å and $x \sim 0.22$. The pumping stripe, which is proton delineated, is 6 μm wide and the laser cavity length is 250 μm.

 0003-6951/83/110937-03$01.00

High pressure measurements on photopumped low threshold $Al_x Ga_{1-x} As$ quantum well lasers

M. D. Camras, N. Holonyak, Jr., and J. J. Coleman
Electrical Engineering Research Laboratory and Materials Research Laboratory, University of Illinois at Urbana-Champaign, Urbana, Illinois 61801

H. G. Drickamer
School of Chemical Sciences and Materials Research Laboratory, University of Illinois at Urbana-Champaign, Urbana, Illinois 61801

R. D. Burnham, W. Streifer, D. R. Scifres, C. Lindström, and T. P. Paoli
Xerox Palo Alto Research Center, Palo Alto, California 94304

(Received 3 March 1983; accepted for publication 25 April 1983)

Data are presented on the continuous (cw) 300 K photopumped laser operation of a low threshold $Al_{x'} Ga_{1-x'} As$–GaAs ($x' \sim 0.30$) single quantum well heterostructure (quantum well size $L_z \sim 60$ Å) subjected to high pressure (0–11 kbar) in a simple opposed anvil apparatus. Beyond ~11 kbar where the central $Al_{x'} Ga_{1-x'} As$ waveguide region undergoes a direct–indirect transition, and the waveguide confinement begins to weaken and deep levels tend to become important, the laser threshold increases rapidly and "quenches" cw 300 K operation. Pulsed 300 K photopumped laser operation of an undoped 121-period $Al_x Ga_{1-x} As$–GaAs ($x \sim 0.5$) superlattice in the pressure range from 0–11 kbar is shown for reference. The pressure coefficients of the quantum well heterostructure and the superlattice lasers are comparable (~11 meV/kbar).

PACS numbers: 62.50. + p,78.45. + h,78.20. − e,42.55.Px

I. INTRODUCTION

High pressure has been known for some time as a convenient method to study the band structure of bulk III-V semiconductors.[1] Most recently high pressure has been used to investigate the behavior of quantum well heterostructure (QWH) laser (diode) emission[2] and superlattice (SL) absorption.[3] Unlike previous work, below we describe high pressure measurements on extremely low threshold single quantum well $Al_{x'} Ga_{1-x'} As$–GaAs lasers[4,5] that, as shown here, can be operated continuously (cw) at 300 K by photopumping in a simple opposed anvil apparatus. This type of semiconductor laser operation (photopumped, cw, 300 K at high pressure) has not been previously demonstrated and has the obvious advantage that doped or undoped samples can be compared. We show in the present work that ultralow threshold (cw, 300 K) QWH samples, with a single undoped GaAs quantum well located in an $Al_{x'} Ga_{1-x'} As$ ($x' \sim 0.30$) waveguide (and carrier reservoir),[4,5] become difficult to operate in stimulated emission at pressures corresponding to the Γ-X band crossover of the barrier and waveguide region. The pressure coefficient of the low threshold QWH (laser) crystal is shown to be comparable (~11 meV/kbar) to that of photopumped undoped SL samples.

II. EXPERIMENTAL PROCEDURE

The QWH's and SL's of interest here have been grown by organometallic vapor phase epitaxy (OMVPE).[6,7] The low threshold QWH[5] consists of an undoped single GaAs quantum well of thickness $L_z \sim 60$ Å centered between two barrier layers of $(L_{z'}/2) \sim 600$ Å $Al_{x'} Ga_{1-x'} As$ ($x' \sim 0.30$) which serve as a carrier reservoir and optical waveguide region.[4] This ~0.12 μm "active region" is confined on one side by ~1 μm of Se-doped ($\sim 3 \times 10^{17}/cm^3$) $x'' \sim 0.85$ $Al_{x''} Ga_{1-x''} As$ and on the other side by ~1 μm of Mg-doped ($\sim 5 \times 10^{17}/cm^3$) $x'' \sim 0.85$ $Al_{x''} Ga_{1-x''} As$.[5] The SL, which is undoped and consists of 121 periods of $L_z \sim 85$ Å GaAs wells and $L_B \sim 80$ Å $Al_x Ga_{1-x} As$ ($x \sim 0.5$) barriers, and is capable of cw 300 K laser operation,[8] has been calibrated in earlier high pressure absorption measurements (~11.5 meV/kbar).[3] In the present experiments the SL, which is known to be "well behaved" in high pressure measurements,[3] is used for the sake of comparison. Both forms of samples are stripped of substrate and contact-layer GaAs by polishing and selective etching. The bare (100) samples ($\lesssim 2$ μm thick) are cleaved into small rectangles and are photopumped with an Ar^+ laser (5145 Å).

The small rectangular experimental samples are subjected to high pressure in a simple opposed-anvil apparatus that is driven by a differential screw. One of the anvils is a 0.250-in. diam, 0.250-in.-thick sapphire and the other is polished tungsten carbide of 0.125-in. diameter. The samples themselves are preloaded in a 0.030-in.-thick Be–Cu gasket that has a 0.024-in. center hole filled with Au. Because Au is soft, does not work harden, and does not oxidize, it is used as the pressure transmitting "fluid". Once the samples are loaded onto the Au, they are "locked" in the gasket center by a small square (0.030 × 0.030 × 0.004 in.) diamond heat sink and window that is compressed into the Be–Cu gasket. This gasket assembly is then easily introduced and centered between the anvils.

The samples are photopumped (under pressure) through the sapphire anvil and the diamond window. The samples with the diamond on top, after a compression cycle to over 11 kbar and then back to 0, appear as shown in Fig. 1. (Most of the dark specks are laboratory dust and ruby "dust" as no special precautions have been taken to establish "clean" conditions.) The (a) sample is 16 μm wide and is the

 0021-8979/83/084386-04$02.40

Wavelength modification of $Al_xGa_{1-x}As$ quantum well heterostructure lasers by layer interdiffusion

M. D. Camras and N. Holonyak, Jr.
Electrical Engineering Research Laboratory and Materials Research Laboratory, University of Illinois at Urbana-Champaign, Urbana, Illinois 61801

R. D. Burnham, W. Streifer, D. R. Scifres, T. L. Paoli, and C. Lindström
Xerox Palo Alto Research Center, Palo Alto, California 94304

(Received 9 May 1983; accepted for publication 17 June 1983)

Data are presented showing that thermal annealing (875—900 °C) can be used to modify the wavelength of a photopumped, low threshold $Al_xGa_{1-x}As$ quantum well heterostructure (QWH) laser from ~8200 to ~7300 Å with a threshold change from 150 to 1700 W/cm². The energy levels of the annealed single quantum well crystal are approximated by fitting a modified Pöschl–Teller potential to the band-edge profile as modified by layer (Al–Ga) interdiffusion. The layer (Al–Ga) interdiffusion coefficient (at 875 °C) is found to be smaller, by a factor of 3–4, than previously reported. We suggest that this is due to the high quality, i.e., low defect density, of the ultralow threshold QWH crystals of this work.

PACS numbers: 42.55.Px, 66.30.Ny, 81.40.Tv, 71.50. + t

I. INTRODUCTION

Recent work[1,2] on quantum well heterostructures (QWH) grown by metalorganic chemical vapor deposition (MOCVD)[3,4] has shown that it is possible to locate a small GaAs well ($L_z < 80$ Å) in an $Al_{x'}Ga_{1-x'}As$ ($x' \sim 0.30$) waveguide region ($L_{z'} \sim 0.12$ μm), which itself is confined on either side by ~1 μm of $x'' \sim 0.85$ $Al_{x''}Ga_{1-x''}As$ (Fig. 1 and the inset of Fig. 2), and observe very low threshold photopumped laser operation. Specifically, on such a QWH it is possible to achieve continuous (cw) 300 °K laser operation at equivalent current densities as low as $J_{eq}(\text{th}) < 100$ A/cm². The properties of these low threshold single quantum well lasers are described in some detail in Refs. 1 and 2. Beyond this work, however, a further important feature is apparent: For a QWH with a small enough single quantum well active region (GaAs), it should be relatively easy to thermally anneal the crystal and shift the laser wavelength by layer interdiffusion, i.e., Al–Ga (barrier-well) interdiffusion. The Al–Ga interdiffusion causes the initially finite square well (inset of Fig. 2) to become rounded (smoothed) as shown in Fig. 3 into a shallower $Al_xGa_{1-x}As$ well, and thus shifts the confined-particle electron and hole states to higher energy. In this paper we show that thermal annealing is, indeed, a convenient method to adjust the wavelength of a QWH laser crystal without necessarily an excessive increase in the threshold requirement. For example, the wavelength can be shifted from ~8200 to ~7300 Å with the threshold for photopumped laser operation remaining as low as $J_{eq}(\text{th}) \sim 700$ A/cm².

II. EXPERIMENTAL PROCEDURE

As in previous work,[1,2] the $Al_{x''}Ga_{1-x''}As$-$Al_{x'}Ga_{1-x'}As$-$Al_xGa_{1-x}As$ ($x = 0$, $x' \sim 0.30$, $x'' \sim 0.85$) QWH crystals of these studies have been grown by MOCVD.[3,4] The lowest threshold crystal employed in this work is shown in Fig. 1, which is an SEM photomicrograph of the cleaved and etched QWH supplying the data in succeeding figures. (See also the inset of Fig. 2.) The lower part of the figure is the GaAs substrate. The arrow labelled QW indicates the $L_z \sim 75$ Å GaAs ($x = 0$) quantum well, which is centered in the $L_{z'} \sim 0.12$ μm, $x' \sim 0.30$ $Al_{x'}Ga_{1-x'}As$ carrier reservoir[1,2] and waveguide region. This region is identified by a pair of arrows and with the label $L_{z'}$. The $x \sim 0.30$ waveguide region is confined on either side (top and bottom) with $L_{z'}/2 \sim 1$ μm of $x'' \sim 0.85$ $Al_{x''}Ga_{1-x''}As$. The outer edges (0.2–0.3 μm) of the confining layers are heavily doped (~10^{18}/cm³) with Se, but this is not particularly important for the experiments of interest here. Finally, on top of the

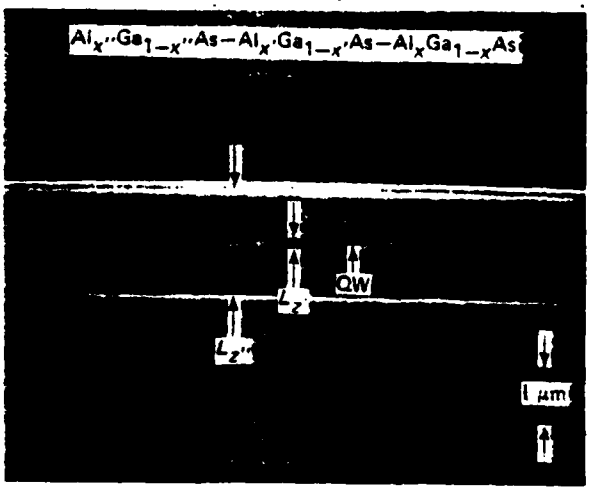

FIG. 1. SEM microphotograph of the cleaved and stained cross section of a single well quantum well heterostructure (QWH) grown by MOCVD at the substrate temperature of 800 °C. The $L_z \sim 75$ Å quantum well QW is confined on both sides by $L_{z'} \sim 0.12$ μm of $x' \sim 0.3$ $Al_{x'}Ga_{1-x'}As$ which itself is confined on both sides by $L_{z''} \sim 2$ μm of $x'' \sim 0.85$ $Al_{x''}Ga_{1-x''}As$ (see inset of Fig. 2). This QWH is sandwiched between a GaAs cap layer at the top and a GaAs substrate on the bottom.

 0021-8979/83/105637-05$02.40

Index of refraction of AlAs-GaAs superlattices

J. P. Leburton and K. Hess
Department of Electrical Engineering and Coordinated Science Laboratory, University of Illinois at Urbana-Champaign, Urbana, Illinois 61801

N. Holonyak, Jr., J. J. Coleman, and M. Camras
Department of Electrical Engineering and Materials Research Laboratory, University of Illinois at Urbana-Champaign, Urbana, Illinois 61801

(Received 2 February 1983; accepted for publication 18 March 1983)

The index of refraction of AlAs-GaAs superlattices is studied both experimentally and theoretically and is compared to the index of the corresponding ternary alloy obtained by intermixing of the superlattice. We find that the index of a superlattice can be 5%–6% higher than the index of the alloy due to zone folding of the states around Γ.

PACS numbers: 78.20.Dj, 78.45. + h

It has been shown by Holonyak *et al.*[1,2] the superlattices can be selectively interdiffused, thus generating patterns of AlGaAs alloy and GaAs-AlAs superlattice regions. These structures have obviously many potential applications in integrated optics. It is therefore desirable to obtain detailed knowledge of the difference in the dielectric function describing the superlattice and the AlGaAs alloy. It is not immediately evident that there are significant differences in the index of refraction of a superlattice versus its disordered alloy, because the index depends mainly on contributions from states around X which probably are influenced only slightly by the superstructure (large effective mass, parallel bands). However, the difference[1] in color of the alloy (yellow) and the superlattice (red) indicates the differences must also exist in the refractive index.

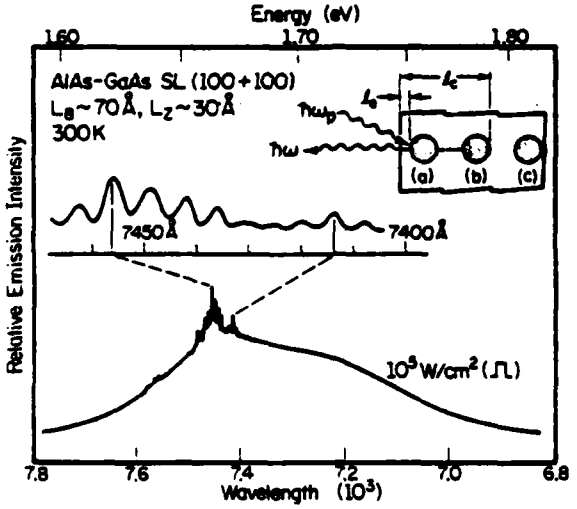

FIG. 1. Photopumped laser operation (300 K, pulsed) of a 100-period AlAs-GaAs superlattice (SL) array of "red" dots or disks [L_B(AlAs)~70 Å, L_z (GaAs)~30 Å] surrounded by impurity-disordered yellow-gap $Al_xGa_{1-x}As$[$x = L_B/(L_B + L_z) \sim 0.7$]. The SL dot (a) (see insert) is photopumped; laser operation occurs from the left cleaved edge to the second SL "red" dot labeled (b), or over a cavity length $l_c \sim 130\ \mu$m which agrees with the fine mode spacing $\Delta\lambda \sim 6$ Å shown on the expanded scale. The edge-to-dot dimension $l_e \sim 18\ \mu$m agrees with the peak-to-peak spacing (7414–7456 Å) of the expanded stimulated-emission spectrum. These mode and spectral data show that the index difference, n(AlAs-GaAs)-n(AlGaAs) > 0, is appreciable. ω_p denotes the pump frequency.

It is the purpose of this communication to show that index differences do exist. We present experimental evidence of reflection at the superlattice-alloy boundaries, and perform a model calculation of the index of refraction showing that the size quantization of states close to Γ introduces subtle differences between alloy and superlattice.

In Fig. 1 we show photoluminescence data obtained on a 100-period AlAs-GaAs superlattice (SL) with barrier size $L_B \sim 70$ Å and well size $L_z \sim 30$ Å. As described elsewhere,[3] this SL when photopumped is capable of continuous 300-K laser operation. Following a relatively low-temperature, short-cycle Zn-diffusion procedure described earlier,[2] with a dot pattern of Si_3Ni_4 serving as a mask to preserve selectively the SL,[1] we obtain the structure shown in the inset of Fig. 1 (see also Fig. 1 of Ref 1). The sample of the inset has a smooth cleaved highly reflecting edge at the left at distance l_e from the first SL dot or disk (a); an irregular edge occurs at the bottom of the sample, and at the right beyond the third SL dot (c) is another irregular edge. Above these dots [(a), (b), (c)] the pattern of SL dots is repeated (not shown). Between the SL dots the crystal has been converted to yellow-gap disordered $Al_xGa_{1-x}As$ alloy [$x = L_B/(L_z + L_B) \sim 0.7$].

The sample of the inset is photopumped (pulsed, $\sim 10^5$ W/cm^2) on the first SL dot, and the spectrum of Fig. 1 is obtained. The sample functions in stimulated emission, with reflection at each dot edge, in the region from the highly reflecting left edge to the second SL dot labeled (b). This is a cavity length $l_c \sim 130\ \mu$m, which is apparently sufficient length to give enough reflection and feedback (at each dot edge) to support the stimulated emission. This behavior agrees with the fact that we observe (visually, not shown) a very clear reflected spot at the left edge of SL dot (b). Also the mode spacing formula

$$\Delta\lambda = \lambda^2[2l_c(n - \lambda dn/d\lambda)]^{-1}, \quad (1)$$

with $(n - \lambda dn/d\lambda) \sim 3.5$, gives $\Delta\lambda \sim 6$ Å, which is in very good agreement with the fine mode spacing shown on the expanded scale (7414–7456 Å) in Fig. 1. Similarly, the spacing of the two expanded-scale peaks in Fig. 1 agrees with the dimension l_e ($\sim 18\ \mu$m). In addition, coarser structure in the spectrum indicates that further reflection (as from the dot edges) exists in the region of length l_c. These data indicate that an index difference, at quantum-well recombination-

 0021-8979/83/074230-02$02.40

Solid State Communications, Vol.48,No.8, pp.671-673, 1983
Printed in Great Britain.

0038-1098/83 $3.00 + .00.
Pergamon Press Ltd.

(25)

QUANTUM WELL LASER OPERATION AT LOW TEMPERATURE IN STRONG MAGNETIC FIELDS

P. Gavrilovic, K. Meehan, and N. Holonyak, Jr.
Electrical Engineering Research Laboratory and Materials Research Laboratory
University of Illinois at Urbana-Champaign, Urbana, Illinois 61801

R.D. Burnham, T.L. Paoli, and W. Streifer
Xerox Palo Alto Research Center
Palo Alto, California 94304

Received 16 August 1983 by J. Tauc

Experimental results on quantum well laser operation in magnetic fields B < 12 T are reported. For B perpendicular (B⊥) to the quantum well a shift toward higher photon energy of ~ 0.5 meV/T is observed, with the laser threshold current decreasing significantly. In parallel magnetic fields (B∥) no significant effect is measured, thus confirming the built-in two-dimensional character of the electron gas.

We report here the results of experiments on the effect of a strong magnetic field (at low temperature) on the energy of stimulated emission from quantum-well heterostructure (QWH) laser diodes. In contrast to the results of experiments on homojunction[1,2] and double heterojunction diodes[3] in which the active region behaves as bulk crystal, the behavior of QWH diodes is governed by the quasi-two-dimensional density of states, a result of the quantum size effect. (See Ref. 4 for a review.) In these earlier experiments, the emission energy corresponds to transitions from donor to acceptor states (homojunction diodes with a heavily compensated active layer) or to transitions from the conduction band to acceptor states (double heterojunction diodes).[3] For the QWH diodes of the present work, however, the transitions are from electron subbands of the conduction band to the heavy-hole or light-hole subbands of the valence band.[4] The laser emission exhibits a linear shift to higher energy with increasing magnetic field B for B perpendicular (B⊥) to the plane of the QW; the energy is independent of B for B parallel (B∥) to the plane of the QW. Simultaneously, the threshold current for lasing with B perpendicular to the quantum-well layers is reduced, while it is unaffected with B parallel to the layers. As will be discussed below, the reduction of the threshold current is a manifestation of the further quantization of the 2-D electron gas by the magnetic field. These observations provide direct experimental proof that the electron gas is quasi-two-dimensional under lasing conditions.

The QWH diodes of this work have been grown by metalorganic vapor phase epitaxy (MOCVD) as previously described.[5] The device structure consists of an undoped single GaAs quantum well of width L_z = 60-80 Å located between two larger (0.06 μm) x' ~ 0.3 $Al_{x'}Ga_{1-x'}As$ barriers, one Se doped (on the substrate side) and the other Mg doped (on the p-contact side). The active region is confined on the substrate side by a 0.9 μm n-type layer of Se-doped Al_x-Ga_{1-x}-As (x" ~ 0.85) and on the other side by a 0.8 μm thick p-type layer of Mg-doped Al_x-Ga_{1-x}-As (x" ~ 0.85).

The wafers are processed into diodes with cavity lengths of 500 μm as described elsewhere.[6] The diodes have either broad area contacts to the p region or are proton-bombarded to produce a 6 μm wide stripe for the active region. The diode dice are mounted p-side down with indium solder onto copper heat sinks. For emission measurements the diodes are mounted in a variable-temperature cryostat which is inserted in the bore of a 12 T superconducting magnet. Temperatures below 4.2 K are obtained by continuously pumping the cryostat. The laser diode output is directed onto the face of a fiber-optic light pipe; the output from the fiber illuminates the entrance slit of a 0.5 m monochromator. The excitation for the diode is provided by either a constant-current source (for DC operation) or by a pulse generator.

In Fig. 1 we show the dependence of the photon energy and excitation current, at lasing threshold, on the magnetic field strength for the transverse orientation, i.e., B perpendicular to the plane of the QW (B⊥). The corresponding data for B parallel to the QW (B∥) are plotted in Fig. 2. The emission energy is taken as that of the dominant mode in the spectrum at each value of B. The spectrum exhibits an increase in energy with magnetic field, starting at ~ 30 kG, in the B⊥ orientation. The data points appear to oscillate about a linear shift or slope because the emission wavelength (and thus the energy) is constrained to values determined by the mode spacing of the laser diode Fabry-Perot cavity. From the experimentally recorded spectra of Fig. 3, it is evident that the magnetic field displaces the center of the emission envelope to higher energy; in addition, the peak energy changes discontinuously. This observation is confirmed

Transient capacitance spectroscopy on large quantum well heterostructures

P. A. Martin, K. Meehan, P. Gavrilovic, K. Hess, N. Holonyak, Jr., and J. J. Coleman
Electrical Engineering Research Laboratory and Materials Research Laboratory, University of Illinois at Urbana-Champaign, Urbana, Illinois 61801

(26)

(Received 28 February 1983; accepted for publication 12 April 1983)

We report transient capacitance measurements on $Al_xGa_{1-x}As$–GaAs–$Al_xGa_{1-x}As$ ($x \sim 0.35$) double heterojunctions with a large quantum well active region ($L_z \sim 800$ Å). It is suggested that the thin GaAs layer acts as a "giant" artificial deep level. It follows then that the band edge discontinuity ΔE_c determines the electron emission rates (from the thin layer), thus making it possible for ΔE_c to be determined by transient capacitance measurements.

PACS numbers: 85.30.De, 73.40.Lq, 68.48. + f, 71.55.Fr

As part of a larger effort, we have been employing deep level transient spectroscopy[1] to examine thin GaAs layers as well as quantum well heterostructure layers.[2] The intent of these measurements has been to determine how the emission rate of electrons (holes) at interfaces or from quantum wells differs from the behavior of bulk crystals. These changes have been anticipated to arise from changes in the energy levels of deep traps close to interfaces and from the two-dimensional final density of states in the quantum well.[3,4] Preliminary experimental results, however, have exhibited peculiarities which, in our opinion, require a very different explanation: the GaAs thin layers *themselves* behave like big traps. We have reported earlier on the dynamics of capture and emission of hot electrons in quantum wells.[5,6] Deep-level transient spectroscopy adds new perspective to this problem and, based on the model employed earlier,[5,6] opens a new method or opportunity to determine band-edge discontinuities. We note that the nature and role of the interface band-edge discontinuities are among the most fundamental problems in the physics of semiconductor heterojunctions,[7] and hence are of much interest.

The experimental samples of the present work have been grown by metalorganic chemical vapor deposition and are nominally doped n-type with Se ($\sim 2\times10^{15}$ cm^{-3}). The double heterojunction (DH) samples consist of a buffer layer of GaAs grown on top of a GaAs substrate, followed by a 1.0-μm confining layer of $Al_xGa_{1-x}As$ ($x \sim 0.35$), a GaAs well ($L_z \sim 800$ Å), and another confining layer of $Al_xGa_{1-x}As$ ($x \sim 0.35$) that is ~ 0.3 μm thick.

For preparation into diodes the DH wafer is first lapped to 5 mil, and Au–Sn is electroplated and alloyed on the substrate side of the wafer. Schottky barriers are then formed on the top AlGaAs confining layer by electroplating 2 μm of Au in a pattern of 11-mil-diam. dots defined by ~ 1200 Å of SiO_2. The Au is applied after the surface has been mildly etched with a dilute solution of 1 HF:7 NH_4F. The resulting devices are separated and attached with silver-filled epoxy to TO-18 headers, and a wire bond to the Schottky barrier completes the diode. These diodes have a forward turn-on voltage of 0.5–0.7 V and a reverse breakdown voltage which varies from diode to diode and is greater than 3 V.

Deep level transient spectroscopy (DLTS) has been performed using a system described elsewhere.[8] In the present work a parallel-plate capacitor was used in place of the second diode. For the DLTS measurements a reverse bias of 1 V is used and 20-μs pulses of varying magnitudes are superimposed on the bias. Two deep levels have been observed (Fig. 1). One, which we label E2, exhibits an energy level at 0.88 eV, a capture cross section of 7.0×10^{-13} cm^2 and a concentration (corrected for the effect of the edge region[9]) of about 5×10^{13} cm^{-3}. E2 behaves as predicted by DLTS analysis and does not show any significant dependence of the signal peak with temperature and the peak height on bias pulse voltage. It is therefore easily attributed to a deep level in the $Al_xGa_{1-x}As$. We have, however, no straightforward explanation of the other peak (E1). The second level, which we label E1, exhibits a peculiar dependence on the forward-bias pulse height and width. This makes fitting to the conventional detailed balance expressions a questionable procedure.

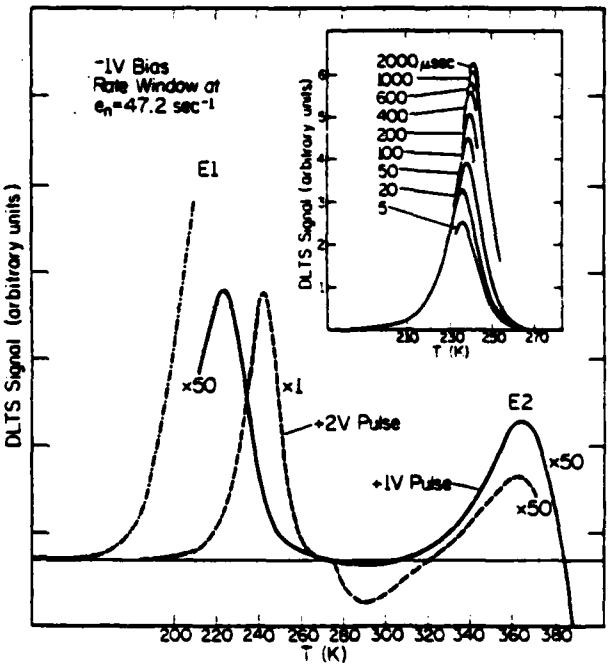

FIG. 1. DLTS scan for 1 V reverse bias with two different bias pulse voltages, showing variation in the height and temperature of the low-temperature peak, E1. The apparent decrease in the signal strength of the second peak (E2) as the bias pulse is increased to 2 V is due to a superimposed minority carrier trap. Inset: variation of peak E1 with bias pulse duration.

 0021-8979/83/084689-03$02.40

Proc. NATO summer school at Miniat. ITALY (1983)

(27)

Superlattices

Karl Hess

Department of Electrical Engineering and
Coordinated Science Laboratory
University of Illinois at Urbana-Champaign
Urbana, IL 61801

1. Introduction

This is a very one-sided review of superlattices and by no means does justice to this rapidly growing field. My intent is to illustrate possibilities inherent in the variability of boundary conditions in finite superlattices or more generally speaking, multiple heterostructure layers.

In recent years, much progress has been made in the technology and basic understanding of superlattices and lattice-matched III-V compound heterostructure layers in general [1]. Two new epitaxial technologies have emerged -- molecular beam epitaxy (MBE) [2] and metalorganic chemical vapor deposition (MOCVD) [3] -- which have opened a variety of new possibilities, including superlattice transport as discussed by Esaki, Tsu, and Chang [4-6], the fabrication of materials exhibiting extremely high mobilities [7], quantum well heterostructure lasers [8,9], planar doped barrier structures [10], and real space transfer switching [11]. More recent research has also concentrated on strained (lattice mismatch) superlattices [12] and on type II superlattices [6].

PRINCIPLES OF HOT ELECTRON THERMIONIC EMISSION (REAL SPACE TRANSFER) IN SEMICONDUCTOR HETEROLAYERS AND DEVICE APPLICATIONS

K. Hess

Department of Electrical Engineering and
Coordinated Science Laboratory
University of Illinois at Urbana-Champaign
Urbana, Illinois 61801

ABSTRACT

The principles of real space transfer and its phenomenological description in terms of the concepts of electron temperature and quasi Fermi levels are reviewed. It is shown that real space transfer is a mechanism to achieve ultrafast switching and storage of charge carriers. The real space transfer-glow cathod analogy, which demonstrates the existence of a new transistor principle, is discussed in detail.

INTRODUCTION

The technologies of molecular beam epitaxy (MBE) and metalorganic chemical vapor deposition (MOCVD) have opened a world of possibilities to create new forms of III-V semiconductor heterolayer materials. Structures hundred times as sophisticated and small as the smallest feature sizes in current silicon technology can be fabricated with ease. This fine tuned variability of structure and boundary conditions offers many opportunities for the development of new device concepts and research in this area is rapidly expanding [1].

Advantages of III-V compounds with respect to steady state mobility and transient electronic transport [1] (velocity overshoot) have long been known. However, the realization of these advantages in applications have been impeded by technological difficulties. MBE and MOCVD have provided a quantum leap in material quality and controlability, which together with the ideas of selective (modulation) doping [2] and achievable abruptness of

Book chapter
Springer (1985)
L. Reggiani, editor

(29)

Hot Electrons in Semiconductor Heterostructures and Superlattices

Karl Hess

Department of Electrical Engineering and
Coordinated Science Laboratory
University of Illinois at Urbana-Champaign
Urbana, IL 61801

Gerald J. Iafrate

U. S. Army Electronics Technology and
Devices Laboratory
Fort Monmouth, NJ 07703

Stimulated emission in strained-layer quantum-well heterostructures

M. D. Camras, J. M. Brown, N. Holonyak, Jr., M. A. Nixon, and R. W. Kaliski
Electrical Engineering Research Laboratory and Materials Research Laboratory, University of Illinois at Urbana-Champaign, Urbana, Illinois 61801

M. J. Ludowise, W. T. Dietze, and C. R. Lewis
Corporate Solid State Laboratory, Varian Associates, Incorporated, Palo Alto, California 94303

(Received 6 June 1983; accepted for publication 27 July 1983)

Stimulated emission data are presented on a large variety of strained-layer quantum-well heterostructures (QWH's) and superlattices (SL's) grown by metalorganic chemical vapor deposition (MOCVD). These structures consist of barrier-well combinations of thickness $L_B, L_z \lesssim 150$ Å made from GaAs-InGaAs, GaAsP-GaAs, and GaAsP-InGaAs. Also employed are higher band-gap confining layers of $In_xAl_yGa_{1-x-y}As$, $Al_yGa_{1-y}As_{1-x}P_x$, and $Al_xGa_{1-x}As$. All of the heterostructures are grown on a GaAs substrate with and, in some cases, without a graded layer. The strain range between 0.2 to 12.5×10^{-3} is examined. Photopumped, these heterostructures operate as *continuous* (cw) 300 K lasers, with thresholds of $1.6–7.5\times10^3$ W/cm^2, for periods of time between 0.5 to > 35 min. Under high-level excitation, the equivalent of $J_{eq}\sim10^3$ A/cm^2, laser operation fails or is quenched by networks of dislocations (with ⟨110⟩ Burger's vectors) that are generated within the strained-layer region of the QWH's or SL's. These dislocation networks, which are revealed via transmission electron microscopy (TEM), occur at a more rapid rate in higher threshold samples and ones with higher built-in strain. The TEM data show, however, that no heterointerface defects (dislocations) are present in the as-grown strained-layer regions but are present in thick (bulk) graded regions.

PACS numbers: 42.55.Px, 78.45. + h, 68.48. + f, 78.55.Ds

I. INTRODUCTION

Since the initial demonstration of III-V compound epitaxy,[1] the question has persisted to what extent layer mismatch can be tolerated in semiconductor heterostructures. For example, early work has shown that in the usual thick-layer form of $GaAs_{1-x}P_x$ ($x\neq0$) grown on GaAs the resulting single heterostructure fails as an improved form of laser or LED because of the large defect density at the heterointerfaces.[2–4] If the heterolayers are thin enough, however, as in the strained-layer superlattices (SL's) first grown by Blakeslee,[5] then presumably the interface defect density can be kept low because of elastic deformation of the layers. Recently Osbourn and co-workers[6] have revived the interest in strained-layer SL's by suggesting that indirect-gap GaP-$GaAs_{1-x}P_x$ strained-layer SL's can, because of zone folding, act direct. This, of course, is not sufficient for the observation of a high level of luminescence, even if the layer sizes are small enough,[7] unless the heterointerfaces are sufficiently free of defects. The argument can be reversed: if a high level of luminescence, specifically stimulated emission, is observed on a strained-layer heterostructure [SL or quantum-well heterostructure (QWH)], then we can conclude that the defect density is low and, without argument, the crystal is direct (or effectively direct). It is, of course, easier to consider a strained-layer SL or QWH consisting of direct-gap quantum-well layers and then determine whether the density of heterointerface defects is large or small, stimulated emission serving as the basis for the determination. Proceeding in this manner, recently we have demonstrated that a strained-layer SL can be grown free enough of defects at heterointerfaces to make possible stimulated emission.[8] This has been demonstrated on $GaAs_{1-x}P_x$-GaAs ($x\sim0.25$) and GaAs-$In_xGa_{1-x}As$ ($x\sim0.2$)[9] strained-layer SL's grown via metalorganic chemical vapor deposition (MOCVD).[10] These SL's have, in fact, been operated *continuously* (cw) as photopumped 300 K lasers but at high excitation level ($J_{eq}\gtrsim10^3$ A/cm^2) prove to be unstable.[9]

In this paper we present a considerable extension of this work. Room temperature and cw laser operation (via photoexcitation) is described on a variety of strained-layer heterostructures. These include SL structures and single or double wells confined by SL sections. The III-V materials GaAs, $In_xGa_{1-x}As$, and $GaAs_{1-x}P_x$ have been used for quantum wells and for coupling barriers, e.g., the barrier-well combinations employed are GaAs-InGaAs, GaAsP-GaAs, and GaAsP-InGaAs. Layer sizes are in the range $L_B, L_z \lesssim 150$ Å. For improved photoluminescence performance, wider-gap confining layers of $Al_xGa_{1-x}As$, $Al_yIn_xGa_{1-x-y}As$, or $Al_yGa_{1-y}As_{1-x}P_x$ have been grown on the samples. Gallium arsenide, with or without the use of graded layers, has been used as the substrate crystal, and strain magnitudes in the range from 0.2 to 12.5×10^{-3} have been considered. The stability of these heterostructures at high excitation level (the equivalent of $J_{eq}\sim10^3$ A/cm^2) has been examined. We show that cw 300 K laser operation is quenched by the generation of a network of dislocations, which indicates that a serious problem exists in the high level operation of strained-layer SL's or QWH's but which does not imply that stable low level operation is not possible.

II. CRYSTAL GROWTH AND SAMPLE PREPARATION

As mentioned, the QWH and SL crystals of interest here have been grown by metalorganic chemical vapor deposition (MOCVD).[10] Epitaxial layers are grown on GaAs:Sn

 0021-8979/83/116183-07$02.40

Broadband tuning ($\Delta E \sim 100$ meV) of $Al_xGa_{1-x}As$ quantum well heterostructure lasers with an external grating

J. E. Epler and N. Holonyak, Jr.
Electrical Engineering Research Laboratory and Materials Research Laboratory, University of Illinois at Urbana–Champaign, Urbana, Illinois 61801

R. D. Burnham, C. Lindström, W. Streifer, and T. L. Paoli
Xerox Palo Alto Research Center, Palo Alto, California 94304

(Received 30 June 1983; accepted for publication 8 August 1983)

$Al_xGa_{1-x}As$-GaAs quantum well heterostructure laser diodes are shown to be tunable over a 100-meV range when operated continuously (cw) at room temperature in an external cavity with a grating to control feedback. The gain profile of the $n = 1$ and $n' = 1'$ (electron-to-heavy hole and electron-to-light hole, $e \rightarrow hh$ and $e \rightarrow lh$) transitions and the $n = 2$ electron-to-heavy hole transitions are clearly outlined by the intensity profile of the selected laser lines. The partial homogeneous broadening of the gain profile agrees with rapid carrier relaxation in the well. The diodes contain a single 60–90-Å GaAs well and are grown by metalorganic chemical vapor deposition.

PACS numbers: 42.55.Px, 42.60.Da, 78.45. + h

Since the successful demonstration, *at room temperature*, of wavelength tuning of a diode laser with an external grating by Rossi and coworkers,[1] III-V heterojunction lasers[2–8] have been operated (300 K) on numerous occasions in such manner and have yielded a variety of tuning ranges ($\Delta\hbar\omega \lesssim 40$ meV), linewidths, and threshold currents. The external grating provides a convenient method for probing the gain profile, selectively influencing the carrier recombination process and, of course, determining the lasing wavelength. Quantum well heterostructure (QWH) lasers have a unique advantage over previously tuned diode lasers in that the active region can be band filled to well above the bulk crystal band edges at moderate current densities[9] and thus are excellent candidates for broadband tuning. The gain profile of the band filled confined-particle transitions provides, at sufficient current level (and lattice temperature), a large energy range for stimulated emission. In this letter we describe the $\Delta\hbar\omega \sim 100$ meV tuning range (8300–7800 Å) obtained with an external grating on a single-stripe (6 μm wide) single well QWH diode operated (300 K) continuously (cw) at $I = 88.5$ mA. The QWH laser diode is shown to exhibit partial homogeneous line broadening. For example, when the grating is tuned to a wavelength ($\lambda \sim 8317$ Å) near the $n = 1$ and $n = 1'$ transitions, the rapid depletion of the excess carriers reduces, as expected,[10] the intensity of the higher energy emission, as high in energy as $\Delta E \sim 2\hbar\omega_{LO}$ ($\lambda \sim 7875$ Å).

The QWH diodes of interest here are grown by metalorganic chemical vapor deposition (MOCVD) as previously described.[11] A low threshold single well QWH design is employed[12,13] that simulates the single well and the high-energy photopumped laser operation shown in Fig. 10 of Ref. 9. An undoped GaAs quantum well of thickness $L_z = 60$–90 Å is grown between two larger $Al_{x'}Ga_{1-x'}As$ ($x' \sim 0.3$) layers of

 0003-6951/83/200740-03$01.00

Wavelength modification ($\Delta\hbar\omega = 10$–40 meV) of room temperature continuous quantum-well heterostructure laser diodes by thermal annealing

K. Meehan and N. Holonyak, Jr.
Electrical Engineering Research Laboratory and Materials Research Laboratory, University of Illinois at Urbana-Champaign, Urbana, Illinois 61801

R. D. Burnham, T. L. Paoli, and W. Streifer
Xerox Palo Alto Research Center, Palo Alto, California 94304

(Received 30 June 1983; accepted for publication 29 August 1983)

Data are presented showing that wavelength modification, of at least 210 Å (from 8180 to 7970 Å), of broad area room temperature pulsed quantum well heterostructure (QWH) laser diodes is possible by thermal annealing. Thermal annealing at 900 °C for 8 h results in only a minor change in the threshold current density, 385–425 A/cm², thus making possible similar wavelength modification (8180–8080 Å) of *continuous* (cw) 300 K stripe-geometry QWH laser diodes.

PACS numbers: 42.55.Px, 73.40.Lq, 81.40.Tv, 81.40.Ef

Recent work[1] has shown that wavelength modification of *undoped* $Al_{x'}Ga_{1-x'}As$-$Al_xGa_{1-x}As$ $[x(t=0)=0]$ quantum well heterostructures (QWH's) by thermal annealing at 875–925 °C (~8 h) results in wavelength shifts from ~8200 to ~7300 Å with the threshold (J_{th}) for photo-pumped (single well) laser operation remaining below the limit for room temperature continuous (cw) operation. The layer (Ga-Al) interdiffusion coefficient at 875 °C has been found previously to be 2.5×10^{-18} cm²/s,[1] or significantly lower than reported in earlier work.[2] Nevertheless, the diffusion length $l=\sqrt{Dt}\sim27$ Å (8 h) indicates immediately that QWH's with well sizes $L_z \lesssim 100$ Å are good candidates for controllable and selectable modification to shorter wavelength by thermal annealing and by well-layer, barrier-layer (Ga-Al) interdiffusion. In fact, it is even possible to determine approximately the position of the energy levels of the resulting QWH by fitting a modified Pöschl–Teller potential to the modified (annealed) band-edge profile.[1] In the present work, we show that a *p-n* QWH (with a single GaAs quantum well, $L_z < 80$ Å) that operators as a cw 300-K laser can be thermally annealed at (875–900 °C) and be shifted to shorter wavelength without a significant change in threshold (J_{th}). We show that annealing of a QWH at 875 °C for 8 h results in small wavelength modification and that ~900 °C annealing leads to a change in photon energy of $\Delta\hbar\omega = 20$–40 meV, or more for annealing periods exceeding 8 h (or 900 °C).

The *p-n* heterostructure crystals of this work are $Al_{x''}Ga_{1-x''}As$-$Al_{x'}Ga_{1-x'}As$-$Al_xGa_{1-x}As$ ($x=0$, $x'\sim0.30$, $x''\sim0.85$, $L_z<80$ Å) QWH's grown by metalorganic chemical vapor deposition (MOCVD).[3,4] The active region consists of an $L_z<80$ Å GaAs quantum well that is located in the center of a larger ($L_{x'}\sim0.13$ μm) $Al_{x'}Ga_{1-x'}As$ ($x'\sim0.30$) layer that acts as a carrier reservoir[4,5] and as a waveguide region (e.g., see the inset of Fig. 2 of Ref. 6). This region is confined on either side by $x\sim0.85$ $Al_{x''}Ga_{1-x''}As$. The *n*-type confining layer ($n_{Se}\sim5\times10^{17}$/cm³) is ~2.8 μm thick; the *p*-type confining layer ($n_{Zn}\sim5\times10^{17}$/cm³) is ~0.6 μm thick. Because of the low Zn concentration in the *p*-type confining layer, the quantum well boundaries (and confined-particle energies) are not modified significantly by Zn diffusion since there is a relatively large threshold concentration for this to occur.[7]

After the thermal annealing of the as-grown QWH's, the crystal is Zn diffused for 10 min at 600 °C to ensure that the *p*-type GaAs cap layer is sufficiently doped for Ohmic contacts. Then the wafer is lapped and polished from the substrate side to a thickness of 100–125 μm. Next the wafer is metallized on the *p* side with 100 Å of Au + 500 Å of Cr + 1000 Å of Au and on the *n* side with 100 Å of Au + 400 Å of Cr + 1000 Å of Au, and is heated at 300 °C for 10 s in a hydrogen atmosphere. The crystals are then cleaved and sawed into dice 250×250 μm and are attached to TO-18 headers. The mesa stripe diodes used for cw 300 K measurements are similarly metallized, but first are etched through the active region with 24-μm stripes protected by photoresist. Also, before the metallization a 120-Å SiO_2 layer is deposited on the surface, and contact stripes of 12 μm are opened centered over the 24-μm mesa stripes.

A thermal anneal carried out in an evacuated quartz ampoule with excess As[1,2] at 875 °C (8 h) causes little shift in wavelength from that of the as-grown crystal.[8] A 900 °C anneal (8 h); however, causes (Fig. 1) a 40-meV shift in wavelength (from 8180 to 7970 Å). The threshold current density is observed to increase from 385 A/cm² (875 °C, 8 h) to 425 A/cm² (900 °C, 8 h), which, actually, is negligible when the difference in diode length is considered (200 vs 230 μm). We note that, indeed, little change is expected in the threshold current since a quantum-well laser diode is modified by thermal annealing into another quantum-well laser diode, with square well uniformly modified into a rounded well.

As seen in Fig. 2, cw 300-K laser operation of a *p-n* QWH is possible after thermal annealing near 900 °C (8 h). The wavelength shift to 8080 Å, as opposed to that of 7970 Å in Fig. 1, is due to uncontrolled variability in the two different annealing runs and also bandfilling differences in pulsed and cw diode operation, not to mention differences in diode geometries. In the case of the former (variable annealing), any change in the layer (Al-Ga) interdiffusion causes a significant shift in the quantum-well shape and well energies (wavelength).[1] We mention that the Fabry–Perot modes drawn on the 5.5 mA (a) curve of Fig. 2 represent only one

 0021-8979/83/127190-02$02.40

Thermal-anneal wavelength modification of multiple-well p-n $Al_xGa_{1-x}As$-GaAs quantum-well lasers

K. Meehan,[a] J. M. Brown, P. Gavrilovic, and N. Holonyak, Jr.
Electrical Engineering Research Laboratory and Materials Research Laboratory, University of Illinois at Urbana-Champaign, Urbana, Illinois 61801

R. D. Burnham, T. L. Paoli, and W. Streifer
Xerox Palo Alto Research Center, Palo Alto, California 94304

(Received 3 October 1983; accepted for publication 23 November 1983)

Data are presented showing that ordinary thermal annealing can be used to modify GaAs square wells into rounded $Al_xGa_{1-x}As$ quantum wells and shift the continuous 300-K laser operation of a p-n multiple-well $Al_xGa_{1-x}As$–GaAs heterostructure laser to higher energy. Transmission electron microscopy is used to show that thermal annealing at 900 °C for 10-h changes, for example, well sizes from 85 to 105 Å and coupling barriers from 95 to 75 Å, which results in a change of laser photon energy of $\Delta\hbar\omega \sim 50$ meV. Bandfilling is minimal in multiple quantum-well lasers, thus making thermal annealing a useful method to "tune" a continuous 300-K quantum-well laser to shorter wavelength as shown here. These thermal annealing experiments indicate that the Al-Ga interdiffusion coefficient at a heterointerface is $D(900) \sim 10^{-18}$ cm^2/s.

PACS numbers: 42.55.Px, 81.40.Ef, 73.40.Lq, 66.30.Ny

I. INTRODUCTION

If we consider an $Al_xGa_{1-x}As$-GaAs heterointerface, say, in a typical double heterostructure (DH) laser with a GaAs active region of thickness $L_z > 500$ Å, and consider what times and temperatures are needed for Al-Ga interdiffusion (or AlGaAs-GaAs layer interdiffusion) for there to be a significant change in the heterostructure, times exceeding 10 h and temperatures exceeding 900 °C are required. That is, the Al-Ga interdiffusion constant is known to be quite small,[1,2] and thermal annealing is not a very viable method to effect an important change in an $Al_xGa_{1-x}As$-GaAs DH laser. In contrast to the relative insensitivity of ordinary $Al_xGa_{1-x}As$-GaAs DH's to thermal annealing as a method of modifying the basic DH structure, and thus wavelength, the small well and barrier dimensions ($L_z < 100$ Å) of quantum-well heterostructures (QWH's) make them ideally suited to this purpose. That is, an as-grown QWH crystal, although highly uniform across its area, often differs in quantum-well size (L_z) sufficiently from the design choice to give a wavelength longer than desired. As recently shown on *single-well* undoped QWH crystals[2] and p-n doped QWH crystals,[3] ordinary thermal annealing can be used to modify a square well (dashed in Fig. 1) to a rounded well (solid profile in Fig. 1), thus shifting the wavelength from longer to shorter ($1 \rightarrow e1$ and $1 \rightarrow hh1$ in Fig. 1). This procedure makes sense because, e.g., at practical annealing times such as $t \sim 10$ h and temperatures ~ 900 °C, the Al-Ga interdiffusion constant is $D(900) \sim 10^{-18}$ cm^2/s and $l = \sqrt{Dt} \sim 20$ Å, which is obviously significant compared to L_z ($l \sim L_z$).

Clearly, for wavelength modification of a QWH laser to be important, it must apply to p-n QWH's that can be fabricated into diode lasers that operate continuously (cw) at room temperature (300 K). This has so far been demonstrated only for the case of a single-well p-n QWH laser,[3] but not for multiple-well designs. Yet it is the latter that are required in many cases because of certain basic differences in the charge-filling behavior of these two forms of QWH's: Specifically, bandfilling and a large spectral width (and tuning range)[4] can be accomplished in the case of a single-well QWH, whereas in a multiple-well QWH bandfilling is minimal (or can be) and the spectral width narrow. In this paper we show that, in fact, multiple-well p-n QWH's that are capable of operating as cw 300-K lasers can, by thermally annealing (at ~ 900 °C), be shifted in energy by as much as $\Delta\hbar\omega \sim 50$ meV and be fabricated into shorter wavelength cw 300-K lasers. In addition, we show directly via transmission

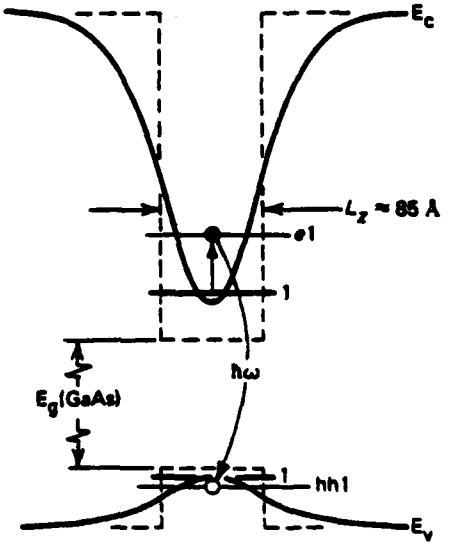

FIG. 1. Schematic diagram of the energy band of an as-grown GaAs quantum well ($L_z \approx 85$ Å, dashed-line profile) and after a 900 °C thermal anneal for 10 h, which results in a rounded $Al_xGa_{1-x}As$ quantum well (solid-line profile). The bound states move up in energy from $1 \rightarrow e1$ and $1 \rightarrow hh1$ as the result of the anneal. The composition of the $Al_xGa_{1-x}As$ well changes ($0 \rightarrow x$) and the well widens (85→105 Å), resulting in a graded interface between the well and the $x' \sim 0.30$ $Al_{x'}Ga_{1-x'}As$ barrier layers.

[a] IBM doctoral fellow.

 0021-8979/84/072672-04$02.40

Impurity-induced disordering of single well $Al_xGa_{1-x}As$-GaAs quantum well heterostructures

K. Meehan,[a] J. M. Brown, M. D. Camras, and N. Holonyak, Jr.
Electrical Engineering Research Laboratory and Materials Research Laboratory, University of Illinois at Urbana–Champaign, Urbana, Illinois 61801

R. D. Burnham, T. L. Paoli, and W. Streifer
Xerox Palo Alto Research Center, Palo Alto, California 94304

(Received 7 November 1983; accepted for publication 8 December 1983)

Transmission electron microscopy and photoluminescence data are used to show that a *single* GaAs quantum well ($L_z \approx 70$ Å) confined by $Al_{x'}Ga_{1-x'}As$ ($x' \sim 0.3$) layers can, via low-temperature (600 °C) Zn diffusion, be interdiffused ("absorbed") into the confining layers (impurity-assisted Al-Ga interdiffusion) and be shifted to higher gap ($x = 0 \rightarrow x' \sim 0.3$) without damaging the crystal or ruining its capability to operate as a continuous 300-K low threshold photopumped laser.

PACS numbers: 66.30.Jt, 73.40.Lq, 42.55.Px, 61.16.Di

Since the recent discovery of impurity-induced disordering of $Al_xGa_{1-x}As$-GaAs superlattices (SL's) via low-temperature (500–600 °C) Zn diffusion,[1–3] this area of work has been extended to include ion implantation with Si and Zn impurities.[4,5] Also impurity-induced disordering of strained-layer superlattices by means of Zn diffusion has been demonstrated.[6] In almost all the studies performed to date, impurity-induced disordering experiments have been conducted on SL systems, which, although of fundamental interest, are not necessarily all that practical. Most practical forms of quantum well heterostructures (QWH's) are not SL's, or not even small SL's of, let us say, at least a half dozen periods. In many cases only one quantum well layer is a necessary or fundamental part of a practical QWH device, e.g., a laser, and it is important in such instances to determine the nature of the resulting heterostructure after impurity-induced layer disordering. We consider this problem and show here that a single GaAs ($x = 0$ $Al_xGa_{1-x}As$) quantum well confined by $Al_{x'}Ga_{1-x'}As$ ($x' \sim 0.3$) barriers can be "disordered" (layer interdiffused) out of existence ($x \rightarrow x'$) by low-temperature impurity diffusion and not cause any noticeable damage in the resulting heterostructure. This is demonstrated by means of transmission electron microscopy (TEM) and comparison of the as-grown crystal with the crystal modified by impurity-induced disordering (or Al-Ga interdiffusion).[1–3] Confirming photoluminescence data are presented showing that the disordered region ($GaAs \rightarrow Al_{x'}Ga_{1-x'}As$) is not damaged. That is, in essence the GaAs quantum well (QW) is "absorbed."

The $Al_{x''}Ga_{1-x''}As$-$Al_{x'}Ga_{1-x'}As$-$Al_xGa_{1-x}As$ ($x'' \sim 0.85$, $x' \sim 0.3$, $x = 0$) QWH crystal used in this work has been grown by metalorganic chemical vapor deposition (MOCVD) as described elsewhere.[7,8] Of particular interest, the QWH crystal employed here has previously been used in thermal annealing layer-modification and wavelength-modification experiments[9] and even earlier has been used, in as-grown form, to demonstrate very low threshold continuous (cw) 300-K photopumped laser operation.[10] A TEM micrograph of the as-grown QWH is shown in (a) of Fig. 1. The top $Al_{x''}Ga_{1-x''}As$ ($x'' \sim 0.85$) confining layer appears faded because of thickness variations in the ion-milled specimen. For present purposes, however, this is unimportant inasmuch as a clear cross section of all of the as-grown layers appears in Fig. 1 of Ref. 9. The most important portion of the QWH in the present experiments is the $Al_{x'}Ga_{1-x'}As$ ($x' \sim 0.3$) waveguide region of thickness $L_{x'} \approx 0.13$ μm with, in its center, an $L_z \approx 70$-Å GaAs QW (an $x = 0$ $Al_xGa_{1-x}As$ QW).

A portion of the QWH crystal with the top GaAs layer removed has been subjected to Zn diffusion at 600 °C for 10 h in one case and for 20 h in another. Masking Si_3N_4 dots of 37-

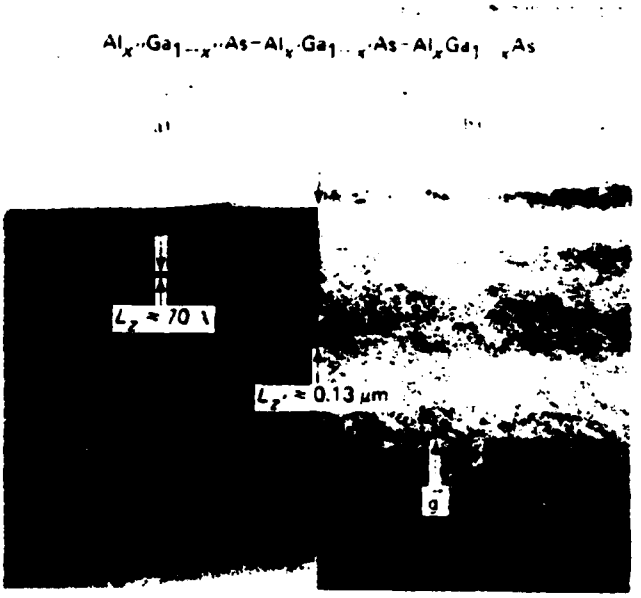

FIG. 1. Transmission electron microscope (TEM) micrographs of (a) an as-grown $Al_{x''}Ga_{1-x''}As$-$Al_{x'}Ga_{1-x'}As$-$Al_xGa_{1-x}As$ ($x'' \sim 0.85$, $x' \sim 0.30$, $x = 0$) quantum well heterostructure (QWH), and (b) the QWH after Zn diffusion at 600 °C for 10 h. As shown in (b), the Zn-induced low-temperature Al-Ga interdiffusion eliminates the $L_z \approx 70$-Å QW ($x \rightarrow x'$), smears the x''-x' heteroboundaries, and broadens the $L_{x'} \approx 0.13$-μm $Al_{x'}Ga_{1-x'}As$ ($x \sim 0.3$) waveguide region, but does not cause damage (dislocations) or ruin the crystalline properties of the $x' \sim 0.3$ center region (electron diffraction pattern inset at lower right). (The TEM g vector is in the 200 direction.)

[a] IBM doctoral fellow.

 0003-6951/84/040428-03$01.00

Stripe-geometry AlGaAs-GaAs quantum-well heterostructure lasers defined by impurity-induced layer disordering

K. Meehan,[a] J. M. Brown, and N. Holonyak, Jr.
Electrical Engineering Research Laboratory and Materials Research Laboratory, University of Illinois at Urbana–Champaign, Urbana, Illinois 61801

R. D. Burnham, T. L. Paoli, and W. Streifer
Xerox Palo Alto Research Center, Palo Alto, California 94304

(Received 5 December 1983; accepted for publication 16 January 1984)

Stripe-geometry AlGaAs-GaAs single quantum-well heterostructure lasers are demonstrated in which the region complementary to the stripe (outside of and defining the stripe) is shifted to higher band gap, and lower refractive index, by low-temperature (600 °C) Zn diffusion. Impurity-induced Al-Ga interdiffusion causes the single GaAs quantum well ($x = 0$, $L_z \approx 80$ Å) outside of the stripe region to be mixed ("absorbed," $x \rightarrow x'$) into the $Al_{x'}Ga_{1-x'}As$ ($x' \sim 0.3$, $L_y \approx 0.18\,\mu$m) bulk-layer waveguide of the crystal.

PACS numbers: 42.55.Px, 73.40.Lq, 66.30.Jt, 85.60.Jb

Previous work has established that AlGaAs-GaAs quantum-well heterostructures (QWH's) are unstable against Zn diffusion,[1-4] even at temperatures (< 600 °C) well below those that are employed (> 600 °C) in the epitaxial QWH crystal growth. Perhaps equally important, Zn or Si implantation, followed by thermal annealing, can be used to interdiffuse (Al-Ga) and disorder, or mix, $Al_xGa_{1-x}As$ ($0 < x < 1$) and GaAs quantum-well layers.[5,6] Either process, diffusion or implantation, can be used to change (*increase*), selectively, the effective energy gap of the layered quantum-well heterostructure to that of ordinary disordered-alloy bulk single crystal. Recent data show that the disordered higher gap bulk alloy is not damaged[7] and, most important, can be arranged in arbitrary geometrical patterns and micropatterns, via conventional photolithography procedures.[2] That is, the as-grown lower gap QWH and the surrounding impurity-disordered higher gap bulk alloy can be arranged in any desired complementary pattern. In this letter we describe the use of this process to construct stripe-geometry QWH laser diodes. The Zn-diffused region not only is shifted to higher energy gap than the as-grown (masked) QWH stripe but also is reduced in index of refraction,[2,8] resulting then in an index-guided laser diode.

The single well *p-n* Al_x-Ga_{1-x}-As-$Al_{x'}Ga_{1-x'}$As-$Al_xGa_{1-x}As$ ($x = 0$, $x' \sim 0.30$, $x'' \sim 0.85$; $L_z \approx 80$ Å) QWH crystal employed in this work is grown by metalorganic chemical vapor deposition (MOCVD),[9,10] and is shown slanting upward from left to right in Fig. 1. Figure 1 is a scanning electron microscope (SEM) micrograph of an etched piece of the *p-n* QWH that on the right has been subjected to Zn diffusion for 1.5 h at 600 °C ($D \sim 2 \times 10^{-12}$ cm²/s). The portion of the QWH on the left is the as-grown crystal. The portion of the crystal at the left between the offset triangular "tick" marks labeled "c" (▽ △) is an as-grown Zn-doped GaAs contact layer (~0.2 μm). Below this is a Zn-doped ($n_{Zn} \sim 5 \times 10^{17}$/cm³) Al_x-Ga_{1-x}-As ($x'' \sim 0.85$) top confining layer that is ~0.6 μm thick. Just below the confining layer is an $Al_{x'}Ga_{1-x'}As$ ($x' \sim 0.30$) waveguide region (the active region), which, as shown, is $L_y \approx 0.18\,\mu$m thick. Slightly above center (at the left) in the waveguide region is a GaAs ($x = 0$) quantum well which is marked (QW) with a triangular "tick" mark (△). The inset in Fig. 1 at the lower right is a ~10× higher magnification transmission electron microscope (TEM) micrograph of a portion of the as-grown waveguide region, a region as wide as that between the "tick" marks at the dimension arrows at the lower left. The inset shows clearly the GaAs quantum well ($L_z \approx 80$ Å). Finally, below the $Al_{x'}Ga_{1-x'}As$ waveguide region is a thick (~2.8 μm) *n*-type ($n_{Se} \sim 5 \times 10^{17}$/cm³) Al_x-Ga_{1-x}-As ($x'' \sim 0.85$) bottom confining layer, and then the *n*-type GaAs substrate (not shown).

Before the Zn diffusion (Zn_2As_3), a Si_3N_4 masking layer ~1000 Å thick is deposited on the crystal and is covered with the photoresist stripe pattern desired. The Si_3N_4 is selectively removed from the region to the right of "c" in Fig.

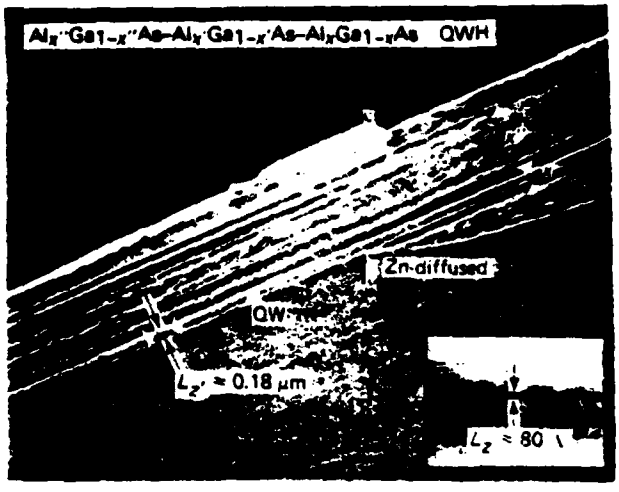

FIG. 1. Etched cross section, viewed by scanning electron microscope, of an Al_x-Ga_{1-x}-As-$Al_{x'}Ga_{1-x'}$As-$Al_xGa_{1-x}As$ ($x = 0$, $x' \sim 0.30$, $x'' \sim 0.85$) quantum-well heterostructure that has been masked with Si_3N_4 on the left and has been Zn diffused (Zn_2As_3) on the right at 600 °C for 1.5 h. On the right ("Zn-diffused") the GaAs ($x = 0$) quantum well interdiffuses (Al-Ga) into the $L_y \approx 0.18$-μm $Al_{x'}Ga_{1-x'}As$ ($x' \sim 0.3$) waveguide region ($x \rightarrow x'$). The inset at the lower right shows at ~10× higher magnification (transmission electron micrograph) an as-grown x' region of the width shown at the $L_y \approx 0.18$-μm dimension arrows (of the lower left).

[a] IBM doctoral fellow.

 0003-6951/84/070700-03$01.00

Disorder of an $Al_xGa_{1-x}As$-GaAs superlattice by donor diffusion

K. Meehan,[a] N. Holonyak, Jr., J. M. Brown,[b] M. A. Nixon, and P. Gavrilovic
Electrical Engineering Research Laboratory and Materials Research Laboratory, University of Illinois at Urbana–Champaign, Urbana, Illinois 61801

R. D. Burnham
Xerox Palo Alto Research Center, Palo Alto, California 94304

(Received 14 May 1984; accepted for publication 14 June 1984)

The Si impurity is diffused (850 °C, 10 h, $x_j \sim 2.4\,\mu$m) into 2.4 μm of $Al_xGa_{1-x}As$-GaAs ($x \gtrsim 0.6$) superlattice (barrier $L_B \approx 320$ Å, quantum well $L_z \approx 280$ Å) and disorders it into bulk-crystal $Al_{x'}Ga_{1-x'}As$ ($x' \gtrsim 0.32$). The as-grown infrared gap superlattice is converted selectively to red gap bulk crystal and, where undiffused and not disordered, is still capable of continuous 300-K photopumped laser operation at a threshold of 4×10^3 W/cm^2 (or $J_{eq} \sim 1.7\times10^5$ A/cm^2, 5145 Å pump photon).

Although quantum well heterostructures (QWH's) and superlattices (SL's) are inherently quite stable, these structures can readily be converted to compositionally disordered bulk crystal with various impurities during relatively low-temperature annealing and diffusion procedures. For example, recently it has been learned that $Al_xGa_{1-x}As$-GaAs QWH's or SL's are unstable against low-temperature (< 750 °C) Zn diffusion.[1–3] Impurity-induced disordering of an $Al_xGa_{1-x}As$-GaAs QWH or SL can be accomplished at temperatures, and anneal cycles, much less than those required for ordinary thermal disordering of the layers.[4–6] Moreover, and of special importance in the present context, ordinary photomasking procedures (Si_3N_4 layers and photolithography) can be employed to create an arbitrary pattern of impurity-induced (higher gap) $Al_{x'}Ga_{1-x'}As$ bulk crystal in the $Al_xGa_{1-x}As$-GaAs QWH or SL crystal.[2] To a lesser extent, ion implantation, followed by thermal annealing, has been shown also to be a viable method to cause impurity-induced disordering of a QWH or SL. Specifically, the two impurities Zn and Si have been implanted and used to disorder (partially) $Al_xGa_{1-x}As$ SL's.[3,7] Zinc diffusion, however, has been the most successful procedure, and a corresponding (equally successful) donor diffusion process would be highly desirable, which is the subject of this paper. We show that the process recently employed by Greiner and Gibbons[8] to diffuse Si into GaAs can be used to disorder an $Al_xGa_{1-x}As$-GaAs SL and thus form higher gap bulk-crystal $Al_{x'}Ga_{1-x'}As$. The Si impurity is amphoteric but here serves as a donor[8] and, as mentioned elsewhere in connection with implantation,[7] could exhibit ideal disordering mechanics along the lines discussed by Van Vechten.[9] Above all, we demonstrate that disordering of an $Al_xGa_{1-x}As$-GaAs SL via Si diffusion can be accomplished selectively.

For these experiments the $Al_xGa_{1-x}As$-GaAs SL's (or QWH's) are grown by metalorganic chemical vapor deposition (MOCVD) as described elsewhere.[10,11] Initially a 1-μm layer of $Al_xGa_{1-x}As$ ($x \gtrsim 0.6$) is grown on the substrate followed by a ~0.4-μm GaAs layer and then the superlattice. The SL as such consists (40 periods) of GaAs quantum wells of thickness $L_z \approx 280$ Å coupled by $Al_xGa_{1-x}As$ ($x \gtrsim 0.6$) barriers of thickness $L_B \approx 320$ Å. A bright-field transmission electron micrograph (TEM) of a section of the SL is shown on the right side of Fig. 1. (The diffused region on the left is described later.)

Prior to Si diffusion into the SL, Si_3N_4 is deposited (for diffusion masking) on the wafer, and for convenience a stripe pattern (15-μm stripes on a 25-μm period, Fig. 2) is developed on photoresist deposited on the Si_3N_4. The Si_3N_4 is then plasma etched (CF_4) leaving 10-μm bare stripes on the wafer. Next the photoresist is removed, and the wafer is cleaned in HCl just before ~100 Å of Si is electron beam evaporated onto the wafer at 7×10^{-7} Torr. Immediately after the evaporation is complete ~0.5 μm of SiO_2 is deposited onto the wafer.[8] The SL, with a small piece of As, is then sealed in a quartz ampoule face down on a "slab" of Si to ensure a uniform temperature across the wafer (with also an overpressure of As). After the diffusion, which is accomplished at 850 °C for 10 h, most of the SiO_2 is removed with NH_4F:HF (7:1, 3.5 min). The remaining SiO_2, Si, and Si_3N_4 are removed in a CF_4 plasma. The sample is then cleaved, with one part employed for TEM specimens and the other samples for photopumping.

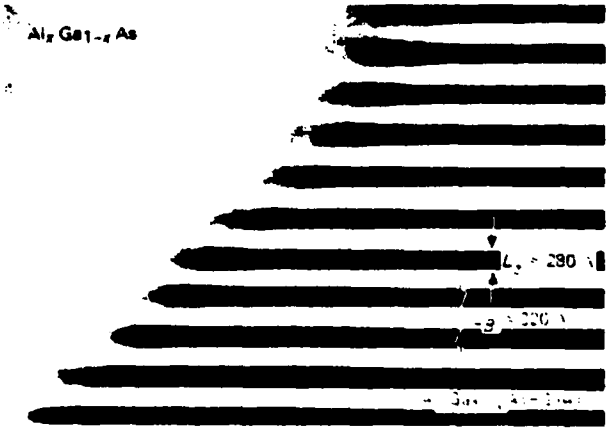

FIG. 1. Bright-field transmission electron micrograph of a 40-period $Al_xGa_{1-x}As$-GaAs superlattice ($x \gtrsim 0.6$, $L_B \approx 320$ Å, $L_z \approx 280$ Å) that on the left has been disordered into bulk-crystal $Al_{x'}Ga_{1-x'}As$ by Si diffusion and on the right is masked (Si_3N_4 protected) as-grown SL that has "survived" the 850 °C (10 h) anneal cycle. The lower part of the 2.4-μm SL is shown and the curved region just at the point in the SL to which the diffusion has penetrated.

[a] IBM doctoral fellow.
[b] Present address: AT&T Bell Labs., Holmdel, New Jersey.

High-energy ($\lambda \lesssim 7300$ Å) 300 K operation of single- and multiple-stripe quantum-well heterostructure laser diodes in an external grating cavity

J. E. Epler, N. Holonyak, Jr., and J. M. Brown
Electrical Engineering Research Laboratory and Materials Research Laboratory, University of Illinois at Urbana-Champaign, Urbana, Illinois 61801

R. D. Burnham, W. Streifer, and T. L. Paoli
Xerox Palo Alto Research Center, Palo Alto, California 94304

(Received 16 February 1984; accepted for publication 22 March 1984)

A set of high performance single- and multiple-stripe $Al_{x'}Ga_{1-x'}As$-$Al_xGa_{1-x}As$ quantum-well heterostructure (QWH) laser diodes coupled to an external grating cavity is used to demonstrate the tuning properties of a semiconductor laser at short wavelength ($\lambda \lesssim 7300$ Å). A single-stripe laser diode (6-μm stripe width) with a single $Al_xGa_{1-x}As$ ($x \sim 0.22$) quantum well of size $L_z \approx 400$ Å is broadly tunable ($7080 < \lambda < 7370$ Å, $\Delta\hbar\omega \sim 70$ meV) and delivers a single dominant longitudinal mode of moderate output power ($P_{out} \sim 50$ mW at 200 mA, pulsed). In continuous (cw) operation ($I = 135$ mA) a single-stripe laser has a 36-meV tuning range, $7168 < \lambda < 7322$ Å. Phase-locked twenty- and forty-stripe diodes (3.5-μm stripe width) from the same QWH wafer are capable of single-longitudinal-mode output at higher power (peak $P_{out} \sim 1.6$ W at an 8.0-A, 200-ns pulse) although at slightly longer wavelength and reduced tuning range ($7225 < \lambda < 7425$ Å). Data are presented illustrating the wavelength dependence of the gain and power output as well as the partial homogeneous broadening and phase-locked nature of the QWH laser arrays. The difference in performance of the multiple-stripe diodes compared with the single-stripe structure can be attributed to the internal coupling of the optical field in neighboring stripes and the reduced threshold current density.

I. INTRODUCTION

An external dispersive cavity has long been recognized as an effective means to improve the spectral output and to probe the internal operation of semiconductor diode lasers.[1-7] A major limitation, however, of more common single heterostructure and double heterostructure (DH) lasers in external-grating operation is the lack of adequate carrier band filling, and thus a small recombination-radiation spectral range and a small gain bandwidth. A large active region size [i.e., bulk-crystal active layer thickness $L_z > 500$ Å] imposes a practical limit (~ 40 meV) on the energy range of the gain profile. In a quantum-well heterostructure (QWH) carrier band filling can be large.[8,9] For example, a photopumped single-well ($L_z \sim 200$ Å) QWH sample can be band filled sufficiently to give laser operation in a $\Delta\hbar\omega \sim 300$-meV range.[8] As a further example, in recent work[7] with QWH laser diodes coupled to an external grating cavity, we have demonstrated 100-meV tunability in continuous (cw) 300 K operation, which is a much greater range than that of ordinary heterojunction lasers ($\sim kT$) but still far less than the "limit" of ~ 300 meV. To obtain the data below, we have, similar to Ref. 7, employed an external grating cavity to investigate the possibility of high power, high-energy tunability of both single-[10] and multiple-stripe[11] high performance QWH diodes. The QWH active region is an $Al_xGa_{1-x}As$ ($x \sim 0.22$) quantum well of size $L_z \approx 400$ Å. The confining layers are $Al_{x'}Ga_{1-x'}As$ ($x' \sim 0.85$). The relatively large size of the quantum well does not easily permit maximum carrier band filling; however, with pulsed excitation of a single-stripe diode, we obtain a 70-meV tuning range ($7080 < \lambda < 7370$ Å) with a single dominant longitudinal mode. The results of the grating experiments indicate a broad, largely homogeneously broadened gain profile capable of supporting narrow line ($\Delta\lambda = 0.3$ Å resolution-limited measurement) operation under high level cw and pulsed room-temperature operation.

The multiple-stripe diodes are spectrally similar to the single-stripe lasers with some important differences, the most apparent being a much greater power output. For example, a forty-stripe diode delivers 1.6 W of peak power (8-A, 200-ns pulse) into a single longitudinal mode ($\lambda \sim 7300$ Å). Also, the multiple-stripe diodes have a lower threshold current density. Thus, the gain profile is centered at longer wavelength (lesser band filling) and has a smaller tuning range (40 meV). The far-field emission generally exhibits a two-lobed pattern in the plane of the junction, which indicates a 180° phase shift between neighboring stripes. These observations are consistent with the concept of a laser array phase locked with the combination of internal mode coupling and external feedback. The similarity with a broad-area diode lasing on physically separate but internally coupled filaments has been previously noted.[12] The performance of the multiple-stripe diodes compared to their single-stripe counterparts indicates that the phase-locked laser array is well suited for high power *tunable* diode laser systems.

II. EXPERIMENTAL PROCEDURE

As in previous work,[7] the $Al_{x'}Ga_{1-x'}As$-$Al_xGa_{1-x}As$ ($x \sim 0.22$, $x' \sim 0.85$) crystals of the present studies have been grown by metalorganic chemical vapor deposition (MOCVD). In Fig. 1 a transmission electron micrograph shows the single 400-Å quantum-well active region of the diodes whose characteristics and operation are described below. The lack of a separate-confinement waveguide structure "sandwiching" the quantum well undoubtedly in-

 0021-8979/84/150670-06$02.40

Far-field supermode patterns of a multiple-stripe quantum well heterostructure laser operated (~7330 Å, 300 K) in an external grating cavity

J. E. Epler and N. Holonyak, Jr.
Electrical Engineering Research Laboratory and Materials Research Laboratory, University of Illinois at Urbana–Champaign, Urbana, Illinois 61801

R. D. Burnham, T. L. Paoli, and W. Streifer
Xerox Palo Alto Research Center, Palo Alto, California 94304

(Received 30 March 1984; accepted for publication 14 May 1984)

A multiple-stripe quantum well heterostructure laser diode operated in an external grating cavity is shown to exhibit the far-field radiation patterns of the "supermode" eigenstates predicted by coupled mode analysis. Data (~7330 Å) are presented on a gain-guided laser array at various continuous (cw, 300 K) operating currents to illustrate the progression of the supermodes from double-lobed patterns (phase shift between emitters) to a single-lobed pattern (no phase shift between emitters). As the cavity wavelength is scanned a cyclical progression (2.8-Å period) of far-field patterns (supermodes) is observed.

Since the successful continuous (cw) 300-K operation of a phase-locked multiple-stripe semiconductor laser,[1] a quantum well heterostructure (QWH),[2] this form of laser and its potential for a higher performance level have attracted increasing attention. Specifically, phase-locked multiple-stripe quantum well heterostructure lasers offer significant improvement in power output[1,3] and reduced beam divergence[4,5] over previous devices. Coupled mode analysis of a multiple-stripe semiconductor laser array[6] predicts the existence of a discrete set of N "supermodes" (N = the number of laser stripes), with each supermode operating at slightly different wavelength. The existence of these supermodes has been confirmed in a recent study by spectrally resolving the spatial profile of the optical intensity on the laser facet.[7] A more direct way to study the supermodes is to "force" a multiple-stripe QWH laser to operate at a given wavelength, e.g., in an external grating cavity,[8–10] and then examine the far-field pattern of the resulting supermode (or supermodes). In this letter we describe this form of multiple-stripe laser operation and confirm directly many of the features of the coupled mode analysis of Ref. 6. Data are presented showing clearly the far-field patterns corresponding to various supermodes, at several currents, for a twenty-stripe (~5-μm centers) QWH diode operating continuously (cw) 300 K near the visible (~7330 Å).

The $Al_{x'}Ga_{1-x'}As$-$Al_xGa_{1-x}As$ ($x' \sim 0.85$, $x \sim 0.22$) QWH crystals of this work are grown by metalorganic chemical vapor deposition (MOCVD) as previously described.[11] The quantum well size is $L_z \simeq 400$ Å, and in the form of ordinary single-stripe lasers this QWH crystal has exhibited excellent short wavelength high power performance.[12] As in earlier work,[9,12] the single- or multiple-stripe pattern is produced by proton bombardment through a thick photoresist mask. An optical microscope is used to verify the actual spacing of the array elements (in this case ~5 μm) by examination of the near-field pattern. After metallization the QWH crystal is cleaved into 250-μm bars and then separated into individual dice that, in turn, are attached junction side down onto copper blocks. The reflectivity of the diode front facet is modified with an Al_2O_3 antireflecting layer and the back facet with an Al_2O_3/Al reflecting coating.

The diode front-facet emission is collimated with an f1.0, 50.8-mm focal length lens. A diffraction grating (7500 Å blaze) oriented with its rulings parallel to the crystal layers disperses the collimated radiation and returns a major fraction to the diode facet in the form of spectral bands (see Ref. 9). Fine control of the grating angle (or cavity wavelength) is accomplished with a piezoelectric transducer built into the (Burleigh) optical mount. The 15-μm travel of the transducer provides a ~6-Å range over which the cavity wavelength can be precisely controlled. The period of a complete cycle through the supermodes is observed to be 2.8 Å, which agrees with the diode longitudinal mode spacing. The displacement of the piezoelectric transducer is assumed linear with applied voltage over a small range (2.8 Å) and is used to obtain the wavelength splitting from supermode to supermode to within 0.1 Å. The resolving power of the grating/lens system is about 0.1 Å, which is sufficient in many circumstances to isolate a single supermode.

A rectangular Al-coated mirror intercepts a small section of the collimated beam and directs it, via a slit, onto a fiber optic "light pipe" which scans the far-field emission pattern. The optical signal (supermode pattern) is monitored with a radiometer/strip chart recorder. The resolution of the system is better than 0.5°. The linear scan of the collimated radiation introduces an error in accordance with the approximation $\tan x \simeq x$, which over small angles (< 30°, full angle) is negligible. A small fraction of the emission is monitored with a 0.5-m Jarrel–Ash monochromator (≲0.2 Å resolution) equipped with a GaAs response photomultiplier and an electrometer/strip chart recorder. Hence, the emission spectrum and far-field pattern can be simultaneously recorded.

The set of far-field patterns shown in Fig. 1 is typical of the cycle of supermodes observed at relatively high injection currents (I = 520 mA, P_{out} = 70 mW, cw). A double-lobed pattern with a 10° spacing between peaks occurs at 7326.7 Å and coincides with the L = 20 supermode (based on the progression of lobe separation). As the cavity wavelength is shifted (via the grating) toward lower energy, the peak separation decreases as the diode is induced to operate in lower order mode configurations. While often a single supermode is dominant, e.g., L = 16 in (b) and L = 11 in (c), often two or

 0003-6951/84/160406-03$01.00

(39)

Effect of layer size on lattice distortion in strained-layer superlattices

J. M. Brown, N. Holonyak, Jr., and R. W. Kaliski
Electrical Engineering Research Laboratory and Materials Research Laboratory, University of Illinois at Urbana–Champaign, Urbana, Illinois 61801

M. J. Ludowise,[a] W. T. Dietze, and C. R. Lewis
Corporate Solid State Laboratory, Varian Associates, Incorporated, Palo Alto, California 94303

(Received 23 January 1984; accepted for publication 2 April 1984)

The accommodation of lattice mismatch in strained-layer GaAs-$In_x Ga_{1-x} As$ ($x \approx 0.27$) superlattices grown by metalorganic chemical vapor deposition has been examined as a function of layer thickness using transmission electron microscopy. The degree of distortion from cubic is shown to be dependent on the layer thickness and at sufficiently large layer sizes ($\gtrsim 180$ Å) dislocations are introduced at the interfaces.

PACS numbers: 61.16.Di, 61.70.Jc, 68.90. + g

It has recently been shown that the lattice mismatch in strained-layer superlattices (SL's) is accommodated by the tetragonal distortion of successive layers of the SL.[1] The degree of distortion is dependent on the amount of lattice mismatch between the two component layers. As in previous work,[1] the results presented in this letter are obtained on strained-layer SL crystals grown by metalorganic chemical vapor deposition (MOCVD),[2,3] specifically on GaAs-$In_x Ga_{1-x} As$ ($x \approx 0.27$) SL's. For these SL's the lattice mismatch is 1.9%, which corresponds to a strain of 9.6×10^{-3}. As shown earlier[4,5] these SL's, for layer sizes $L_B, L_z \lesssim 150$ Å, will operate as continuous (cw) 300-K photopumped lasers for ~ 5 min ($J_{eq} \sim 10^3$ A/cm^2) before failing, thus providing powerful evidence that the layer interfaces for the as-grown SL are defect-free. This letter presents, for these same high quality SL's (new samples), the results of a transmission electron miscroscope (TEM) study of specimens in which the lattice mismatch is kept constant but the layer size is varied from SL to SL, with the quantum wells and barriers being held equal in size ($L_z = L_B$). At $L_z = L_B \gtrsim 180$ Å dislocations are introduced at the interfaces, which is in reasonable agreement with theoretical considerations.[6]

The strained-layer GaAs-$In_x Ga_{1-x} As$ ($x \approx 0.27$) SL's of interest here have been grown by MOCVD as extensively described elsewhere.[2,3] Unlike ordinary SL's, however, the crystals of this work have three separate SL's grown in series from smaller to larger size, and then from the largest size the intermediate size SL and the smallest are repeated to give a symmetrical "stack" of five SL's in the entire series that are unwarped. Two of these SL stacks have been prepared: (a) $L_B = L_z \approx 85$, 120, 180, 120, 85 Å and (b) $L_B = L_z \approx 35$, 160, 240, 160, 35 Å.

The SL crystals are prepared for examination in a Philips 420 TEM by sectioning (cleaving) normal to the plane of growth [(100) plane] so that the layers can be imaged in cross section. The specimens are then mechanically thinned and ion milled to the point of electron transparency, the specimen normal being the [110] direction. As reported previously,[1] another SL specimen with 150-Å layers has shown considerable departure from cubic structure, there being an alternate expansion and contraction of successive layers in the growth direction. In the case of the SL sections of the present work with layer sizes 35 and 85 Å, no measurable distortion from cubic could be seen in selected-area-diffraction patterns as is shown in Fig. 1(a) ($L_B, L_z \approx 35$ Å). The electron diffraction patterns obtained from the superlattices show two distinct features. (i) Satellite peaks are seen in the growth direction equally spaced around all the diffracted peaks in the pattern. These reflect the variation in composition in the growth direction and are separated from the main diffracted beams by a distance in reciprocal space Δg given by[7]

$$\lambda = \frac{[ah/(h^2 + k^2 + l^2)]g}{\Delta g}, \tag{1}$$

where λ is the wavelength of the compositional modulation and is equal to twice the layer size, h, k, l are the Miller indices of the diffracted beam, g is the reciprocal lattice vector of the diffracted beam, and a is the lattice parameter. It can be seen from this equation that as the layer size increases, the satellite spots get closer to the main diffracted spots, and at layer sizes of about 120 Å become indistinguishable in the present measurements. (ii) As the layer size increases, the main diffracted beam splits into two in the growth direction. This splitting increases with the order of the diffracted spot and does not therefore result from the periodic variation in composition but must be crystallographic in origin. The superlattice consists of two crystal structures which give rise to the two diffracted beams in the growth direction. Dark field imaging using the two beams reveals alternating contrast which confirms that the different layers have different lattice spacings. There appears to be no splitting in the growth plane within the accuracy of our measurements, the diffraction pattern indicating that the superlattice consists of two tetragonal crystal structures. The satellite peaks due to the periodically varying composition are clearly seen in the 35-Å layers in the 004 diffraction spot shown in Fig. 1(a). For larger layer sizes, however, the tetragonal distortion in the SL becomes visible in the selected-area-diffraction pattern as a splitting in the growth direction, which is evident in Fig. 1(b) ($L_B, L_z \approx 180$ Å). The satellite spots are much closer to the main beam as the layer size increases.

The heterointerfaces between the layers in these

[a] Now at Hewlett-Packard Research Laboratories, Palo Alto.

(40)

Journal of Crystal Growth 68 (1984) 370–382
North-Holland, Amsterdam

GROWTH AND CHARACTERIZATION OF AlGaAs/GaAs QUANTUM WELL LASERS

R.D. BURNHAM, W. STREIFER and T.L. PAOLI

Xerox Palo Alto Research Center, Palo Alto, California 94304, USA

and

N. HOLONYAK, Jr.

Electrical Engineering Research Laboratory and Material Research Laboratory, University of Illinois at Urbana-Champaign, Urbana, Illinois 61801, USA

Quantum well heterostructure (QWH) lasers have unique and desirable characteristics. A review of a variety of QWH lasers, including infrared and visible, single and multiple stripe devices, will be discussed. Emphasis will be on advances made in the last three years, including broad band tuning with an external grating, wavelength modification by annealing and index-guiding by impurity-induced disordering.

1. Introduction

Although the first reports of semiconductor lasers appeared in 1962 [1–4], it was not until 1970 that continuous, room temperature laser operation was demonstrated [5,6]. This achievement required the implementation of lattice-matched heterostructures [7], which were fabricated by improved crystal growth techniques. Since the early 1970's, much effort has been devoted to refining both the laser structure and crystal growth. Recently, one of these techniques, metalorganic chemical vapor deposition (MOCVD), has become increasingly popular as a consequence of its versatility and economy. The chemistry of MOCVD growth of III–V compounds was pioneered by Manasevit as early as 1968 [8]; however, it was Dupuis and Dapkus [9] who demonstrated that high laser quality AlGaAs/GaAs heterostructures can be achieved by MOCVD. MOCVD can also produce wafers of excellent uniformity, as evidenced by laser measurements of threshold from various parts of a wafer [10–12].

Fig. 1. Transmission electron micrograph of portion of an $Al_xGa_{1-x}As/AlAs/GaAs$ superlattice (SL grown by MOCVD). The size of the composite $AlAs-Al_xGa_{1-x}As-AlAs$ ($x = 0.2$) barriers is $L_b = 105$ Å and for the GaAs quantum wells $L_z = 90$ Å. The herringbone pattern of {111} planes (spacing 3.26 Å) corresponding to the crystal [100] direction upward and [110] normal to the figure make possible accurate layer measurements and identification of monolayer fluctuations in AlAs layer size at (a) and (b).

2. Ultra-thin layers and abrupt interfaces

MOCVD is also advantageous in that very abrupt interfaces and very thin layers can be grown

0022-0248/84/$03.00

IEEE - EDL-5, 266 (1984)

(41)

Two-Dimensional Numerical Analysis of the High Electron Mobility Transistor

D. Widiger*, K. Hess, and J. J. Coleman

Abstract

We develop a two-dimensional model for the High Electron Mobility Transistor (HEMT) including conduction outside the quantum well. The model uses the continuity and power balance moment equations for both inside and outside the well, with electron concentration and average energy as dependent variables, and with parameters determined by Monte Carlo simulation. We show that conduction outside the well is dominant in the "pinch-off" region and that consequently the speed advantage of the HEMT over conventional devices does not arise from high saturation velocities in the quantum well but rather from a lower access resistance as suggested by a velocity profile calculation. It is further demonstrated that several effects which are unimportant in conventional FET's are of significance in the HEMT. Among these effects are electronic heat conduction and to some extent real space transfer.

This work is supported by Army Research Office Contract DAAG 29-82-K-0059, the Joint Services Electronics Program, and the Office of Naval Research, N0014-76-C-0806.

The authors are with the Department of Electrical Engineering and Coordinated Science Laboratory, University of Illinois, Urbana, IL 61801.

*IBM Resident Study Program

Proc. of the IEDM, San Francisco 1984

TWO-DIMENSIONAL TRANSIENT SIMULATION OF THE HIGH ELECTRON MOBILITY TRANSISTOR

D. Widiger, I. C. Kizilyalli, K. Hess, and J. J. Coleman

The Department of Electrical Engineering and Coordinated Science Laboratory,
University of Illinois, Urbana, IL 61801.

ABSTRACT

We develop a model for the High Electron Mobility Transistor (HEMT) which simulates conduction both inside and outside the quantum-well subbands and includes hot electron effects within the framework of average-energy-dependent parameters in macroscopic transport equations. At 77K we see significant velocity overshoot and bulk conduction. From transient simulations it is seen that the current-switching speed is a function of the electron transit time. From this we conclude that the advantage of the excellent conduction in the quantum well is not in a high saturation velocity at pinch-off but rather in a low access resistance. We also conclude that for the HEMT current saturation cannot be explained in terms of a velocity saturation mechanism at the drain edge of the gate. Finally, from steady-state calculations at 300K, we find that although velocity overshoot is reduced, the basic effects are similar to those seen at 77K.

INTRODUCTION

The recently-developed High Electron Mobility Transistor (HEMT) [1] is a field-effect device which takes advantage of the high mobility, two-dimensional electronic system generated by the technique of modulation-doping [2],[3]. This technique introduces carriers into high-purity GaAs from donor ions in an adjacent layer of $Al_xGa_{1-x}As$, the electrons and ions separated by the built-in heterojunction potential. The spatial separation from impurity scatterers and the high screening of the dense electronic system contribute to the higher mobility. The HEMT controls such a high-mobility conducting layer in a field-effect transistor arrangement.

THE MODEL

To accurately model transport in the HEMT one must account for the important high-field effects such as velocity saturation, velocity overshoot, and negative differential resistance. The model we have proposed [4] does this by using the Boltzmann moment equations of continuity and drift/diffusion [5]

$$\frac{\partial n}{\partial t} = \nabla\cdot[-e\mu n\nabla\psi+\nabla Dn] \tag{1}$$

and power balance and energy flux

$$\frac{\partial nE}{\partial t} = -j\cdot\nabla\psi-nB \\ -\alpha\nabla\cdot[-\mu nE\nabla\psi+\nabla DnE] \tag{2}$$

where n is the electron concentration, j is the current density, ψ is the potential, μ, D, and B are the mobility, diffusion, and energy loss parameters all taken as functions of the average energy E in a fashion similar to that of Buot and Frey [6], and α is a dimensionless constant dependent on the power-law nature of the scattering and is set to 4/3, the value for deformation-potential scattering. The functional dependencies on E are determined from Monte Carlo simulations under steady-state and homogeneous conditions and from experimental data [7]. The power balance equation (2) is slightly modified from that given in [5] which assumes a Boltzmann distribution to determine the energy flux term (the term in brackets) by assuming in addition a power law scattering rate.

The model also includes transport in the quantum well by simulating a single quantum well system coexisting with the bulk system. Only the lowest quantum subband is included in the quantum system, whereas the second and higher quantum subbands are counted to the bulk system. This incorporates the important properties of both quantum and bulk transport. The transport equations are similar to those for the bulk system. The two systems are coupled by assuming 1) local quasi-equilibrium between the quantum system and the bulk system, and 2) the diminishing of the proportion of quantum well electrons to bulk electrons as kT_e becomes comparable to the energy difference between the first two quantized energy levels. We have in addition assumed zero conduction in the AlGaAs. The significance of transfer into the AlGaAs (real space transfer [8]) can be estimated from the results for the average energy.

A rectangular device geometry is used. The boundary conditions at the source and drain are assumed to be the result of the one-dimensional, equilibrium problem. By this choice we model ideal source and drain contacts. The potential at the gate-insulator interface is fixed at the gate potential corrected for the built-in

INTERFACE STRUCTURE OF GaAs/AlAs SEMICONDUCTOR SUPERLATTICES PREPARED BY MOCVD

S.J. JENG, C.M. WAYMAN

Department of Metallurgy and Mining Engineering and Materials Research Laboratory, University of Illinois, Urbana, IL 61801, USA

and

G. COSTRINI and J.J. COLEMAN

Electrical Engineering Research Laboratory and Materials Research Laboratory, University of Illinois, Urbana, IL 61801, USA

Received 13 April 1984

The heterointerfaces in GaAs/AlAs semiconductor superlattices grown by the MOCVD technique have been examined on the atomic scale using high-resolution transmission electron microscopy and were found to be atomically smooth and without defects.

1. Introduction

Semiconductor superlattice structures are of interest because of their special electronic and optical properties [1–3]. Electrons and holes can be confined to two-dimensional quantum states in thin semiconductor layers or at semiconductor heterointerfaces, and high-mobility electronic devices can be made. These quantum effects are sensitive to the detailed nature of the interfaces, which in turn are closely dependent on the conditions of epitaxial growth. Metal-organic chemical vapor deposition (MOCVD) [3,4] can produce uniform epitaxial layers with atomically smooth interfaces. The process is carried out near atmospheric pressure and the ultrahigh-vacuum equipment required for molecular beam epitaxy (MBE) [5] is not necessary. In this report, the results of a recent study of MOCVD superlattice structures performed by both conventional and high-resolution transmission electron microscopy are presented. These data show that the interfaces of these superlattices are atomically smooth and defect free.

2. Experimental methods

Two GaAs/AlAs superlattices, with GaAs and AlAs layer thicknesses of 20 and 100 Å respectively, were grown on {100} GaAs substrates using the MOCVD growth process. Slabs from such specimens were then cleaved on {110} planes, and the two slabs were cemented together edge-to-edge in twin orientation with the superlattice side in the middle as described by Pettit et al. [6]. After mechanically thinning to ≈500 μm in thickness the specimens were ion milled to electron transparency using a cold stage and argon beam at a low incidence angle. The superlattice structures were then observed in cross section. The {110} cleavage planes are preferred because of their ease of cleavage, after which the desired heterointerfaces are oriented edge-on. Also, it should be noted that a {110} projection is the most "open" projected structure in the zincblende case. Electron microscopy was performed using a Philips EM420 microscope with a LaB_6 filament source and line resolution of 2 Å, operated at 120 kV.

0 167-577x/84/$ 03.00

J. Appl. Phys., submitted

(44)

Conditions for Uniform Growth of GaAs by Metalorganic Chemical Vapor Deposition in a Vertical Reactor

G. Costrini and J.J. Coleman

Electrical Engineering Research Laboratory, Materials Research Laboratory

Univeristy of Illinois at Urbana-Champaign, Urbana, Illinois 61801

Abstract

The uniformity of epitaxial growth of GaAs by metalorganic chemical vapor deposition (MOCVD) in a vertical-flow rotating-disk reactor has been investigated. Observations of the thickness of the epitaxial layer versus radial distance on the susceptor surface are made for various conditions of carrier gas flow and growth temperature. A model is proposed in consideration of hydrodynamic and thermal boundary layer effects at the susceptor surface. The effects of a parasitic processes in the limit of smaller boundary layers and transition to source input rate-limited growth in the limit of thicker boundary layers are described

Stripe-geometry $Al_xGa_{1-x}As$-GaAs quantum well heterostructure lasers defined by Si diffusion and disordering

K. Meehan, P. Gavrilović, and N. Holonyak, Jr.
Electrical Engineering Research Laboratory and Materials Research Laboratory, University of Illinois at Urbana–Champaign, Urbana, Illinois 61801

R. D. Burnham and R. L. Thornton
Xerox Palo Alto Research Center, Palo Alto, California 94304

(Received 4 September 1984; accepted for publication 16 October 1984)

The use of Si diffusion and impurity-induced layer disordering, via a Si_3N_4 mask pattern, to construct stripe-geometry $Al_xGa_{1-x}As$-GaAs quantum well heterostructure lasers on n-type substrates is described. This leads to a convenient form of index-guided buried-heterostructure laser that is easily constructed and replicated (in various geometries) on commonly available n-type GaAs substrate.

Modern methods of crystal growth have made it relatively easy to realize the basic ultrathin layered structure of a quantum well laser.[1] In some respects a more difficult matter is that of how to convert, laterally or transversely, the layered heterostructure into some form of stripe geometry, which is a more or less standard form for semiconductor lasers. Possibly an ideal way to convert a layered structure into a stripe geometry, or indeed into an arbitrary shape, is by impurity-induced disordering.[2,3] For example, Zn diffusion into an $Al_xGa_{1-x}As$-GaAs quantum well heterostructure (QWH) or superlattice (SL), which can be masked,[3,4] intermixes Al and Ga, intermixes high-gap and low-gap layers, and increases (by the transformation of thin layers to bulk crystal) the energy gap of initially quantum well regions. If this is applied to the usual QWH grown on an n-type wafer, the Zn-disordered region creates a considerable lateral shunt adjacent to the as-grown QWH stripe.[4,5] This can, of course, be avoided by the use of a p-type substrate.[4,6] These (p substrates), however, are less common, lower in mobility, and less useful for integrating other devices on the same substrate. For an n-type substrate with various n-type epitaxial layers grown first and then quantum wells and p-type layers on top, the conversion of this structure to a ("p up") stripe-geometry laser requires (on its sides or edges) a donor disordering process, preferably one that can be accomplished by simple impurity diffusion. Such a disordering process has recently been demonstrated.[7] Silicon has been diffused into an $Al_xGa_{1-x}As$-GaAs SL and, where not masked, has converted the SL to higher gap bulk crystal. In the present letter we describe the use of Si diffusion and layer disordering, via a Si_3N_4 mask pattern, to construct stripe-geometry QWH lasers (buried heterostructure lasers) grown on n-type substrates.

The double-well QWH wafer used in this work has been grown by metalorganic chemical vapor deposition (MOCVD)[8,9] and previously has been used in thermal annealing and quantum well broadening experiments.[10] The active region (see Fig. 2 of Ref. 10) consists of two $L_z \simeq 85$-Å GaAs quantum wells ($x = 0$ $Al_xGa_{1-x}As$) that are coupled with an $L_B \simeq 95$-Å $Al_{x'}Ga_{1-x'}As$ ($x' \sim 0.3$) barrier. The wells and barrier are located approximately in the center of a large ($L_z \simeq 0.23$ μm) $Al_{x'}Ga_{1-x'}As$ ($x' \sim 0.30$) waveguide. The quantum wells and the waveguide are undoped. This region is confined on the substrate side by an n-type $Al_{x''}Ga_{1-x''}As$ ($n_{Se} \sim 5\times10^{17}/cm^3$, $x'' \sim 0.85$) layer (~ 1.2 μm) and on the top side by a ~ 1.7-μm-thick p-type $Al_{x''}Ga_{1-x''}As$ ($n_{Mg} \sim 5\times10^{17}/cm^3$, $x'' \sim 0.85$) layer. A 0.8-μm Zn-doped GaAs cap layer, on a 0.5-μm Mg-doped $Al_yGa_{1-y}As$ ($y \sim 0.15$) transition layer, is grown on top for metallization and current contacts.

As with Zn-induced disordering in a pattern forming a stripe active region,[5] the initial wafer preparation is the same. A 0.1-μm Si_3N_4 masking layer is deposited on the QWH wafer. Using photoresist lithography and CF_4 plasma etching, we prepare a set of 24-μm Si_3N_4 stripes on 20-mil centers. The p-type GaAs cap and p-type $Al_yGa_{1-y}As$ transition layer are then selectively removed except under the Si_3N_4 stripes. These layers are removed between the stripes so as not to impede the Si diffusion. After the diffusion and disordering, a narrow ~ 24-μm as-grown QWH p-type stripe remains; at its edges, of course, the stripe is converted to n type by the Si diffusion (see Fig. 1).

Prior to the diffusion the wafer is cleaned using a short HCl etch to remove any surface oxides, and then a thin (~ 100 Å) Si layer is electron beam evaporated onto the sur-

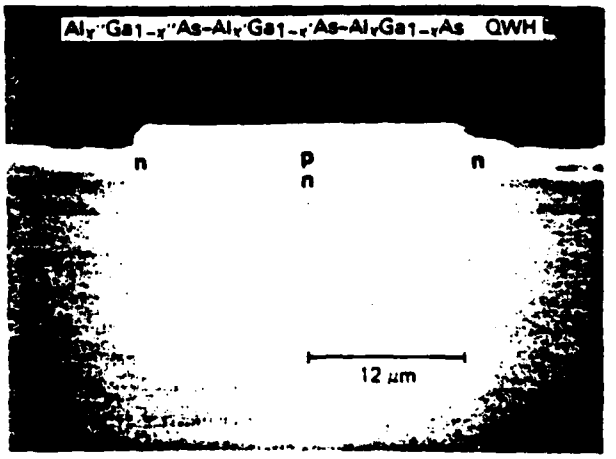

FIG. 1. Scanning electron microscope (SEM) image of an etched 24-μm-wide $Al_{x''}Ga_{1-x''}As$-$Al_{x'}Ga_{1-x'}As$-$Al_{x''}Ga_{1-x''}As$ ($x'' \sim 0.85$, $x' \sim 0.30$, $x = 0$) quantum well heterostructure (QWH) laser stripe (end view) defined by Si diffusion and disordering. The as-grown p-n QWH is shown in the center (24 μm). The Si diffused and disordered areas (no quantum wells) are the regions converted to n type on the left and the right.

J. Appl. Phys. 57, (15 May, 1985)

(46)

DONOR-INDUCED DISORDER-DEFINED BURIED-HETEROSTRUCTURE $Al_xGa_{1-x}As$-GaAs QUANTUM WELL LASERS

K. Meehan, P. Gavrilovic, J.E. Epler,[a] K.C. Hsieh, and N. Holonyak, Jr.

Electrical Engineering Research Laboratory and Materials Research Laboratory

University of Illinois at Urbana-Champaign, Urbana, Illinois 61801

R.D. Burnham, R.L. Thornton, and W. Streifer

Xerox Palo Alto Research Center, Palo Alto, California 94304

Abstract

A simple form of buried heterostructure $Al_xGa_{1-x}As$-GaAs quantum well laser is described that is realized by impurity-induced layer disordering (donor-induced disordering). The layer disordering, and the resulting band-gap shift to higher energy (and lower index), is accomplished by Si diffusion in a stripe pattern defined by a Si_3N_4 mask. Single mode lasers of stripe width 3 μm and 6 μm are demonstrated that operate continuously at 300 K in the threshold current range of 10-25 mA and with single-facet power levels as high as 10-20 mW.

J. Appl. Phys. 57, (1 Jan, 1985)

(47)

SUPERMODES OF MULTIPLE-STRIPE QUANTUM WELL HETEROSTRUCTURE LASER DIODES OPERATED (cw, 300 K) IN AN EXTERNAL GRATING CAVITY

J.E. Epler and N. Holonyak, Jr.,

Electrical Engineering Research Laboratory and Materials Research Laboratory

Univeristy of Illinois at Urbana-Champaign, Urbana, Illinois 61801

R.D. Burnham, T.L. Paoli, and W. Streifer

Xerox Palo Alto Research Center

Palo Alto, California 94304

The far-field supermode patterns of a phase-locked multiple-stripe quantum well heterostructure (QWH) laser diode are described as a function of injection current and emission wavelength, the latter controlled by an external grating. The external-grating cavity is used to isolate single or multiple supermodes of the multiple-stripe QWH laser (P_{out} > 170 mW cw, $\lambda \sim 7400$ Å). The progression of supermode patterns consists of a discrete set of mode configurations for each longitudinal mode of the spectrum. The progression is cyclic with a ~ 2.8 Å period which corresponds to the longitudinal mode spacing of the diode. Under high gain conditions, i.e., near the center of the recombination-radiation spectrum or at higher current levels, continuous tunability is observed with gradual transitions between supermode eigenstates. As the gain is reduced (low current) the number of supermodes observed decreases until only the in-phase pattern, i.e., each emitter at the same phase, remains above threshold. The far-field patterns range from a double-lobe pattern with a 10° peak separation (5 μm between emitter phase reversals) to a narrow (< 2° full angle half power) single-lobe in-phase pattern. The experimental data are compared to the results of coupled mode analysis.

J. Appl. Phys. 57, (1 Feb, 1985)

48

PRESSURE DEPENDENCE OF $Al_xGa_{1-x}As$ LIGHT EMITTING DIODES NEAR THE DIRECT-INDIRECT TRANSITION

R.W. Kaliski, J.E. Epler, and N. Holonyak, Jr.
Electrical Engineering Research Laboratory and Materials Research Laboratory
University of Illinois at Urbana-Champaign, Urbana, Illinois 61801

M.J. Peanasky, G.A. Herrmannsfeldt, and H.G. Drickamer
School of Chemical Sciences, Department of Physics and
Materials Research Laboratory
University of Illinois at Urbana-Champaign, Urbana, Illinois 61081

M.J. Tsai, M.D. Camras, F.G. Kellert, C.H. Wu, and M.G. Craford
Opto-Electronic Laboratory, Hewlett Packard Corporation
Palo Alto, California 94304

Abstract

High pressure studies on high quality $Al_xGa_{1-x}As$ double heterostructure (DH) light emitting diodes (LED's) grown by liquid phase epitaxy (LPE) are presented. The $Al_xGa_{1-x}As$ active region varies in composition from $x \sim 0.25$ to ~ 0.53, i.e., through the critical region of the direct-indirect transition ($x \equiv x_c \approx 0.45$). The pressure coefficient of the Γ conduction band is observed to decrease ($\sim$ 1 meV/kbar for $x \sim 0.25$ to $x \sim 0.53$) with increasing Al concentration, which is in accord with alloy disorder and band edge bowing. Indirect-gap (X) recombination radiation of significant intensity is observed and provides evidence for the high quality of the LPE diodes. High pressure measurements, and the increase in energy of the direct band edge and

J. Appl. Phys. 57, (1 Feb, 1985)
(49)

HYDROSTATIC PRESSURE MEASUREMENTS ($\lesssim$ 12 kbar) ON SINGLE- AND MULTIPLE-STRIPE QUANTUM-WELL HETEROSTRUCTURE LASER DIODES

J.E. Epler, R.W. Kaliski, and N. Holonyak, Jr.
Electrical Engineering Research Laboratory and Materials Research Laboratory
University of Illinois at Urbana-Champaign, Urbana, Illinois 61801

M.J. Peanasky, G.A. Herrmannsfeldt, and H.G. Drickamer
School of Chemical Sciences, Department of Physics and
Materials Research Laboratory
University of Illinois at Urbana-Champaign, Urbana, Illinois 61801

R.D. Burnham and R.L. Thornton
Xerox Palo Alto Research Center, Palo Alto, California 94304

Short wavelength $Al_{x'}Ga_{1-x'}As$-$Al_xGa_{1-x}As$ ($x' \sim 0.85$, $x \sim 0.22$) quantum well heterostructure (QWH) laser diodes (well size $L_z \approx 400$ Å) that operate continuously (cw) at 300 K are subjected to hydrostatic pressure ($\lesssim$ 12 kbar). The emission spectrum and the light intensity versus current (L-I) curves are monitored to determine the pressure dependence of the direct (Γ) bandgap and the threshold current. The bandgap exhibits a linear pressure dependence with a noticeable change in slope at ~ 4.5 kbar, similar to previously reported results for $Al_xGa_{1-x}As$-GaAs QWH diodes. The threshold current increases monotonically with pressure, reflecting the increasing loss of carriers to the X- and L-bands. The short-wavelength cw limit of the system, i.e., a gain-guided laser with a 400-Å $Al_xGa_{1-x}As$ ($x \sim 0.22$) quantum well and no separate waveguide region, is determined to be ~ 6980 Å.

J. of Superlattices and Microstructures, Academic 1985

(50)

GENERAL MODEL OF THE TRANSVERSE DIELECTRIC CONSTANT OF GAAS-ALAS SUPERLATTICES

K. B. Kahen, J. P. Leburton and K. Hess

Department of Electrical Engineering and Coordinated Science Laboratory, University of Illinois
Urbana-Champaign, Illinois 61801

A general model of the transverse dielectric constant of GaAs-AlAs superlattices is presented. The model is based on treating separately the individual contributions from the Γ, X, and L valleys, enabling us to understand better the general trends of the overall dielectric constant. An accurate $\vec{k}\cdot\vec{p}$ band calculation is used to determine the bulk band structure around the three symmetry points and a realistic Kronig-Penney model is used to calculate the influence of the superlattice periodicity on the bulk band structure. The resulting dielectric constant shows a small polarization effect due to the anisotropy of the superstructure and a large amount of fine structure corresponding to different transitions between the quantized levels. The influence of the barrier and well thicknesses, L_B and L_Z, respectively, is also important and it is shown that for a constant value of $\bar{x}=L_B/(L_B+L_Z)$, the real part of the zero frequency dielectric constant increases as a function of L_B. Finally, the real parts of the dielectric constants of a superlattice and the corresponding AlGaAs alloy, characterized by the same value of $\bar{x}$, are compared and it is found that at zero frequency the superlattice dielectric constant is slightly larger with the difference increasing for higher frequencies.

Accepted 9/3/84 JDow

(59)

Send a copy of this sheet plus camera-ready copy to I. Superlattices & Microstructures
Academic Press 1985
24-28 Oval Rd
London NW1 7DX
United Kingdom

TWO-DIMENSIONAL NUMERICAL ANALYSYS OF THE HIGH ELECTRON MOBILITY TRANSISTOR

D. Widiger, I. C. Kizilyalli, K. Hess, and J. J. Coleman
The Department of Electrical Engineering and Coordinated Science Laboratory,
University of Illinois, Urbana, IL 61801.

(Received 13 August 1984 by John D Dow)

Electrical properties of the High Electron Mobility Transistor (HEMT) are determined. The continuity and power balance equations are modeled with electron concentration and average energy as dependent variables and with Monte-Carlo-generated parameters. Conduction in both the quantum well and the bulk are included, represented respectively with one-dimensional and two-dimensional finite difference schemes. Important effects observed are velocity overshoot, electronic heating and heat conduction, real space transfer, and transfer of carriers from the quantum well to the bulk in pinch-off. It is concluded that the speed of the HEMT over conventional devices does not arise from high saturation velocities in the quantum well but rather from a lower access resistance.

This work is supported by Army Research Office Contract DAAG 29-82-K-0059, the Joint Services Electronics Program, and the Office of Naval Research, N0014-76-C-0806. D. Widiger is part of the IBM Resident Study Program.

IEEE Transactions on ED submitted

(52)

Two-dimensional Transient Simulation of an Idealized High Electron Mobility Transistor

D. Widiger*, I. C. Kizilyalli, K. Hess, and J. J. Coleman

Abstract

We develop a model for the High Electron Mobility Transistor (HEMT) in which we include both hot electron effects and conduction outside the quantum subband system using hydrodynamic-like transport equations. With such a model we can assess the significance of the various physical phenomena involved in the operation of the HEMT. We calculate results with a two-dimensional numerical technique for both steady-state and transient operation. For a 3 micron device at 77K, we determine a transconductance of 450 mS/mm, a current-switching speed of 6 ps, and a capacitive charging speed of 4 ps per fan-out gate which corresponds to the performance measured by other workers. We also see that electronic heating, velocity overshoot, and conduction outside the quantum well are significant near the pinch-off point. We conclude that the advantage of HEMT is twofold. The excellent conduction in the quantum well results in a low access resistance and the low impurity concentration in the GaAs results in optimum overshoot effects.

The authors are with the Department of Electrical Engineering and Coordinated Science Laboratory, University of Illinois, Urbana, IL 61801. This work is supported by Army Research Office under Contract DAAG 29-82-K-0059, the Joint Services Electronics Program, and the Office of Naval Research under Contract N0014-76-C-0806. D. Widiger is part of the IBM Resident Study Program.

* The present address of D. Widiger is International Business Machines 120/023, 9500 Godwin Dr., Manassas, Va. 22110.

Materials Letters. submitted

(53)

Interface Characteristics of GaAs/$Al_xGa_{1-x}As$ Superlattices Grown by MOCVD

S.J. Jeng and C.M. Wayman

Department of Metallurgy and Mining Engineering and
Materials Research Laboratory
University of Illinois

and

J.J. Coleman and G. Costrini

Electrical Engineering Research Laboratory and
Materials Research Laboratory
University of Illinois
Urbana, IL 61801

ABSTRACT:

The structure and quality of the heterointerfaces of AlAs/GaAs semiconductor superlattices grown by the MOCVD technique have been examined on the atomic scale using high resolution electron microscopy lattice imaging. The interface of either GaAs grown on AlAs ($Al_xGa_{1-x}As$) or AlAs ($Al_xGa_{1-x}As$) grown on GaAs is atomically smooth and without defects in both cases, and the interface quality is not degraded by increasing either the layer size or the Al composition.

INTRODUCTION:

In semiconductor devices, crystalline defects can be non-radiative recombination centers which reduce the carrier lifetime and, therefore, the quantum efficiency in optoelectronic devices. Impurities, furthermore, can

END

FILMED

5-85

DTIC